8-2022

Ribonucleotide Reductase Subunit Switching in Hepatoblastoma Drug Response and Relapse

Anthony Brown
University of Tennessee Health Science Center

Ribonucleotide Reductase Subunit Switching in Hepatoblastoma Drug Response and Relapse

Abstract

Hepatoblastoma is the most common primary liver cancer in infants and young children. Despite being a very rare cancer that accounts for only 0.5-2% if all childhood cancer cases, HB has the largest increase in incidence among childhood cancers in the United States and worldwide. The five-year survival rate of children with the aggressive forms of HB, including those that have developed metastatic or recurrent diseases, is less than 40% due to the lack of effective treatment. We aim to identify targetable mechanisms underlying the progression and drug resistance of high-risk HB. Our recent work on HB mouse and organoid models, patient-derived xenografts (PDX) and primary patient samples revealed a significant upregulation of ribonucleotide reductase (RNR) subunit M2 (RRM2) in high-risk HB. RNR is the sole enzymatic complex in mammal cells that converts ribonucleotides to deoxyribonucleotides and plays a critical role in regulating cell division and DNA repair. We found standard chemotherapy agents as well as two RRM2 inhibitors, triapine and MK1775, werecapable of reducing RRM2 expression effectively in vitro. However, we found a significant induction of another RNR subunit M2B (RRM2B) in treated cells in corresponding to RRM2 reduction. While no changes in drug response were noticed in RRM2B knockout (KO) HB cells. RRM2B levels in HB cells showed a strong impact on cells' ability to recover after chemotherapy. RRM2BOE HB cells showed a significant increase in their colony formation potential after chemotherapy where RRM2BKO cells formed much fewer colonies after treatment compared to the control cells. Interestingly, we noticed a reversed subunit switch from RRM2B to RRM2 during the recovery period when cell proliferation was restored. RRM2, indeed, had a much higher enzymatic activity in converting ribonucleotides to deoxyribonucleotides than RRM2B and promoted cell growth much more efficiently than RRM2B when both were overexpressed in HB cells. Finally, combining the RRM2 inhibitor MK1775 with standard chemotherapy in HB PDX models, although showing no additional benefit in reducing tumor size, significantly delayed tumor relapse after drug withdrawal. In this study, we demonstrated an intriguing switching between two RNR subunits, RRM2 and RRM2B in HB cells undergoing drug treatment and during their recovery afterwards. Our data suggest that RRM2 supports HB growth while its switching to RRM2B is critical to tumor cell survival under drug treatment. When tumor relapses, there is a reversed subunit switch from RRM2B to RRM2 to supports the recurrent growth of the tumor, which can serve as a potential therapeutic target in preventing HB relapse.

Document Type

Dissertation

Degree Name

Doctor of Philosophy (PhD)

Program

Biomedical Sciences

Research Advisor

Liqin Zhu Ph.D.

Keywords

Cancer; Hepatoblastoma

Subject Categories

Medicine and Health Sciences | Neoplasms | Oncology | Pediatrics | Therapeutics

UNIVERSITY OF TENNESSEE HEALTH SCIENCE CENTER

DOCTOR OF PHILOSOPHY DISSERTATION

Ribonucleotide Reductase Subunit Switching in Hepatoblastoma Drug Response and Relapse

---

Author:
Anthony Brown

Advisor:
Liqin Zhu, *Ph.D.*

A Dissertation Presented for The Graduate Studies Council of
The University of Tennessee Health Science Center
in Partial Fulfillment of the Requirements for the Doctor of Philosophy degree from
The University of Tennessee

in

Biomedical Sciences: Cancer and Developmental Biology
College of Graduate Health Sciences

July 2022

DEDICATION

I would like to dedicate this dissertation first and foremost to my mother, Katrina Brown, who supported me throughout my education and if not for her, I would not be where I am, and more importantly, would not be the person I am today. To my friends, Lucas Gunnels, Cooper Luton, Logan Boles, and Madison Boles, who whether they knew it or not, pushed me to go further than I ever thought possible and made me strive to be better. I could not ask for better friends. To my fiancée Kate Chambers who has supported me endlessly, through all the late nights, listening to my presentations even though you had no idea what I was saying. You have been the light of my life and I don't know if I would have made it without you. Finally, to my dog Lily, I know you won't read this, but you have brought so much joy into my life and gave me a reason to not stay in lab all day.

ACKNOWLEDGEMENTS

First, I would like to give me sincerest gratitude to Dr. Liqin Zhu who took me under her wing and allowed me to pursue my passion in her lab. Your mentorship, guidance, and unwavering support for me and my project has gotten me through this Ph.D. at times when I was unsure if I would make it. You have prepared me to be a successful scientist and I could not have asked for a better place to do it.

I would like to thank my committee members Dr. Joseph Opferman, Dr. Mark Hatley, Dr. Gerard Grosveld, and Dr. Evan Glazer for supporting me and guiding through this process. You have all always provided amazing feedback and gave new ways to look at and approach my project which would not be completed without all of your help.

I am thankful for the rest of the Zhu lab, Dr. Liyuan Li, Dr. Li Fan, Dr. Tian Cheng, Dr. Kaushik Dey. You all have provided so much help to me throughout my years in the lab and someone always had experience I needed for an experiment. Your expertise has guided me and allowed me to put forth work I am proud of.

I would like to thank my collaborators Dr. Stefano Cairo and Dr. Emilie Endorse for their help and guidance with in vivo experiments, Dr. Shondra Miller, and Dr. Baranda Hansen for your knowledge, expertise, and help with Crispr/Cas9 knockouts, Dr. Qingfei Pan for your incredible computational work that really provided insight for my project, and Dr. Nikolai Timchenko for your help with Co-IP experiments.

I am especially thankful for my friends at St. Jude, in no particular order, Brennan Bergeron, Dr. Jianzhong Hu, and Joseph Miller. You all have provided not only scientific input and advise for my project but also genuine friendship and were always up to talk when I needed a break. It was an honor to get my Ph.D. alongside you guys.

And finally, to my friends and family, I could not have done it without you. Your encouragement helped push me along and you all mean the world to me.

ABSTRACT

Hepatoblastoma (HB) is the most common primary liver cancer in infants and young children. Despite being a very rare cancer that accounts for only 0.5-2% of all childhood cancer cases, HB has the largest increase in incidence among childhood cancers in the United States and worldwide. The five-year survival rate of children with the aggressive forms of HB, including those that have developed metastatic or recurrent diseases, is less than 40% due to the lack of effective treatment. We aim to identify targetable mechanisms underlying the progression and drug resistance of high-risk HB.

Our recent work on HB mouse and organoid models, patient-derived xenografts (PDX) and primary patient samples revealed a significant upregulation of ribonucleotide reductase (RNR) subunit M2 (RRM2) in high-risk HB. Ribonucleotide reductase (RNR) is the sole enzymatic complex in mammal cells that converts ribonucleotides to deoxyribonucleotides and plays a critical role in regulating cell division and DNA repair. We found standard chemotherapy agents as well as two RRM2 inhibitors, triapine and MK1775, were capable of reducing *RRM2* expression effectively in vitro. However, we found a significant induction of another RNR subunit M2B (RRM2B) in treated cells in corresponding to RRM2 reduction. While no changes in drug response were noticed in *RRM2B* knockout (KO) HB cells. RRM2B levels in HB cells showed a strong impact on cells' ability to recover after chemotherapy. Overexpression (OE) of RRM2B in HB cells showed a significant increase in their colony formation potential after chemotherapy where $RRM2B^{KO}$ cells formed much fewer colonies after treatment compared to the control cells. Interestingly, we noticed a reversed subunit switch from RRM2B to RRM2 during the recovery period when cell proliferation was restored. RRM2, indeed, had a much higher enzymatic activity in converting ribonucleotides to deoxyribonucleotides than RRM2B and promoted cell growth much more efficiently than RRM2B when both were overexpressed in HB cells. Finally, combining the RRM2 inhibitor MK1775 with standard chemotherapy in HB PDX models, although showing no additional benefit in reducing tumor size, significantly delayed tumor relapse after drug withdrawal.

In this study, we demonstrated an intriguing switching between two RNR subunits, RRM2 and RRM2B in HB cells undergoing drug treatment and during their recovery afterwards. Our data suggest that RRM2 supports HB growth while its switching to RRM2B is critical to tumor cell survival under drug treatment. When tumor relapses, there is a reversed subunit switch from RRM2B to RRM2 to supports the recurrent growth of the tumor, which can serve as a potential therapeutic target in preventing HB relapse.

TABLE OF CONTENTS

LIST OF TABLES

LIST OF FIGURES

LIST OF ABBREVIATIONS

ABC	ATP binding cassette
AFP	Alpha fetal protein
ALL	Acute lymphoblastic leukemia
AP1	Activator protein 1
cAMP	Cyclic AMP
CDK2	Cyclin dependent kinase 2
ChIP-Seq	Chromatin Immunoprecipitation Sequencing
ClFTP	Tri-phosphorylated clofarabine
CREB	cAMP response binding protein
Ctnnb1	β-Catenin
CYP	Cytochrome P450
dNTPs	Deoxyribonucleotide triphosphate
DOX	Doxorubicin
EGFR	Epidermal growth factor receptor
EMT	Epithelial mesenchymal transition
GS	Glutamine Synthetase
GSEA	Gene set enrichment analysis
GSK-3β	Glycogen synthase kinase - 3β
HAT	Histone acetyltransferase
HB	Hepatoblastoma
HCC	Hepatocellular carcinoma
HDAC	Histone deacetylase
HDAC	Histone deacetylases
HPC	Hepatic precursor cell
hRFC	human folate carrier
IC50	50% Inhibitory concentration
IHC	Immunohistochemistry
LC/MS	Liquid chromatography/mass spectrometry
MD	Moderately differentiated
MDR1	Multi drug-resistance gene 1
NCSLC	Non-small cell lung cancer
NF-Y	Nuclear factor Y
NF-κβ	Nuclear factor kappa-B
NICD	Notch intercellular domain
NICD1	Notch intercellular domain 1
NSG	Nod skid gamma
PD	Poorly differentiated
PNR	Prominin1CreERT2; RosaNICD1/+; RosaZsG
PPTR	Prominin1CreERT2; Ptenflx/flx; Tp53flx/flx; RosaZsG
PRETEXT	Pretreated extent of tumor
PYWAYRRM2	Ribonucleotide reductase subunit M2 associated pathways
PYWAYRRM2B	Ribonucleotide reductase subunit M2B associated pathways
RNR	Ribonucleotide Reductase

ROS	Reactive oxygen species
RRM1	Ribonucleotide reductase subunit M1
RRM2	Ribonucleotide reductase subunit M2B
SCU	Small cell undifferentiated
SNP	Single nucleotide polymorphism
TCGA	The cancer genome atlas
TdT	tdTomato
TFAM	Mitochondrial Transcription Factor A
WD	Well differentiated
WDF	Well differentiated fetal
5-FU	Fluorouracil

CHAPTER 1. INTRODUCTION

Hepatoblastoma

Hepatoblastoma (HB) is extremely rare accounting for only 1% of all malignancies in the pediatric age group, with less than 1.5 cases per million children under the age of 18.[1] HB, which makes up more than two-thirds of the pediatric liver malignancies has recently been reported to have the highest increase in incidence rates of pediatric malignancies possibly due to the increased number of survivors of premature birth and the predisposition to develop HB in infants with a birth weight lower than 1500g.[2] With the advancement of surgical procedures and chemotherapy, the 5-year overall survival rate has reached greater than 80%.[3]

However, about one fifth of patients with HB have lung metastasis at the time of diagnosis.[4, 5] For children with metastatic HB, the survival rate drops dramatically, a recent study looking exclusively at children with metastatic HB showed a 5-year overall survival rate of just 23.7%.[6]

Challenges in Hepatoblastoma Research

Clinical and basic research on HB remains challenging due to a small patient population and limited research resources. Over a 15-year period from 1994 to 2006 the Society of Pediatric Oncology Liver Tumors Strategy Group (SIOPEL) performed 2 international clinical trials to test therapeutic strategies on high-risk HB with a total patient number of 216.[7] In comparison to a more common pediatric solid, neuroblastoma, which is the most common extra-cranial solid tumor in infants and children,[8] between the years 1991-2020 there were 9087 children enrolled in 2 international clinical trials.[9]

The rarity of HB has also limited the number of research models available for HB. There are currently on two cell lines publicly available for HB; HepG2 and Huh6, with both being from low grade tumors.[10]Similar to cell lines, there is a lack of mouse models available as well. As of six years ago there were only around 4 reported transgenic mouse models that were able to produce HB tumors and one of them only produced tumors 38% of the time.[10] Patient-derived xenografts (PDXs) have been established for HB in recent years, however, metastasis are rare in either HB genetic or PDX mouse models. Highlighting the need for new research models for HB and more specifically models that recapitulate the more advanced disease state.

Development of a Metastatic HB Mouse Model in Our Laboratory

Our lab has reported the development of a HB genetic mouse model, *Prominin1*^{CreERT2}*;NICD1* (Notch intercellular domain 1)*/+; Rosa*^{ZsG} (PNR) mouse (**Figure 1-1**) in which the Notch signaling pathway was activated in Prom1-expressing

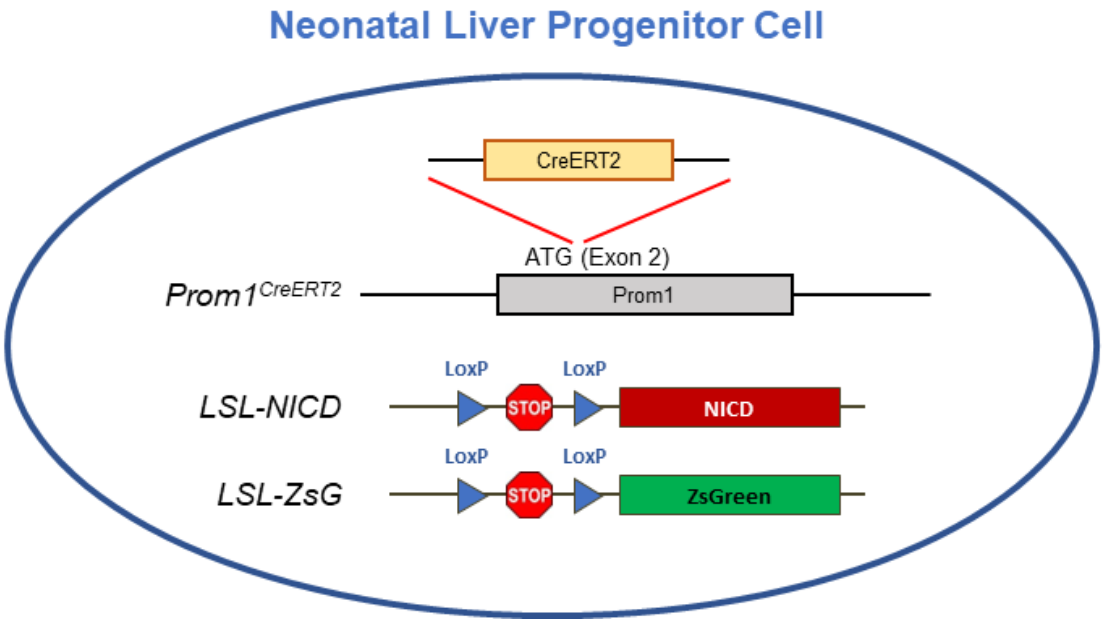

Figure 1-1. Schematic diagram of PNR mouse model.

liver progenitor population in neonatal mice to drive HB development.[11] Notch has been shown to play an important role in the development, repair, and homeostasis of the liver.[12] Detailed histopathological review has confirmed that tumors generated in our PNR model recapitulate the fetal and embryonal subtypes of HB.[11] These tumors expressed common HB diagnostic markers such as β-catenin (*Ctnnb1*) and glutamine synthetase (*GS*).[11] While this PNR model was able to produce HB in neonatal mice, it had a low metastasis rate of 1.9%.[13]

In order to develop a high-risk HB mouse model that would allow us to gain further insight into the biological mechanisms driving advanced progression of HB, our lab chose a cancer stem cell (CSC) based approach to promote metastasis in the PNR model. CSCs have been widely reported to be tightly associated with advanced cancer development such as metastasis, drug resistance, and relapse.[14] Recent 3D organoid models provided an efficient means to enrich CSCs from primary tumors.[15] To enrich the potential metastatic initiating CSCs from the PNR tumors, our lab isolated primary tumors from the PNR mouse model and cultured the tumor cells in a 3D cell culture system using Matrigel as the base and a chemically defined medium for liver cancer cells.[13] These organoids could be readily established from the primary PNR tumors and showed a consistent and significant upregulation in the expression of liver stem cell markers compared to their parental tumors. They were then orthotopically transplanted into CD-1 nude mice where a subset of the organoids were highly tumorigenic and metastatic (**Figure 1-2**). The metastatic rates for these tumorigenic organoids significantly increased to 28-42%, a drastic increase from the parental PNR model.[13] By using a cancer organoid based approach, our lab was able to generate a highly efficient model of high-risk HB.

Upregulation of Ribonucleotide Reductase M2 in HB Metastasis

In order to determine potential drivers behind the increased metastasis observed in the organoid transplantation model, we performed a large RNAseq transcriptomic comparison of the primary tumors in the genetic models and metastatic tumors in the organoid transplantation model, as well as the PNR organoids with the normal organoids grown from wildtype mouse liver. We found Ribonucleotide reductase M2 (RRM2) to be one of the top genes significantly upregulated in the highly tumorigenic PNR organoids and metastatic tumors. RRM2 is essential for proliferating cells and catalyzes the formation of deoxyribonucleotides for DNA synthesis.[16] It has been reported to be upregulated in several other cancers including breast, cervical, lung, and adult liver cancer.[17-20] We confirmed that RRM2 expression was tightly associated with HB progression in patients, with higher grade tumors showing high levels or RRM2 expression. There have been several inhibitors that have been developed to target RRM2 or the RNR complex, two of which are triapine and MK1775.[21, 22] When testing these RRM2 inhibitors as well as standard chemotherapies were used on the HB cell line HepG2, we found that all treatments were able to effectively lower RRM2 protein levels which was expected due to the various mechanisms in which they inhibit proliferation.

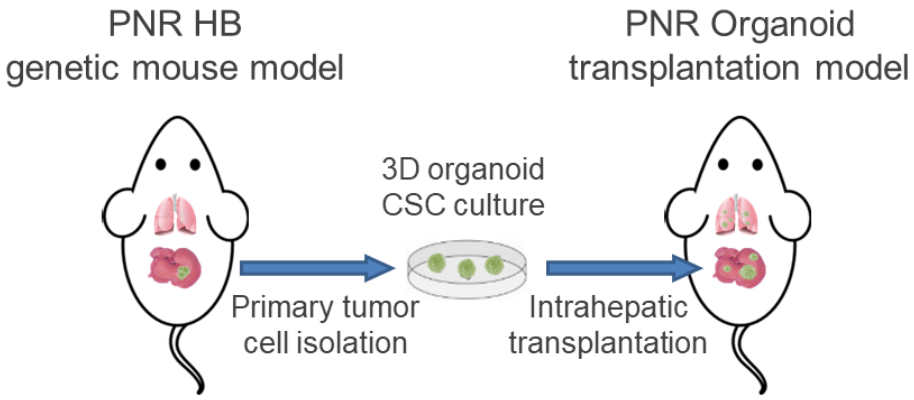

Figure 1-2. Schematic diagram of orthotopic transplantation model.

Interestingly, we found that and isoform of RRM2, ribonucleotide reductase subunit M2B (RRM2B), was significantly induced by treatment. This dynamic switching from RRM2 to RRM2B following drug treatment was also found in a HB PDX cell line that was developed in a collaborating lab, as well as HB214 PDX tumors in vivo. We found that RRM2B has a much lower expression in treatment naïve cells and tumors and was not associated with HB progression in patients. Although RRM2B has been associated with stress response[23] its role in cancer is unclear. Our finding on this drug-induced RRM2 to RRM2B switching in HB cells and tumors suggests that these two RNRM2 isoforms might have distinct role in HB development and drug response.

Hypothesis and Specific Aims

Drug treatment-induced switching of the two RNR2 subunits, RRM2 and RRM2B, is critical to HB cell survival and drug resistance.

I propose to test this hypothesis via the following two specific aims to determine the biological functions of RRM2 and RRM2B in HB development and drug resistance, and the effects of their pharmacological inhibition on advanced HB development. Successful completion of this project will yield essential evidence to support RNR as a novel therapeutic target of high-risk HB.

Aim 1: Elucidate the Function of RRM2 and RRM2B in HB Development and Drug Resistance

To determine the role of RRM2 and RRM2B in HB development and drug resistance, we will use genetic approaches to up- and down-regulate RRM2 and RRM2B expression in HB cells and test their effects on HB cell growth, drug resistance, and long-term cell survival.

Aim 2: Determine if RNR Is a Potential Therapeutic Target for HB

The high expression of RRM2 in aggressive HB tumors suggests that targeting RRM2 enzymatic activity may serve as an effective therapeutic strategy for high-risk HB patients. RRM2 inhibitors have been previously developed and showed a promising efficacy in treating many refractory adult cancers such as colorectal, breast and ovarian cancers, particularly when combined with standard chemotherapies. Upregulation of RRM2B in response to drug treatments could lead to a novel targeting strategy in combination with our chemotherapy agents. We will determine the efficacy of RRM2 inhibitors either targeting RRM2 directly or upstream targets as monotherapies and in combination with standard chemotherapies. We will identify the most effective in vitro treatment and validate their efficacy using PDX’s in vivo.

The proposed study will determine the therapeutic value of RRM2 and RRM2B and potentially lead to a novel target for drug design as well as mechanistic insights into the role of RNR in HB drug resistance.

CHAPTER 2. PEDIATRIC LIVER CANER, RNR, AND DRUG RESISTANCE

Pediatric Liver Cancer

Hepatoblastoma

HB occurs typically within the first 3 years of life and is possibly congenital in familial syndromes, such as Beckwith Weidmann syndrome, Simpson-Golabi-Behmel syndrome, Sotos syndrome, familial adenomatous polyposis coli, and constitutional trisomy 18.[24, 25] HB is exceedingly rare in children above age of five where HCC is the most diagnosed liver cancer.[26,27] In pediatric liver cancer, alpha fetoprotein (AFP) is the most important biomarker, which is elevated in 90% HB caces.[28] AFP levels are usually extremely high in neonates (500,00 ng/mL) but decrease throughout infancy. This can sometimes make it difficult for clinicians to determine if an individual's AFP level is within a normal range.[29] Similarly, some benign tumors such as infantile hemangiomas and mesenchymal hamartomas show an increased level of AFP expression and so AFP maker by itself, cannot confirm HB.[29]

HB Cell of Origin

HB is an embryonal tumor that is derived from hepatic precursor cells (HPC) at various maturation stages and that frequently contains heterogenous cell types. HB can show various levels of epithelial or mesenchymal differentiations.[30] The epithelial components of hepatoblastomas exhibit features of embryonal and fetal development.[30] Immunohistochemistry (IHC) and electron microscopy in HB shows small epithelial cells with a phenotypic characteristic somewhere between hepatic and biliary cells. These cells have expression of CK-7, albumin, and OV-6 which are expressed in oval stem cells typical in adult liver.[31]

HB Molecular Subtypes

The term "hepatoblastoma" was introduced in 1962 based on the presence of hepatic epithelial parenchyma resembling fetal or embryonal liver. The current classification has been broken down into an epithelial subtype which is further broken down into fetal and embryonal, and a mixed epithelial and mesenchymal type. The classification of HB must be performed on pre-treated samples as post-treatment specimens may show areas of HB indistinguishable from HCC or well-differentiated fetal (WDF) HB morphology as a consequence of therapy-induced differentiation/-maturation.[32] The Pretreatment extent of tumor (PRETEXT) system is used to help determine the classification of HB and HCC tumors, which consists of two components, the PRETEXT group and annotation factors. The PRETEXT group describes the extent of tumor within the liver while the annotation factors help to describe the associated

features such as vascular involvement (portal vein or hepatic/inferior vena cava), extrahepatic disease, multifocality, tumor rupture, and metastatic disease (to both lungs and lymph nodes).[33]

Epithelial Hepatoblastoma

Epithelial HB is broken down into many different subtypes such as WDF and small cell undifferentiated (SCU). WDF HB is composed of small uniform cells with a central nucleus without nucleoli and an abundant eosinophilic or clear cytoplasm (**Figure 2-1A**).[34] The cells arrange in trabeculae one to two cells thick and rarely may be in an acinar arrangement. The diagnosis of WDF can only be made on pretreated primary resected tumors. Immunostaining of WDF HB shows strong positive expression of glutamine synthetase while β-catenin usually appears membranous and cytoplasmic. The diagnosis of pure WDF HB identifies as a very low-risk patient group.[27, 35]

Another subtype of epithelial HB is SCU which, in the past was assigned the worse prognosis, and was represented as the "anaplastic variant of HB".[36] HB with a SCU phenotype have a high nuclear to cytoplasmic ratio, pale vesicular to hyperchromatic nucleus, scant cytoplasm, and indistinct cell borders (**Figure 2-2A, B**).[27, 36] SCU areas are difficult to distinguish post chemotherapy and like WDF should be diagnosed prior to treatment.[27, 36]

Mixed Hepatoblastoma

Mixed HB is comprised of both epithelial and mesenchymal elements. The most common mesenchymal elements are osteoid and cartilage with muscle, fat, primitive spindle cell mesenchyme being less frequent (**Figure 2-3A, B**).[27, 37] These components are features of this tumor subtype and not a result of chemotherapy or other changes.

Genetics of HB

HB tumors are for the most part, genetically simple. In a study of 112 patients with pediatric liver tumors, somatic mutations in the exonic regions were very rare (.52 per Mb on average).[38] There were 26 genes that were the most frequently mutated in a cohort including *CTNNB1*, *ARID1A*, *TERT* (promoter region), *ITPR2*, *APC*, and glycogen synthase kinase-3β (GSK)-3β.[38] The most common underlying mutation in HB patients is a mutation in *CTNNB1*, with the incidence of such mutation in several independent studies ranging from 46% to 89% and an average of approximately 60%.[39] Mouse models for HB induced by anthraquinone, oxazepam, or diethanolamine strikingly all showed a 100% incidence of β-catenin mutations.[40, 41] These mutations in the Wnt signaling pathway in HB which are predominantly a deletion in exon 3[40] lead to over activation of this pathway.[42, 43] Another study of 125 HB cases divided the patients into three groups based upon age: "tween HB (age> 8, 6 cases)", "child HB (age = 2-8, 38 cases)", and

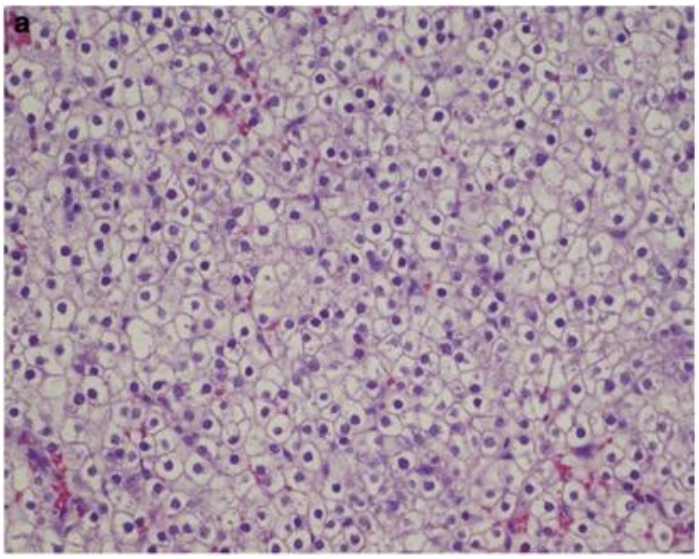

Figure 2-1. Well differentiated hepatoblastoma histology.
Staining of WDHB showing cells with round, centrally placed nuclei. (H&E, 400x). Reprinted by permission from Nature Springer: Modern Pathology. Towards an international pediatric liver tumor consensus classification: proceedings of the Los Angeles COG liver tumors symposium., López-Terrada, D., Alaggio, R., de Dávila, M. *et al.* 2014. https://doi.org/10.1038/modpathol.2013.80 [34].

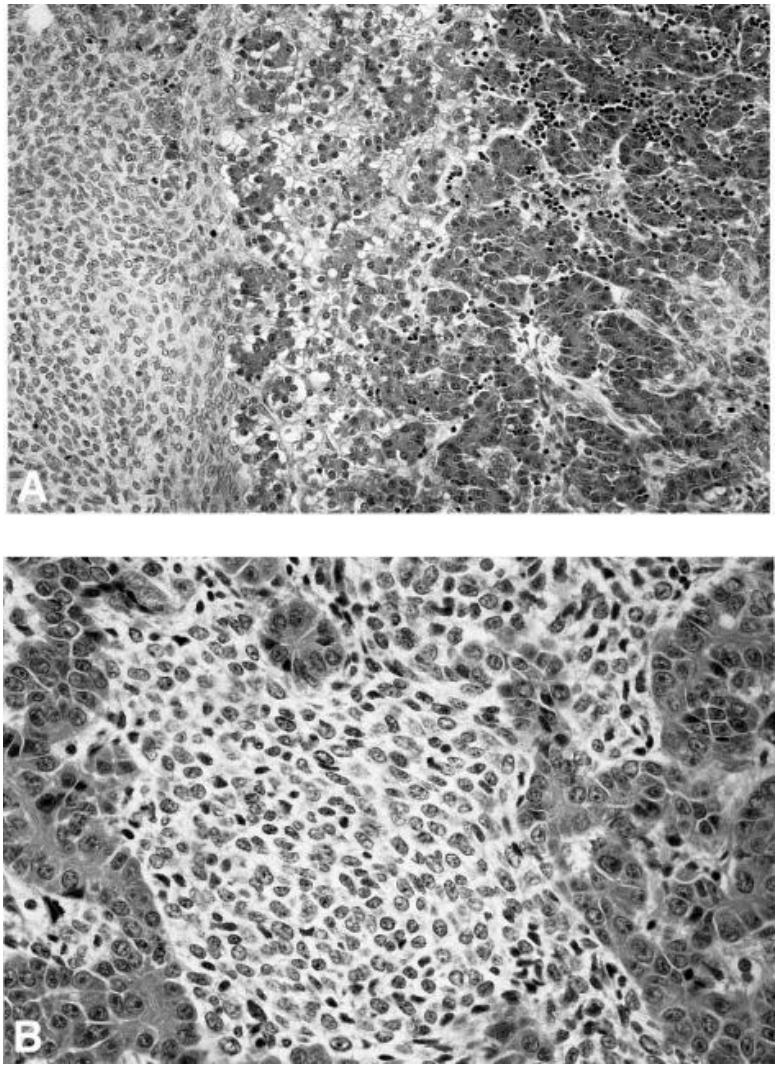

Figure 2-2. Small cell, undifferentiated hepatoblastoma histology.
(A) Small cells forming a sheet on the left are in contrast to the appearance of fetal histology in the center and embryonal histology on the right (H&E, 200x). (B) Small cells intermingling with hepatoblastoma cords exhibiting embryonal histology (H&E, 400x). Reprinted with permission. Haas JE, Feusner JH, Finegold MJ. Small cell undifferentiated histology in hepatoblastoma may be unfavorable. Cancer 2001;92:3130-4http://dx.doi.org/10.1002/1097-0142(20011215)92:12<3130::aid-cncr10115>3.0.co;2-#. [36].

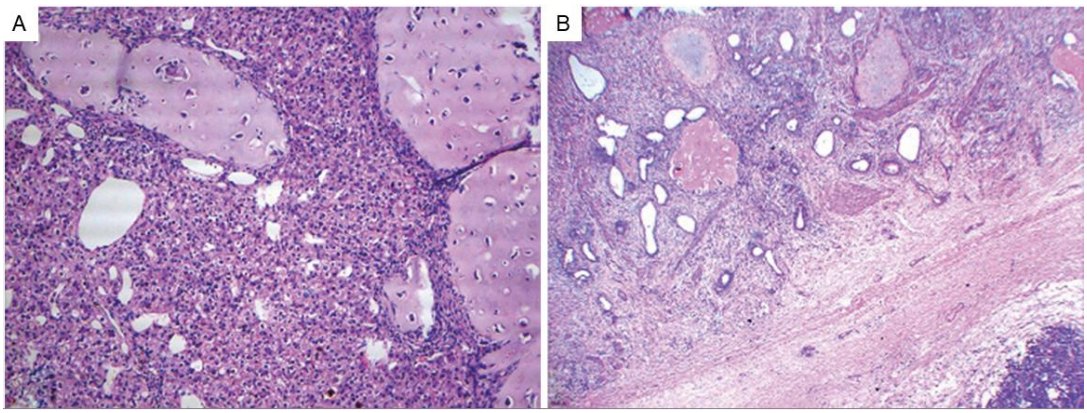

Figure 2-3. Mixed hepatoblastoma histology.
(A.) Mixed hepatoblastoma: Fetal subtype admixed with islands of osteoid (H&E, 100x). (B.) Mixed hepatoblastoma: Epithelial component admixed with cartilage, osteoid, and smooth muscle with immature mesenchyme in the background (H&E, 400x). Reprinted with permission. Kiruthiga KG, Ramakrishna B, Saha S, et al. Histological and immunohistochemical study of hepatoblastoma: correlation with tumour behaviour and survival. J Gastrointest Oncol 2018;9:326-337. http://dx.doi.org/10.21037/jgo.2018.01.08. [37].

"infant HB (age <2, 81 cases)".[44, 45] TERT promotor mutations were highly enriched in tween HB cases.[44] Deletion of the exon 3 region in β-catenin was observed at a higher rate in child HB.[45] One study, looking specifically at germline mutations in HB, found that they occur at a relatively low rate (3.1%) of the 147 patients sampled.[46] APC germline mutations were the most common in 5 of the 9 patients and interestingly, germline mutations of APC were mutually exclusive with somatic β-catenin mutations.[46]

WNT/β-Catenin Pathway

The WNT/β-catenin pathway is complex due to the high number of ligands and receptors involved as well as the variety of intracellular responses it can elicit (**Figure 2-4**).[47] This signaling pathway is highly conserved and plays an important role in key functions including cell proliferation, differentiation, migration, genetic stability, apoptosis, and stem cell renewal.[48] In the canonical pathway, β-catenin is the major intracellular transducer and plays an important role in the entire pathway. The activation of β-catenin is controlled by a complex consisting of APC, AXIN-1, AXIN-2, casein kinase -1α, protein phosphatase 2A, and GSK-3β.[49] As previously mentioned, several of these genes, β-catenin, APC, and GSK-3β all have frequent germline and somatic mutations in HB patients, highlighting the importance of this pathway in HB development.

Notch Signaling Pathway

The Notch signaling pathway plays an important role in normal liver development through its role in maintenance, morphogenesis, and proper development of the biliary tree.[12] There are four different Notch receptors, NOTCH1, NOTCH2, NOTCH3, and NOTCH4 as well as five canonical ligands, Delta-like 1 (DLL1), DLL3, DLL4, Jagged 1 (JAG1), and JAG2. Among these receptor-ligand pairs, NOTCH2-JAG1 seems to be the most important for liver development and has been associated with developmental disorders such as Alagille syndrome.[12] For normal liver development hepatoblasts differentiate into hepatocytes or cholangieocytes. NOTCH2 however, has been shown to delay this maturation process and is overexpressed in 92% of HB.[50] Another member of the Notch signaling pathway, DLK1, which is a marker for bi-potential liver precursor cells (hepatoblasts), has also shown to be elevated in HB[51] suggesting that NOTCH2 is maintaining the hepatoblast population during development resulting in HB.

Treatment and Drug Resistance of Hepatoblastoma

The most common therapy for patients diagnosed with HB is complete surgical resection, but the surgical procedure varies from organization to organization.[52] Tumors that have been defined as very low risk using the PRETEXT system can be recommended for resection without prior chemotherapy.[28] If patients are deemed low-risk, then it is suggested to perform upfront resection followed by adjuvant treatment. For the

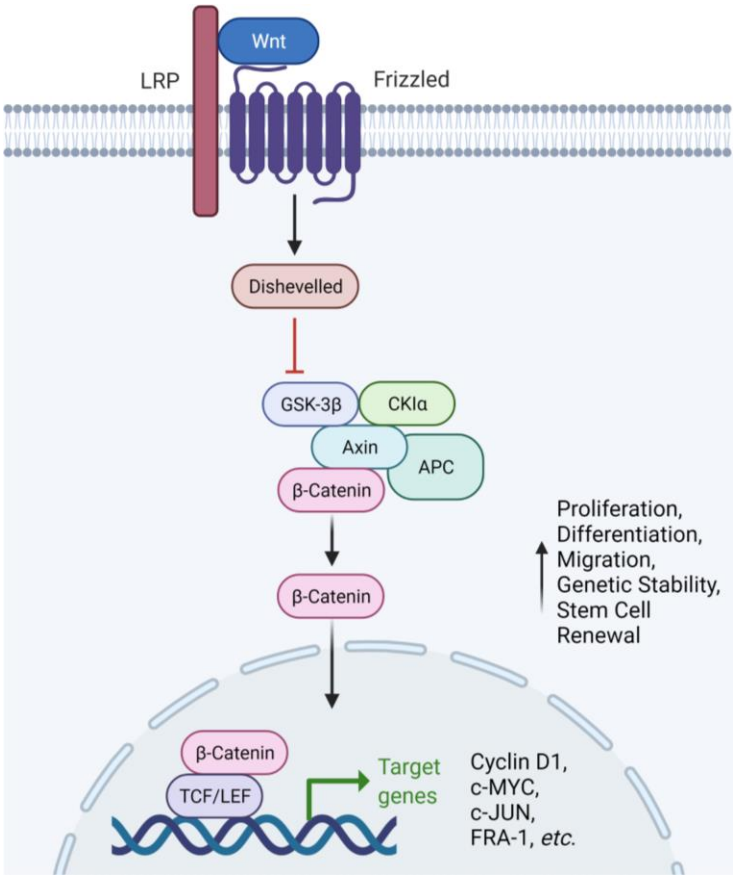

Figure 2-4. Wnt/β-catenin pathway.
Wnt proteins bind to frizzled receptors and the LRP co-receptor which acts to suppress the activity of glycogen synthase kinase-3β (GSK-3β). This prevents phosphorylation of downstream molecules allowing β-catenin association with TCF/LEF transcription factors in the nucleus and upregulation of their target genes. Adapted with permission from "Wnt Beta-Catenin Signaling Pathway", by BioRender.com (2022). Retrieved from https://app.biorender.com/biorender-templates.

intermediate to high-risk groups, they receive neoadjuvant chemotherapy prior to resection, then adjuvant treatment as well.[28] The chemotherapy regiment for HB is either C5V, which is a combination of cisplatin, 5- fluorouracil, and vincristine for low-risk patients, or C5VD, which is similar to C5V with the addition of doxorubicin for higher risk patients.[28] Tumor size and vascular invasion were significant predictors of metastatic disease in univariate analysis; moreover, tumor size at diagnosis and vascular invasion were also significant independent factors.[32] Resection of the tumor should be done prior to long term exposure to chemotherapy due to the risk of drug resistance which has been reported.[28] Patients with tumors that show resistance to chemotherapy or are diagnosed at a very-high risk stage are referred for liver transplantation. While rare, metastasis and relapse do occur in patients at a rate of 20% and 12% respectively.[53, 54] Patients where tumor resection or liver transplantation is possible have a 5 year overall survival rate of ~90%.[55] however, for patients that are unable to have surgery or relapse following treatment the survival rate drops drastically to 35% and 43% respectively.[53, 55]

Hepatocellular Carcinoma

HCC represents the other ~20% of malignant pediatric liver tumors. HCC is usually more clinically challenging compared to HB as tumors present themselves as large, unresectable lesions.[27] HCC is commonly found more in the later years of adolescence and is more frequent in males than females (3:1).[56] HCC in children is usually split into two groups; The first are those associated with metabolic or genetic diseases such as hemochromatosis, hereditary tyrosinemia, progressive familial cholestasis, bile salt export pump disease, multidrug resistance protein 3 defect and tight junction protein 2 deficiency, alpha-1-antitrypsin deficiency, glycogen storage diseases, and less often, biliary atresia and viral hepatitis.[27] The second group arises in patients without chronic liver illness. Fibrolamellar HCC (FL-HCC) is a subtype found more commonly in children and has a greater survival when compared to non-fibrolamellar subtypes (57% vs 28%).[57] Differences in the epidemiology of HCC largely is a result of the prevalence of perinatally acquired HBV infection. In certain areas of the world HCC has been reported as the most common pediatric liver malignancy.[58] In contrast to HB, recent data has shown that the incidence rate of pediatric HCC is declining in some areas[59] or has remained relatively stable over the last 20 years[57] possibly due to the introduction of the hepatitis B vaccine.

HCC Cell of Origin

Due to pediatric HCC accounting for only .4% of all childhood malignances[60], and limited data having been published, the origin of HCC was debated for quite a while. Recent studies have shown that HCC originates from mature hepatocytes not HPC's.[61, 62]

HCC Molecular Subtypes

Pediatric HCC uses the same system as HB for its staging and classification, PRETEXT. These tumors, histologically, are broken down into three main classifications, well differentiated (WD), moderately differentiated (MD), and poorly differentiated (PD) tumors as well as FL-HCC which has some distinct characteristics that don't fit into the other subtypes.

Well Differentiated HCC

WDHCC presents itself as a uniform tumor of hepatocytes arranged in trabeculae at least 3 cells think with frequent bile production. The nodule is usually separated from the surrounding liver by a distinct pseudocapsule. The individual cells have a vacuolated cytoplasm with round nuclei and mild nuclear pleomorphism. Staining of WDHCC shows variable expression of GPC3 and GS with negative β-catenin nuclear staining.[63, 64]

Moderately Differentiated HCC

MDHCC has a larger cell arrangement with trabeculae 15 to 20 cells thick, lined with sinusoids and moderate bile production. The cells themselves have large nuclei with prominent nucleoli as well as an abundance of cytoplasm with eosinophilic cytoplasmic globules. About 50% of MDHCC show positive GPC3 and HS staining. Similar to WDHCC, β-catenin is low to negative with a few tumors showing weak nuclear expression.[27]

Poorly Differentiated HCC

PDHCC contains sheets or nests of small cells that no longer resemble hepatocytes. The nuclear to cytoplasmic ratio is high with a large degree of nuclear pleomorphism. Numerous spots of necrosis and mitosis are noted throughout the tumor. Unlike WD and MD HCC, nuclear expression of β-catenin is strong and diffuse as well as strong GPC3 staining[65]

Fibrolamellar HCC

FL-HCC is a distinct subtype of HCC that has a propensity to arise in younger patients and account for 24 of pediatric HCC cases.[57] FL-HCC is characterized by large abnormally shaped cells with a low nuclear to cytoplasmic ratio and abundant eosinophilic cytoplasm.[60] These tumors show fibrous and lamellar stroma through out and have a central stellate scar.[66] FL-HCC is also characterized by the presence of a DNAJB1-PRKACA chimeric transcript that has been reported in 100% of cases due to 400-kilobase deletion on chromosome 19.[67]

Genetics of Pediatric HCC

Pediatric HCC has been reported to have numerous genetic alterations including gain of chromosomes 1q, 8q, 17q and loss of chromosomes such as 4q. Gene expression profile of HCC patients have found abnormalities in important signaling pathways including TP53, mitogen activated protein kinase, WNT/β-catenin, epidermal growth factor, and transforming growth factor-beta pathways specifically in hepatitis-associated HCC.[27, 42, 68]

Treatment of Hepatocellular Carcinoma

Unfortunately, pediatric HCC usually presents itself as largely chemoresistant. Up till now, surgical resectability is the biggest prognostic predictor upon diagnosis.[69] Other determinants include lymphovascular invasion, extrahepatic disease, and metastatic disease. Children diagnosed with HCC usually present at the more advanced stage with only 20% of the tumors able to be resected upon diagnosis.[70] There have been treatment regimens designed for pediatric HCC with the main one being a combination of cisplatin and doxorubicin (PLADO). A SIOPEL-1 study analyzed the outcome of 37 pediatric HCC patients, who received PLADO treatment prior to surgical resection. A partial response was measured in 49%, while no response or disease progression was observed in the rest. Resection was possible for 17 (46%) of the 37 children with resection being successful in 36%. At a follow up of 75 months, the survival rate of the children was only 28%.[60] For tumors that are not resectable following treatment, the only curative option is liver transplantation similar to HB. There have been some more recent studies on the effect of sorafenib, a multi-kinase inhibitor against Raf and vascular endothelial growth factor receptor, which showed promising therapeutic effects in adults and is currently being examined in children.[71] Due to the limited effective treatments for pediatric HCC, only 20% to 30% of HCC patients respond to therapy, highlighting the need for more effective treatments of pediatric liver malignancies.[72]

Ribonucleotide Reductase

Ribonucleotide reductase (RNR) is a heterodimeric tetramer that is responsible for the generation of deoxyribonucleotides from ribonucleotides for DNA synthesis and repair.[73] RNR consists of two ribonucleotide reductase M1 (RRM1) subunits and two Ribonucleotide reductase M2 (RRM2) or M2B (RRM2B) subunits.[74] In cellular organisms, RNRs synthesize the four deoxyribonucleoside triphosphates (dNTPs) required for DNA replication and repair by removal of the 2'-OH of a ribonucleoside di- or triphosphate molecule via a stable tyrosyl radical.[73] This catalytic activity requires oxygen to produce the tyrosyl radical by a non-heme Fe-O-Fe center in the smaller RRM2 subunit.[74] As the driver for maintaining the homeostatic levels of all four of the dNTPs, RNR is also highly important in cancer development. Uncontrolled proliferation, which is a defining feature of cancer, must be supported by a balanced supply of dNTP.[16] If dNTPs levels are insufficient or even elevated, this will cause replication stress and

further promote genomic instability and increased mutagenesis.[75, 76] Enhanced mutagenesis via imbalanced dNTP levels occurs mainly by two mechanisms, DNA misinsertion and impaired proofreading.[76, 77] Excess levels of dNTPs can lead to competition between different nucleotides for pairing to the template base which will result in misincorporation. DNA polymerase proofreading is also reduced in the presence of excess dNTP levels through a phenomenon known as next-nucleotide effect. This results from the chain extension occurring before the mismatched nucleotide can be removed.[78]

Ribonucleotide Reductase Subunits

RRM1 Regulation and Expression

RRM1 is the large subunit of the ribonucleotide reductase (RNR) complex and has been shown to act as the scaffold. It contains part of the substrate binding site as well as binding sites for allosteric regulators.[79] In non-proliferating or quiescent cells RRM1 levels cannot be detected whereas in proliferating cells RRM1 protein shows a consistent level throughout the cell cycle.[80, 81] Interestingly, RRM1 mRNA levels vary during the cell cycle with minimal levels being expressed during G_0/G_1 and maximal levels being reached during S phase.[82]

RRM1 in Cancer

Even though RRM1 acts as the scaffold for the RNR complex, many studies have been done both preclinically and clinically that suggest it plays a more important role in cancer. Studies have shown that RRM1 is involved in the suppression of cell migration and metastases.[79] Some preclinical data has shown its overexpression in Ras-transformed fibroblasts limited tumor development and metastasis suggesting that RRM1 is a tumor suppressor.[83] In addition, overexpressing RRM1 using an adenovirus in lung carcinomas had a protective effect and increased the transgenic mice survival.[84] Conversely, other studies have shown that inhibiting RRM1 through shRNA significantly inhibits the cell's ability to replicate.[85]

RRM1 has been shown to be associated with gemcitabine resistance when lung cancer cell lines are incubated with the drug. Investigators noticed an increase in RRM1 mRNA and protein in a dose dependent manner with gemcitabine incubation in the culture media.[86] Gemcitabine resistance in RRM1 overexpressing cells has also been evaluated in NCI-H23 non-small cell lung cancer (NSCLC) cells which showed a three-fold increase in RRM1 expression and a twelve-fold increase in the 50% inhibitory concentration (IC_{50}) when compared to the control cells.[87] The role of RRM1 in gemcitabine resistance has also been verified with the reversion of RRM1 expression. Using siRNA to inhibit RRM1 in gemcitabine resistant MIA PACa-2 pancreatic cancer cells showed an increase in gemcitabine sensitivity similar to the parental cells.[88]

Increased sensitivity to gemcitabine has also been reported in other cancers infected with RRM1 siRNA including lung, biliary tract, and pancreatic.[87, 89-91] Clinically RRM1 has been associated with gemcitabine resistance as well. One study in NSCLC performed a randomized trial including 100 patients with advanced stage disease, comparing gemcitabine and cisplatin versus gemcitabine, cisplatin, and vinorelbine versus gemcitabine and vinorelbine followed by vinorelbine and ifosamide. In the group with 20 patients treated with gemcitabine and cisplatin there was a significant increase in overall survival (13.7 months vs 3.6 months) and progression-free survival (8.4 months vs 2.7 months) in patients with low RRM1 mRNA expression compared to those with high RRM1 expression.[92] Another study showed that patients with high RRM1 expression had significantly poorer clinical outcomes and was also associated with poorer overall survival on adjuvant chemotherapy in pancreatic cancer.[93] All this together shows that RRM1 is important in cancer progression and resistance to chemotherapy treatment.

RRM2 Regulation and Expression

RRM2 acts as the rate limiting step for the catalytic formation of deoxyribonucleotides as its expression level is tightly regulated by cell cycle.[73] RRM2 is both regulated at the transcriptional level as well as at the protein level by enzymatic degradation. Several transcription factor binding sites have been identified in the RRM2 promotor including one for E2F4, which represses RRM2 expression during G_1 and one for E2F that regulates enzymes involved in DNA replication.[94, 95] At amino acids 30-32, RRM2 contains a KEN box, which binds to Cdh1-anaphase-promoting complex that forms during mitosis which leads to ubiquitination and subsequent degradation via the proteosome.[76, 96, 97] RRM2 amplification has been reported in studies that looked at hydroxyurea resistance in human cells lines.[98] Human RRM2 gene amplification from a homogenous staining chromosome region always accompanied altered transcriptional regulation. Cell line clones that were resistant to either gemcitabine or hydroxyurea showed a unique binding pattern of several transcription factors including activator protein 1 (AP-1), Sp1, cyclic AMP (cAMP)-response element binding protein (CREB), and nuclear factor kappa-β (NF-κβ).[99] DNA damage which activates checkpoint kinase 1 (Chk1) can upregulate RRM2 expression through the E2F1 transcription factor.[100] Upregulation of nuclear factor Y (NF-Y) which is induced by the inhibition of histone deacetylases (HDAC) or activation of the HIF-1α/STAT3 signaling pathway have both been shown to increase RRM2 transcription and contributes to gemcitabine resistance.[101, 102] More recently there have been several studies that have shown the importance of long non-coding RNA (lncRNA)/microRNA (miRNA) in the role of RRM2 regulation.[103-105]

RRM2 in Cancer

Both RRM1 and RRM2 work together to perform the enzymatic function of RNR and other physiological functions, and as previously mentioned, RRM1 upregulation has been shown to confer resistance to gemcitabine. Although gemcitabine specifically targets RRM1, both overexpression of RRM1 and RRM2 was found to establish

gemcitabine resistance in pancreatic cell lines.[106] This suggests that these two subunits play a role together in catalysis and regulation of drug resistance. However, RRM2 is increased during late G_1 and early S phase of the cell cycle while RRM1 levels remain relatively constant.[80] Due to its more complex and varible regulation mechanisms compared to RRM1, RRM2 maybe even more important in the occurrence of chemoresistance. Studies have found that in chemoresistance samples, both mRNA and protein levels of RRM2 were elevated. Microarray data of Doxorubicin (DOX) resistant breast cancer lines showed high expression of RRM2.[107] Peripheral blood samples from imatinib-resistant patients showed increased RRM2 mRNA levels.[108] Another patient microarray dataset showed RRM2 overexpression in tamoxifen-resistant patients and was correlated with resistant cell lines and xenograft tumors and was also found to be significantly associated with early tumor recurrence in patients.[109] RRM2 upregulation has been reported to induce chemoresistance to cisplatin and fluorouracil (5-FU) through activation of the epidermal growth factor receptor (EGFR)/AKT proliferative pathway.[103] Not only is RRM2 important for chemoresistance it is also highly associated with disease progression and proliferation. In rat hepatoma cells a 200-fold difference in RNR activity was observed between the fast growing and slow growing cells.[110] Because RRM2 is highly associated with cell proliferation, its expression has been surveyed using the ONCOMINE database. RRM2 was reported among the top 10% of most overexpressing genes in 73 out of the 168 cancer types.[16] During DNA damage in TP53+ cells RRM2 is degraded and an isoform RRM2B is upregulated in response.[111, 112] However, in TP53- cells RRM2 is overexpressed in response to DNA damage to help provide nucleotides for DNA repair and recovery from replication stress (**Table 2-1**).[112, 113] RRM2 is an important mediator of cancer progression and chemoresistance, especially to DNA targeting agents.

RRM2B Regulation and Expression

RRM2B, although encoded by an independent gene, is an isoform of RRM2 sharing roughly 80% homology with it.[114] RRM2B, in contrast to its isoform RRM2, lacks a KEN box motif at the N-terminus and is continuously expressed throughout the cell cycle at low levels.[111] RRM2B is believed to play an essential role in DNA repair, mitochondrial DNA (mtDNA) synthesis, and stress response.[115] The regulation of RRM2B expression demonstrates the cells' ability to adapt and their tendency to survive. In early G_1-phase, cell exposure to stressors such as DNA damage or hypoxia, drives the expression of RRM2B via the transcription factor TP53.[116] Progressing though the cell cycle after stress to the cell, RRM2B expression increases and reaches its highest level in the G_1/S transition. At the same time RRM2B is bound to RRM1 to provide nucleotides for DNA synthesis and repair.[73] Interestingly, even though RRM2B is regulated by TP53, TP53 contains homozygous mutations in 50-60% of human cancers.[117] Furthermore, there are tumors with high expression of RRM2B with TP53 deficiencies and continues to influence mitochondrial function, implicating that mitochondrial homeostasis, with respect to RRM2B, is independent of TP53 function.[118] There have been some studies showing that RRM2B is also transcriptionally regulated via P73, a TP53 family member.[119] Other studies have shown binding of the tumor suppressor FOXO3 to the

Table 2-1. Comparison between RRM2 and RRM2B subunits.

Characteristic	RRM2	RRM2B
Contains Radical Tyrosine Residue	Yes	Yes
Contains Non-Heme Iron Group	Yes	Yes
Forms Complex with RRM1	Yes	Yes
Cell Cycle Regulated	Yes	No
Generates dNDPs for DNA Synthesis	Yes	No
Generates dNDPs for DNA Repair	Yes, in $p53^-$ cells	Yes, in $p53^+$ cells
Generates Mitochondrial DNA (mtDNA)	No	Yes
Induced in Response to Cell Stress	No	Yes
Inhibitors	Yes	No

RRM2B promotor activating transcription.[120]

RRM2B in Cancer

The deregulation of RRM2B expression has been reported in numerous cancer types including gastric, prostate, and colon.[121-123] As mentioned previously, RRM2Bs' role in providing dNTPs for DNA repair and synthesis is exploited by cancer cells. Alongside its catalytic role, RRM2Bs' upregulation of P21 also further progresses cancer due to P21 acting as a carcinogen and anti-apoptotic agent. In Akt overexpressing cancers RRM2B may play a tumorigenic role and promote drug resistance.[124] In TP53+ cells, RRM2B is induced after DNA damage takes place. Paradoxically, DNA damage is believed to take place within a few hours of the damage occurring, however RRM2B induction takes longer.[125] Even though they perform similar enzymatic functions, little is known about RRM2B compared to RRM2.

Drug Resistance in Cancer

Resistance to cancer therapy, especially in the case of pediatric cancers, regarding chemotherapies and radiation therapy has been studied for many decades. Unfortunately, as novel chemotherapeutics have been discovered and tested, such as tyrosine kinase inhibitors, monoclonal antibodies, and immune-oncology approaches have resulted in new more drug resistance mechanisms. These mechanisms for drug resistance can include molecular changes at the intracellular, transcellular, and intercellular levels as well as effects on genetics, epigenetics, transcriptional and translational activity in the cells. I will cover some such mechanisms below.

Drug Resistance Through Metabolism

In contrast to adult cancers, particularly carcinomas that harbor more gene mutations and activated oncogenes, pediatric cancers are genetically "quiet".[126] However, there are genetic mutations that do occur that specifically affect drug resistance. Cytochrome P450 (CYP) proteins are involved in drug metabolism for numerous chemotherapeutic agents that work on agents called prodrugs that must be metabolized before they begin to take effect. One such mechanism of resistance is genetic variations in these CYP proteins that can cause hypometabolism of these agents and diminish their efficacy.[127-129] These single nucleotide polymorphisms (SNPs) can also increase CYP protein activity therefore increasing drug metabolism.[127] Other involved proteins include glutathione s-transferases (GSTs), thiopurine methyltransferase (TPMT), methylenetetrahydrofolate reductase, and UDP glucuronosyltransferase 1 family member, polypeptide A1. Variations in these proteins have been shown to affect drug metabolism in many cancers including osteosarcoma,[130, 131] medulloblastoma,[132] neuroblastoma,[133] acute lymphoblastic leukemia (ALL),[134] and HB.[135]

Drug Efflux or Influx

A major class of proteins that control cellular influx and efflux of molecules are ATP binding cassette (ABC) proteins. These proteins act as pumps by directly binding to ATP and using direct energy conversion to expel molecules in or out of the cell. One of the ABC proteins, multidrug resistance protein 1 (MDR1) has been shown to be overexpressed in pediatric solid tumors and leukemias and is correlated with drug resistance and poor survival.[136, 137] Other ABC family members such as MRP1, MRP2, and ABCB1 have also been implicated in pediatric cancer drug resistance.[138, 139] MRP2 has been shown to be highly expressed in HB tumors and its expression shows a reverse correlation with cisplatin resistance, the most common drug used in the treatment for HB.[140] These proteins can be overexpressed in tumors usually through another oncogenic pathway such as MYCN amplification in neuroblastoma,[141] or MDK expression in ALL.[142] ABC proteins can also have germline or somatic mutations that increase their enzymatic activity, which decreases drug exposure to the cells and increases resistance.[143, 144]

Absorption of chemotherapeutic agents into the cell is equally as important. Some cytotoxic agents are only able to enter the cell via direction of high concentration gradients that occur only through active transport and change in expression or activity of these transports can cause drug resistance.[145] One such mechanism is in the case of methotrexate resistance which is usually caused by a gene mutation in human folate carrier (hRFC) in ALL patients. This mutation in the transporter reduces the tendency of the drug to bind to the protein.[146]

Manipulation of DNA Damage Response

One of the hallmarks of cancer is its uncontrolled proliferation, therefore, many chemotherapies are designed to target DNA synthesis which is important for replication. Targeting DNA synthesis leads to activation of TP53, CHEK1, CHEK2, and other DNA response pathways. TP53, which acts as a tumor suppressor and controls many pathways in the cell in response to stress as well as DNA damage repair pathways is commonly mutated in more than 5% of all pediatric cancers.[126] Silencing of this protein, either by somatic mutations or epigenetic regulation has been associated with increased rates of relapse as well as worse prognosis upon diagnosis.[147, 148] Another method for suppression of TP53 is by increased activity of its regulators such as MYCN and MYC either by amplification, translocation or epigenetic-driven overexpression. MYC amplification has also been shown to be associated with RRM2B amplification due to its close proximity on chromosome 8. Amplification of RRM2B is correlated with worse prognosis in some cancers including breast.[149] MYC promotes MDM2 activation which ubiquitinates TP53 leading to its degradation. Other components of DNA repair pathways have also been shown to have mutations in some pediatric cancers such as ATM, ATR, PTEN, and CHEK1, and are associated with a worse prognosis.[150-152]

Suppression of Apoptosis

Apoptosis is the controlled death of the cell which is normal to an organism's growth and development. Apoptosis can be induced by a number of different mechanisms, one of which is through the activation of TP53 following DNA damage. TP53 promotes the expression of numerous pro-apoptotic genes including BCL2 family members, NOXA, and PUMA. These proteins translocate to the mitochondria where they bind to other BCL2 family members and release pro-apoptotic proteins BID, BIM, BAK, and BAX which cause the release of cytochrome C and the activation of caspase cleavage which leads to apoptosis. Alteration of this pathway via changes in BCL2 family member proteins is common in childhood cancers. The overexpression of anti-apoptotic BCL2, BCL2L1, and MCL2 driven by increased signal transduction[153], alternative splicing[154], or epigenetic dysregulation[155], leads to sequestering of their pro-apoptotic counterpart and a decrease in apoptosis. As mentioned previously, mutations in TP53 are quite common and these mutations can lead to an impaired binding to DNA and a decrease in the expression of pro-apoptotic BCL2 family members upon DNA damage.

Treatment-induced Resistance

Cancer cells are also able to respond to chemotherapy treatments which adds another layer of complexity to their treatment. Targeted therapies, using small molecule inhibitors or monoclonal antibodies have been designed over the last 20 years and have proved to be less toxic than conventional chemotherapy that targets all proliferating cells. However, since the introduction of these drugs, unique drug resistance mechanisms have developed in response. One such example is the use of mTOR inhibitors like sirolimus, everolimus, and temsirolimus which target the mTOR/PI3K/AKT pathway that is over activated in numerous cancers.[156-159] Even though these drugs showed some benefits specifically in combination therapy, tumors were found to develop a gain of function point mutation in mTOR which made it unresponsive to first- and second-generation inhibitors[160]. Other tumors were found to have overcome mTOR inhibition by upregulating other members of the AKT pathway like MYC[161] or IDO1.[162] Another instance of this is treatment induced resistance is with the fusion protein BCR-ABL. The use of imatinib for the treatment of BCR-ABL fusion-positive chronic myelogenous leukemia made significant improvements for the overall survival of this disease.[163] However, tumors treated with imatinib have developed resistance in some cases by selecting a population of cells that are unresponsive to the original drug.[164, 165] The use of monoclonal antibodies has been quite advantageous in the treatment of pediatric tumors.[166, 167] One mechanism of resistance to drugs is loss of expression of the target antigen such as CD20 or CD30 in lymphomas.[168, 169] In the case of some drugs, tumors have also been shown to upregulate ABC proteins in response to treatment which results in higher expression during therapy or if there is recurrence of the tumor and leads to increased drug efflux out of the cell.[170] Finally, in the case of HB, treatment with cisplatin has been shown to cause mutations in tumors treated prior to resection due the adducts generated on the DNA.[171, 172] These mutations appeared in drug resistance and relapsed cases and were commonly in genes associated with inhibition of apoptosis (*BIRC5*),

DNA repair (*BRCA1*, *RAD54L*, and *EXO1*), or other genes associated with cancer (BRAF and NOTCH1).[172] All this together shows that there are many unique ways for cancer cells to develop chemotherapeutic resistance and more research needs to be done on resistance mechanisms.

Cancer Cell Plasticity

A unique characteristic of cancer cells is their plasticity, the ability to shift between a differentiated state with limited tumorigenic potential and an undifferentiated state or cancer stem cell like state, which is responsible for tumor growth.[170] One of the aspects of this cell plasticity is epithelial-mesenchymal transition (EMT) which transitions differentiated epithelial cells into a more mobile ECM-secreting mesenchymal cell. EMT has also been associated with chemotherapy resistance in tumors as well, for example, EMT related genes are highly expressed in breast cancer and have been associated with resistance to EGFR and PI3K inhibitors in NSCLC.[173, 174] The HB cell line HepG2 has been reported to have high expression of the transcription factor TWIST which is known to induce EMT. Inhibition of the TWIST protein was able to sensitize cells to cisplatin treatment.[175]

Targeting RNR

Due to RNRs' essential role in DNA synthesis and cell replication it has been a target for chemotherapy for some time. There are two current methods for targeting RNR. The first is targeting RRM1 using nucleoside analogs because it contains the allosteric binding sites as well as forms half of the binding pocket with RRM2. The second is using redox active metal chelators that specifically target the non-heme iron group in RRM2 that is essential for its catalytic function mentioned above. Some siRNA inhibitors have been developed for RRM2 and RRM2B but need further clinical validation to determine their efficacy.

RRM1 Inhibitors

One of the first nucleoside analogs to be developed and approved for clinical use was gemcitabine which is still used as a frontline therapy for several tumors.[176] Gemcitabine's active form (F_2CDP) forms an irreversible covalent bond between RRM1 and the sugar of F_2CDP.[177] Interestingly F_2CDP cannot fully inactivate its target unless RRM1 binds to RRM2 or RRM2B to form the holocomplex. Only the complex forms the site to which F_2CDP binds (**Figure 2-5**).

Another group of clinically successful nucleoside prodrugs are clofarabine, cytarabine, nelarabine, azacytidine, decitabine, cladribine, and fludarabine. These nucleoside prodrugs are used to treat hematological malignancies[178] and although the metabolites for these compounds are believed to target RRM1, this process has only been

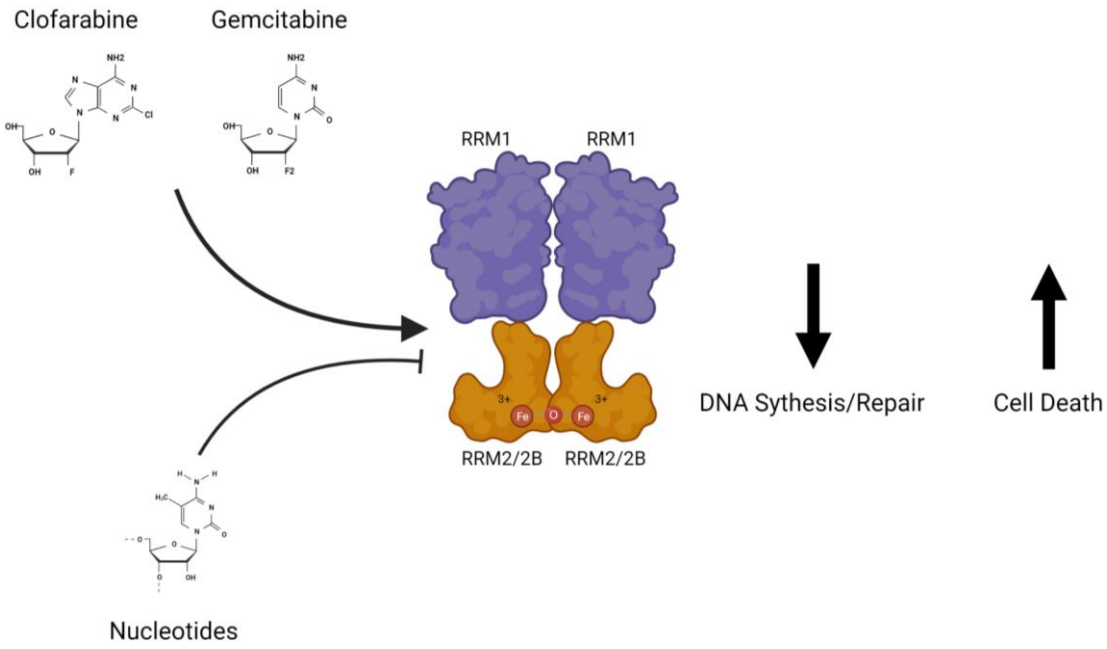

Figure 2-5. Schematic representation of RRM1 inhibition.
Nucleoside analogs clorfarabine and gemcitabine bind to RRM1 in the enzymatic pocket, preventing other nucleotides from being generated for DNA synthesis and repair. Created with BioRender.com.

elucidated for clofarabine.[179] Tri-phosphorylated clofarabine (ClFTP) is the most abundant metabolite of clofarabine and it was originally thought to be the only metabolite that inhibited RRM1, binding in a similar way as dATP.[178] However, after further investigation it was discovered that the dephosphorylated metabolite also inhibits RRM1. CIFTP binds reversibly to RRM1 and initial treatment shows almost complete inhibitions of the enzyme activity but after prolonged exposure the RNR activity recovers to about 50%. The diphosphate form binds to the same location as F_2CDP mentioned previously, however it does not covalently bind and can be reversed.[179] Even though nucleoside analogs have been successful in the treatment of cancer, they have their drawbacks as well. They are prodrugs that are dependent on other enzymes to gain activity.[178] Furthermore, only specific metabolites have inhibitory effects, and a steady state equilibrium may prevail that diminishes the inhibitory effect of the drug or possibly increases its toxcity.[180]

RRM2 Inhibitors

RRM2 has been targeted more by chemotherapy than RRM1 since it is more cell cycle regulated and has significantly higher expression during the G_1/S phase in replicating cells. Most RRM2 inhibitors attempt to target the non-heme iron tyrosine radical essential for its function using radical scavengers or iron chelators.[181] Hydroxyurea (**Figure 2-6A**), which has been used for a long time in the treatment of cancer, specifically in leukemia[182, 183] does both. Hydroxyurea is not specific to RRM2 however, it does interfere and bind with other metalloenzymes such as carbonic anhydrase or matrix metalloproteinases.[184] The structure of hydroxyurea has been used to derive other RRM2 inhibitors such as didox which has been shown to be effective in resistant renal cell carcinoma[105] and help prevent tamoxifen resistance in breast cancer.[185]

Another RRM2 specific inhibitor is triapine (**Figure 2-6A**) which has been used in clinical trials for solid tumors such as head and neck squamous cell carcinoma.[186] Triapine is a thiosemicarbazone that even shows some efficacy against tumors that are resistant to hydroxyurea[187]. The initial mechanism of action for triapine was thought to inhibit RRM2 through iron chelation at its active site.[188] However, the mechanism was later thought to be incorrect when a metal bound form of triapine (Fe(II)-(3AP)), was able to generate reactive oxygen species (ROS) that inhibited RRM2 under aerobic conditions.[189] Recent studies have shown that the Fe(II)-(3AP) form of triapine is the active form and inhibits RRM2 at a faster rate via the production of ROS rather than by iron chelation.[190]

In 2013 a new compound called COH29 (**Figure 2-6B**) was developed to target a novel binding site on RRM2 near the C-terminal tail. Initial studies with this compound showed that it was blocking the assembly of RRM1 and RRM2 holocomplex and it was able to overcome hydroxyurea and gemcitabine resistance in some tumor cells.[191] It is still a relatively novel compound so more studies into its mechanism of action are needed.

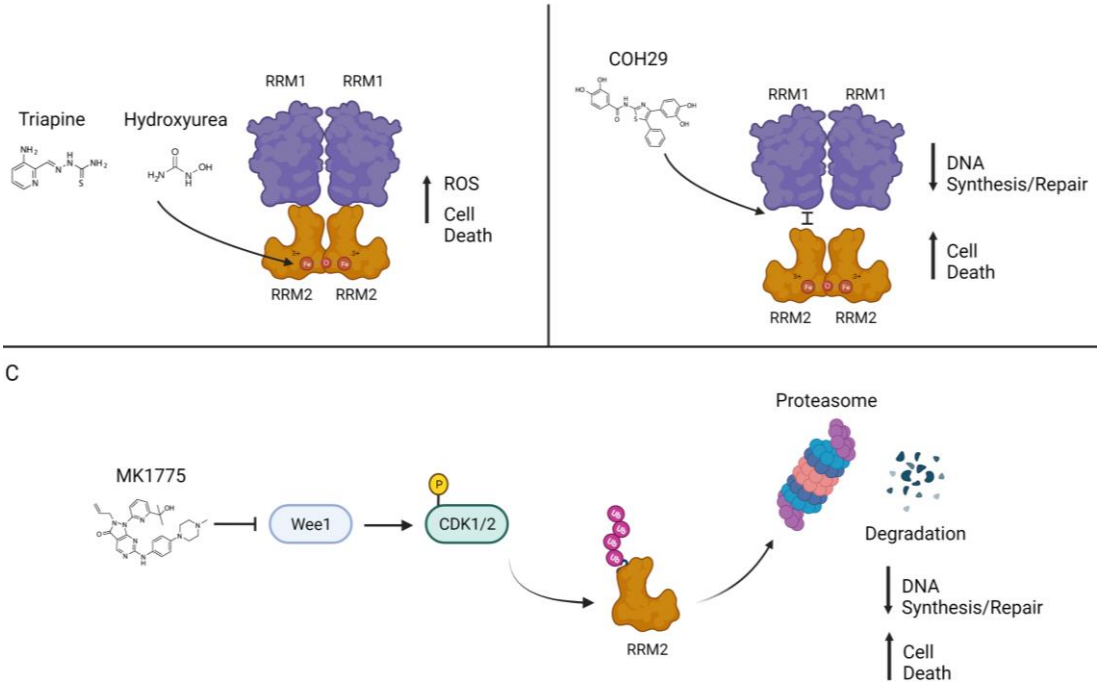

Figure 2-6. Schematic representation of RRM2 inhibition.
(A) Iron chelators triapine and hydroxyurea targeting the non-heme iron group of RRM2. (B) COH29 binds to RRM2 preventing the RNR complex formation. (C) MK1775 inhibits Wee1 leading to increased activation of CDK1/2. This leads to RRM2 ubiquitination and degradation via the proteasome. Created with BioRender.com.

Besides targeting RRM2 directly, another method of RRM2 inhibition is by targeting upstream regulators. One such drug, MK1775 (**Figure 2-6C**), works in this manner. MK1775 is a Wee1 inhibitor and effects RRM2 regulation. Inhibition of Wee1 leads to activation of the cyclin dependent kinase (CDK2) which targets RRM2 for ubiquitination and subsequent degradation via the proteosome. MK1775 has shown promising tumor inhibition in combination with other small molecule inhibitors in some cancers such as Ewing sarcoma.[192]

RRM2B Inhibitors

Due to RRM2B's low level of expression in cells no specific inhibitors have been developed for it. However, as mentioned before RRM2B shares 80% homology with RRM2 and the iron contents of RRM2B and RRM2 were found to be almost identical.[114] Iron chelators that were known to target RRM2 were also tested against RRM2B to see if they could inhibit activity. One drug, Deferoxamine (DFO) showed a 158-fold inhibition of RRM2B over RRM2, however this was the only compound found to be effective.[114] As previously mentioned, RRM2B is crucial for cell survival, so specific RRM2B inhibitors are needed.

CHAPTER 3. METHODOLOGY

Mice

Animal protocols were approved by the St. Jude Animal Care and Use Committee. All mice were maintained in the Animal Resource Center at St. Jude Children's Research Hospital (St. Jude). RRM2- and RRM2B- manipulated HepG2 cells were surgically injected into the liver of two-month-old NSG (NOD scid gamma) mice (JAX) at 5×10^4/mouse in 2 ml cold growth factor-reduced (GFR) matrigel (Corning, Corning, New York) using a 5-ml Hamilton syringe and a 27-gauge needle (Hamilton Company, Bonaduz, Switzerland). Animal survival curves and their median survival were determined by the Kaplan–Meier method in GraphPad Prism 7 and significance between median survival was determined using unpaired two-tailed students t test.

Liver Cell Isolation

Liver tissues were rinsed with ice cold PBS and minced (0.5-1mm^3), then incubated with Papain digestion solution (10U/ml Papain [Worthington]; 1mM NAC [Sigma], 12μg/ml DNase I [Sigma] in Advanced DMEM/F12 [Gibco]) for 20–60 min at 37°C with regular shaking and pipetting. Digestion was terminated after obtaining a homogenous cell suspension by adding cold Advance DMEM/F12. The suspension was then filtered through a 70 μm cell strainer (Corning) and centrifuged at 400×g for 5 min. The pellet was washed twice with cold Advance DMEM/F12, followed by centrifugation at 400×g for 5 min.

Mouse Liver Stem Cells Culture

Cells isolated from mouse liver tissues were resuspended in liver stem cell culture medium. Advanced DMEM/F12 (Gibco) supplemented with 2% B27, 1% N2 (both from (Gibco), 10% Pen-Strep, and 10% L-Glutamine was used as basic medium, and mixed with 50% Wnt3A conditioned media (ATCC, CRL-2647™) supplemented with 1.25mM N-Acetylcysteine (Sigma), 10nM Gastrin (Sigma), and growth factors, including 50ng/ml EGF (Peprotech), 1μg/ml R-spondin1, 100ng/ml Noggin, 100ng/ml FGF-10, 50ng/ml HGF (all from R&D), and 10mM Nicotinamide (Sigma). Cells were then seeded in 60mm culture plates (Corning) coated with growth factor-reduced Matrigel (Corning). Cells formed liver spheroids after 3 days in culture. To passage, liver spheroids were lifted from Matrigel using dispase (Corning), collected using a 40μm cell strainer (Corning), and dissociated into single cells using accutase (Gibco). Passaging was performed at a 1:3 ratio once every 5–7 days.

Ultrasound-guided Intrahepatic Cell Injection

Mice were anesthetized with 2–3% isoflurane/O2, positioned ventrally, and secured on the heated platform. Warmed Aquasonic 100 (Parker Laboratories) coupling gel was applied to the surface of the abdominal skin, and the right liver lobe was imaged using a VEVO-770 High Resolution Ultrasound system (FujiFilm VisualSonics). A 22G catheter (BD) was inserted gently through the skin perpendicular to the incident plane of the transducer into the ultrasound field of view. The catheter needle was then removed to leave the plastic housing for injection. 10 µl of cell suspension was drawn using a pre-cooled 25µl Hamilton syringe with a 27G needle. The needle was then placed in the injector housing and guided into the right liver lobe within the US field of view using stereotactic controls. Cells were injected and the needle was retained in situ for 1 min to allow the implant to solidify. The needle was then slowly removed, followed by the gentle removal of the catheter. The animal was then removed from the bed and monitored until recovery.

PDX Establishment and In Vivo Studies

PDX were established and efficacy studies were performed as described previously.[193, 194] The in vivo studies were performed at XenTech. Fragments from HB-214 PDX were engrafted in the interscapular region of 6–12-week-old female athymic nude mice (Athymic NudeFoxn1nu, ENVIGO, Gannat, France). After latency period, mice bearing tumor between 62 and 256 mm3 were randomly assigned to each treatment arm according to their tumor volume to obtain homogenous mean and median tumor volume in each arm. The control group was not treated during all the course of the experiment. Irinotecan HCl trihydrate (MedChem, Monmouth Junction, New Jersey) (dissolved in 99% NaCl 0.9%; 2.5mg/kg) was administrated intraperitoneally daily for five consecutive days per week for three weeks or first for three consecutive days then one day off followed by five consecutive days per week for two weeks. MK-1775 (MedChem) (dissolved in 0.5% Methylcellulose; 60mg/kg) was administrated orally three time per week for three or four weeks. Treatments were stopped prematurely if toxicity was observed. Tumor volumes were measured two to three time per week depending on the tumor growth. Tumors diameters (length and width) are measured with a caliper (digimatic Solaire, IP67) and tumor volume (TV) is calculated using the formula TV (mm3) = [length (mm) x width (mm)2]/2, where the length and the width are the longest and the shortest diameters of the tumor measured perpendicularly, respectively. All animals were weighed at tumor measurement time and were observed every day for physical, behavior, and clinical signs.

Immunohistochemistry

Liver and tumor tissues were fixed in neutral buffered formalin for one day at room temperature and submitted to HistoWiz Inc. (Brooklyn, NY) for paraffin processing and embedding. Paraffin sections were cut at 4 µm and analyzed using

direct fluorescence microscopy, H&E staining, IHC, and RNAscope.[195]. IHC protocol is as follows, using a Tissue-Tek II slide staining set, slides were immersed in Xylene (Fisher Scientific, X3S-4) for 5 mins, Xylene for 5 mins, 100% ethanol for 5 mins, 95% ethanol for 5 mins, 70% ethanol for 5 mins, and finally 50% ethanol for 5 mins. Slides were then steamed in a Classis Prestige Medical autoclave containing IHC antigen retrieval solution (Invitrogen, 00-4955-58). After slides are allowed to cool to room temp overnight, slides are immersed in water for 5 mins x 2, 1% PBS with 0.1% Triton X100 (Sigma Aldrich, 93443-100ml) for 5 mins, 3% hydrogen peroxide (Honeywell Fluka, Seelze, Germany) for 5 mins, water for 5 mins x 2, and finally in 1% PBS with 0.1% Triton x100 for 5 mins. Antibodies were stained using M.O.M. kit (Vector Laboratories Inc, BMK-2202) and Vectastain Elite ABC HRP kit (Vector Laboratories Inc, PK-6100). Antibodies used included anti-Ki67 (Abcam, Cambridge, MA, USA, ab16667, 1:200). Slides are washed in 1% PBS with 0.1% Triton X100 for 5 mins x 2. and stained with hematoxylin for 5-45 seconds (Vector Labratories Inc, H3404). Slides are then washed with water for 5 mins x 2 and mounting is done using 50% ethanol for 5 mins, 70% ethanol for 5 mins, 95% ethanol for 5 mins, 100% ethanol for 5 mins, xylene for 5 mins, and finally a second xylene for 5 mins. Slides are then mounted with Permount (Fisher Scientific, SP15-100).

RNAscope Staining

RNAscope in situ hybridization of RRM2 and RRM2B mRNA transcripts was performed according to the manufacturer's protocol (Advanced Cell Diagnostics, Hayward, CA, USA).

Immunoblotting Assay

Cells were lysed using radio-immunoprecipitation assay (RIPA) buffer (Thermo Fisher Scientific, Waltham, MA, Cat #89900) supplemented with protease and phosphatase inhibitors (Thermo Fisher Scientific, #78440) and 0.5M Ethylenediaminetetraacetic acid (EDTA) (#78440, Thermo Fisher Scientific). Lysates were centrifuged at 14,000 rpm for 15 minutes at 4°C. Protein concentrations were determined using Pierce™ BCA Protein Assay Kit reagent (Thermo Fisher Scientific, #23227). 15µg of protein were loaded and separated by electrophoresis on NuPAGE™ 4 to 12% Bis-Tris, 1.0, Protein gel (Invitrogen, Waltham, MA). Antibodies were used according to the manufacturers recommended conditions anti-p53R2 + RRM2 antibody (abcam, Cambridge, United Kingdom, ab209995, 1:10000), anti-RRM2 antibody (abcam, ab172476, 1:5000). Molecular weight marker EZ-Run™ prestained protein ladder (Thermo Fisher Scientific, BP3603500,) was used to confirm the expected size of the proteins of interest. Immunoblots were developed with SuperSignal™ West Femto Maximum Sensitivity Substrate (# 34095, Thermo Fisher Scientific) and imaged on a LiCor ODYSSEY Fc (LiCor Inc. Lincoln, NE, Model # 2800). Equal protein loading was confirmed using anti-vinculin antibody (abcam, ab219649, 1:5000).

Cell Growth Assay

5 x 10^4 Cells were seeded in a 6-well plate in triplicate (Day 0) and allowed 24 hours to settle and adhere. After 24 hours plates were imaged on a Lionheart FX imager (Biotek) using a protocol enabling us to image the exact same location on the plates on days 1 through 5 to monitor growth. Image J was used to measure cell surface area and determine fold change. Experiment was repeated two more times and significance was determined using unpaired two-tailed students t test.

CTG Viability Assay

For cell viability a Cell Titer Glo (CTG) assay was used, HepG2 (1,500 cells/well) was seeded on a 384 well plate in 30 ml and incubated for 24 hours. Drug treated cells and their respective controls were incubated for 72hours. For quantification, CellTiter-Glo 2.0 (#G9243 Promega) was added to each well in a 1:1 v/v ratio. Plates were then covered to keep from light and incubated at RT on an orbital shaker at 150 RPM for 30mins. After the incubation, plate was read on a synergy H4 plate reader for luminescence. Dose effect curves for each drug were calculated using Prism software, version 9 (GraphPad). For drug combinations, responses were analyzed using SynergyFinder2.0[196]. Drugs used were cisplatin (#479036-5G Sigma Aldrich), gemcitabine (#AC456890010 Fisher Scientific), vincristine (#AAJ60907MA Fisher Scientific). triapine (#50-136-4826 Fisher Scientific), MK1775 (#M4102 LKT laboratories, Saint Paul, Minnesota), doxorubicin (#BP25161 Fisher Scientific), sorafenib (#NC0749948 Fisher Scientific), SN-38 (#S4908-50MG Selleck Chemicals, Harris County, Texas), deferoxamine mesylate (#AC461770010, Acros Organics, Geel, Belgium), KU60019 (#S1570, Selleck Chemicals). All concentrations were seeded in triplicate and the experiment was repeated two more times. Significance was determined using the Extra Sum of Squares f test.

RRM2 Knockdown

Lentivirus particles were added to HepG2 at a MOI of 3 (Dharmacon V3SH7669-226296450 (RRM2) VSC6544 (GAPDH), and VSC6572 (Scramble)). Cells were selected using puromycin at a concentration of 2 µg/mL until cells in control wells were dead. A doxycycline dose curve was performed to determine optimal dose of doxycycline without loss of cell viability. 500 ng/ml of doxycycline was the optimal dose, and all future experiments were performed using that concentration. Target sequence for RRM2 was (5’ – AGAACCCATTTGACTTTAT – 3’).

RRM2 and RRM2B Knockout by CRISPR/Cas9

$RRM2B^{KO}$ cells were generated using CRISPR/Cas9 technology. Briefly, 4 × 10^5 HepG2 cells were transiently transfected with pre-complexed ribonuclear proteins

(RNPs) consisting of 100 pmol of chemically modified sgRNA 5' – UUCAUUUACAAUUCCAUCAC- 3', Synthego, 35 pmol of Cas9 protein (St. Jude Protein Production Core), and 500 ng of pMaxGFP (Lonza) via nucleofection (Lonza, 4D-Nucleofector™ X-unit) using solution P3 and program EN-158 (HB214) or CA-138 (HepG2) in a 20 μL cuvette according to the manufacturer's recommended protocol. Five days post nucleofection, cells were single-cell sorted by FACs to enrich for transfected GFP^+ cells, clonally selected, and verified for the desired targeted modification (out-of-frame indels) via targeted deep sequencing using gene specific primers with partial Illumina adapter overhangs (F– 5' TCCATAGTTTACTGGTAGTGGGAT-3' and R – 5' AGACATCTTGTCTTTGGCTGAATTT-3', overhangs not shown) as previously described.[197] Briefly, approximately 1×10^4 cells were lysed and used to generate amplicons flanking the gRNA cut site with partial Illumina adapters in PCR #1. During PCR #2 amplicons were indexed and pooled with other amplicons to create sequence diversity. Additionally, 10% PhiX Sequencing Control V3 (Illumina) was added prior to running the sample on an Miseq Sequencer System (Illumina) to generate paired 2 X 250 bp reads. Samples were demultiplexed using index sequences and fastq files were generated. NGS analysis of clones was performed using CRIS.py.[198] Knockout clones were identified as clones containing only out-of-frame indels. $RRM2^{KO}$ was attempted in HepG2 $RRM2B^{OE}$ cells using the same protocol (sgRNA 5' – CGGUCUUGCUGGCCAGGA – 3'). Final clones or pools were authenticated using the PowerPlex® Fusion System (Promega) performed at the Hartwell Center for Biotechnology at St. Jude Children's Research Hospital. Final clones tested negative for mycoplasma by the MycoAlert™ Plus Mycoplasma Detection Kit (Lonza).

RRM1 Co-Immunoprecipitation Assay

Protein extracts were prepared as previously described.[199] Protein extracts (50 μg) were loaded in 4 %-20 % gradient gels (Bio-Rad, Hercules, CA) and transferred to nitrocellulose membranes (Bio-Rad). RRM1 was immunoprecipitated from whole cell extracts using an improved Trueblot (Rockland Immunochemical, Limerick, PA) protocol as previously described[199] with polyclonal antibodies (abcam, ab13714), and the presence of RRM2 and RRM2B in the precipitated fraction was examined by immunoblotting with the same antibodies mentioned above (abcam, ab209995).

Clonogenic Assay

HepG2 or HB214 (5×10^5 /well) cells were seeded in a 6-well plate and incubated for 24 hours. The medium was replaced with medium containing treatment in the concentration stated in the different experiments and the respective controls. After incubation for 72hours cells were trypsonized and seeded (1×10^4/well) in a new 6-well plate in duplicate with fresh medium and allowed to incubate for 14 days. On day 14 wells were washed with PBS and incubated with 6% glutaraldehyde (#BP2547-1 Fisher) and 0.05% w/v crystal violet (#C581-25 Fisher) for 30 minutes. After

incubation wells were washed with ddH_2O and allowed to dry. Plates were then imaged on an Epsom V850 scanner and Image J was used to determine the cell area. Experiment was repeated two more times and significance was determined using unpaired two-tailed students t test.

RRM2 and RRM2B Overexpression

pLVX-IRES-tdTomato-FlagAkt1 vector was obtained from Addgene (#64831) and flagakt1 was removed creating pLVX-IRES-tdTomato (RTD) control vector. RRM2 and RRM2B fragments were generated using HepG2 endogenous DNA and PCR amplified using Clone Amp HiFi (Takara #639298). Fragments were purified on a DNA gel and extracted (Qiagen #28706), fragments were then inserted into the RTD control vector creating pLVX-IRES-tdTomato-RRM2 and RRM2B respectively. Plasmids were expressed in *E. Coli* DH5α competent cells (NEB #C2987H) and purified (Qiagen #12165). Purified plasmid was sent for sanger sequencing and the verified plasmids were sent to the vector core for viral packaging. HepG2 cells were transduced with lentiviral particles at a M.O.I of 3 and the FASC sorted for tdTomato expression.

Quantitative RT-PCR

The total RNA in cells were extracted using RNeasy® Mini Kit (#74106 Qiagen) and the concentration and purity of the RNA were measured by nanodrop spectrometer. SuperScript® III First-Strand Synthesis SuperMix for qRT-PCR (#11752-250 Invitrogen) was used for cDNA synthesis from 1 μg total RNA. FastStart Universal SYBR® Green Master (ROX) (#0491385001 Roche, Mannheim, Germany) was used to perform the quantitative PCR assay on the 7900HT Sequence Detection System (Applied Biosystems, Carlsbad, CA, USA). The results were analyzed using $2^{-\Delta\Delta Ct}$ Method, with *ATCB* as the internal reference gene. Experiments were performed in triplicate and repeated two more times. Significance was determined using unpaired two-tailed students t test. The primers were as follows: RRM2: CTGGAAGGAAAGACTAACTTCTT (Forward), CGTGAAGTCAGCATCCAAGG (Reverse); RRM2B: CCTGCGATGGATAGCAGATAG (Forward), GCCAGAATATAGCAGCAAAAGATC (Reverse); ATCB: GTTGTCGACGACCAGCG (Forward), GCACAGAGCCTCGCCTT (Reverse).

Nucleotide Detection via Targeted LC/MS

Cells were cultured in 6-well plates to ~85% confluence and washed with 2 mL ice cold 1X Phosphate-Buffered Saline (PBS). The cells were then harvested in 300 μL freezing 80% acetonitrile (v/v) into 1.5 mL tubes and lysed by Bullet Blender (Next Advance) at 4 °C followed by centrifugation at 21,000 x g for 5 min at 4 °C. The supernatant was dried by speedvac and reconstituted in 7.5 μL of 66% acetonitrile and 2 μL was separated by a ZIC-HILIC column (150 × 2.1 mm, EMD Millipore) coupled

with a Q Exactive HF Orbitrap MS (Thermo Fisher) in negative detection mode. Metabolites were eluted within a 45 min gradient (buffer A: 10mM ammonium acetate in 90% acetonitrile, pH=8; buffer B: 10 mM ammonium acetate in 100% H2O, pH=8). The MS was operated by a full scan method followed by targeted selected ion monitoring and data-dependent MS/MS (tSIM/dd-MS2). MS settings included full scan (120,000 resolution, 350-550 m/z, 3 x 106 AGC and 50 ms maximal ion time), tSIM scan (120,000 resolution, 1 x 105 AGC, 4 m/z isolation window and 50 ms maximal ion time) and data-dependent MS2 scan (30,000 resolution, 2 x 105 AGC, ~50 ms maximal ion time, HCD, Stepped NCE (50, 100, 150), and 10 s dynamic exclusion). Data were quantified using Xcalibur software (Thermo Fisher Scientific) and normalized by cell numbers. Ribonucleotide and deoxyribonucleotides were validated by authentic standards.

RNA Extraction, Sequencing, and Data Analysis

The total RNA was extracted from HepG2 cells at different conditions using RNeasy® Mini Kit (#74106 Qiagen) following the manufacturer's protocol. The TruSeq Stranded mRNA LTSample Prep Kit (Illumina) was used for library preparation, and PE-100 sequencing was performed using an Illumina HiSeq X Ten instrument (Illumina). All relevant sequencing data will be available at GEO. The adapters used in library preparation were identified by FastQC (v-0.11.5) (https://www.bioinformatics.babraham.ac.uk/projects/fastqc/) and trimmed from the raw reads by cutadapt (v-1.13) (https://doi.org/10.14806/ej.17.1.200) with the default parameters. RSEM (v-1.3.0)[200], coupled with Bowtie2 (v-2.2.9)[201], were used to quantify the expression of genes based on the reference genome hg38 (GRCh38) with gene annotation from GENCODE (release v32). The Transcripts Per Million (TPM) values were extracted and further transformed to log2(TPM+0.1) for subsequent analysis. The differential expression analysis was conducted using limma R package (v-3.42.2).[202] The gene set enrichment analysis (GSEA) was performed by the fgsea R package (v-1.12.0) (https://doi.org/10.1101/060012) with MSigDB dataset (v-6.1)[203] and visualized by NetBID software (v-2.0.2). To evaluate the accuracy of gene expression quantification, Salmon (v0.9.1) was employed to calculate the TPM values of genes. The Spearman correlation coefficient and *p*-value were calculated from the TPM values of genes co-identified by RSEM and Salmon using the stats R package (v3.6.1).

Hub Gene Identification of RRM2 and RRM2B in HB and HCC

We used a scalable software for gene regulatory network reverse-engineering from big data, SJARACNe (v-0.1.0)[204], to reconstruct context-dependent signaling interactomes from the gene expression profiles of 46 HB patient samples collected from GSE75271[205] and 374 HCC patient samples collected from TCGA-LIHC[206], respectively. The parameters of the algorithm were configured as follows: *p* value threshold $p = 1e\text{-}7$, data processing inequality (DPI) tolerance $€ = 0$, and number of bootstraps (NB) = 200.

We used the adaptive partitioning algorithm for mutual information estimation. Both the upstream and downstream first neighbors of RRM2 or RRM2B were extracted and considered as the hub genes in each context.

Gene Set Enrichment Analysis of RRM2 and RRM2B Hub Genes

To identify the cellular processes regulated by RRM2 and RRM2B, we first applied a hypergeometric distribution method for the gene set enrichment analysis using the "funcEnrich.Fisher" function from the R package NetBID (v-2.0.2).[207] Only the HALLMARK and KEGG gene sets from the MSigDB database (v-6.1)[203] were used. The p values of the enrichment analysis of both HB and HCC patient cohorts were further combined with the Stouffer method embedded in the "combinePvalVector" function from NetBID. We then picked the top 10 most significantly enriched gene sets by the hub genes of RRM2 and RRM2B respectively and introduced the Gene Set Enrichment Analysis (GSEA) on both HB and HCC primary patient samples and HepG2 cell lines of different conditions. The differential expression analysis of primary patient samples was performed between RRM2/RRM2B-high and -low which were defined as the top 1/3 and bottom 1/3 in each cohort. The visualization was completed by ggplot2 (v-3.3.4, Wickham H (2016). ggplot2: Elegant Graphics for Data Analysis. Springer-Verlag New York. ISBN 978-3-319-24277-4 (https://ggplot2.tidyverse.org/).

Statistical Analysis

Experimental data were analyzed using the unpaired two-tailed Students t test. Drug response curves were analyzed with GraphPad software using the Extra Sum of Squares f test. Kaplan Meier curves for survival were analyzed with GraphPad using the log-rank test.

CHAPTER 4. RIBONUCLEOTIDE REDUCTASE SUBUNIT SWITCHING IN HEPATOBLASTOMA DRUG RESPONSE AND RELAPSE

Introduction

Hepatoblastoma (HB) is a rare type of primary liver cancer that only affects very young children.[208] Although accounting for only 0.5-2% of all cancer cases in children,[209] HB has the largest increase in incidence among childhood cancers in the United States and worldwide.[210] Most HB tumors are sensitive to chemotherapy and children with HB have an excellent overall five-year survival of >80%. But for children diagnosed with high-risk HB, this number drops to below 40% even with multidisciplinary therapies.[35] Studies in many adult solid tumors have found that tumor cells can develop drug resistance during the course of treatment via various mechanisms as part of their adaptation to stress conditions.[211, 212] This raised an intriguing question as to whether HB cells in high-risk tumors, with their known cellular and molecular heterogeneity and plasticity,[172] can similarly evoke a self-defense machinery when treated by anti-cancer drugs to increase their chance of survival.

Recent work in our lab using HB mouse and organoid models,[13] patient-derived xenografts (PDX) and primary patient samples revealed a significant upregulation of ribonucleotide reductase (RNR) in high-risk HB. RNR is the sole enzymatic complex in mammalian cells that converts ribonucleoside diphosphate (NDP) to deoxy-NDP (dNDP).[213] It plays a critical role in regulating the total rate of DNA synthesis during cell division and DNA repair. [214-216] RNR is a heterodimeric tetramer composed of two large RNR subunit M1 (RRM1) and two small RNR subunit M2 (RRM2)[16]. RRM2 has the catalytic domain of RNR and is tightly cell-cycle regulated.[21] Therefore, it is not surprising that RRM2 upregulation has been found in many adult cancers.[217-221] There is another low-expressing RNR M2 subunit, RNR subunit M2B (RRM2B), which has a lower catalytic activity than RRM2 and is not cell-cycle regulated.[222] It has been found that RRM2B can be induced in a p53-dependent manner under certain stress conditions and becomes the dominant M2 subunit to support DNA repair.[116, 223] Since there is little known about the involvement of RNR in pediatric cancer, we decided to investigate RNR dynamics regarding to its role in HB progression and drug response.

Results

RRM2, Not RRM2B, Is Associated with Disease Progression in HB Patients and Promotes HB Cell Growth

We previously generated a HB mouse model by targeting a population of *Prom1*-expressing neonatal liver progenitors with an activating *Notch* mutation, *NICD* (Notch intercellular domain), *Prominin1*^{CreERT2}; *Rosa*$^{NICD1/+}$; *Rosa*^{ZsG} (PNR) mice.[11] PNR mice

developed frequent primary tumors in the liver but rare metastases. We then reported the generation of multiple cancer organoid lines derived from the PNR tumors. PNR organoid lines varied in their in vivo tumorigenicity with a subset being tumorigenic and metastatic upon orthotopic transplantation and the others generating no tumors in vivo (**Figure 4-1A**).[13] To pinpoint the molecular mechanisms driving metastasis in the PNR models, we performed a comparative RNAseq analysis of metastatic and nonmetastatic PNR-T and PNR-O samples to identify genes associated with metastasis. The same analysis was done for a hepatocellular carcinoma (HCC) mouse model, PPTR (*Prominin1*^{CreERT2}*; Pten*$^{flx/flx}$*; Tp53*$^{flx/flx}$*; Rosa*^{ZsG}) mice, and combined to identify genes commonly associated with liver cancer metastasis (**Figure 4-1B)**.[11, 13] Among the top upregulated genes in metastatic PNR and PPTR tumors and organoids was *Rrm2* (**Figure 4-1C, D**), the catalytic M2 subunit of the ribonucleotide reductase (RNR) complex. RNR catalyzes the formation of deoxy-ribonucleoside diphosphate (dNDP) from NDP. We found that the expression of the other two RNR subunits, *Rrm1* and the other catalytic subunit *Rrm2B*, did not show consistent association with the metastatic potential of tumors and organoids from both models (**Figure 4-1C, D)**. We then wanted to validate that *Rrm2* and not *Rrm2B* was associated at the protein level in our PNR model. Due to RRM2Bs close homology with RRM2, there are no antibodies targeting RRM2B specifically. However, using a dual antibody that recognizes both Rrm2 and Rrm2B, immunohistochemistry (IHC) showed a consistent increase in the number of Rrm2/Rrm2B$^+$ cells in metastatic tumors compared to primary tumors (**Figure 4-2A**). To further validate that RRM2 was associated with HB progression and not RRM2B, we performed an RNA in situ hybridization assay called RNAscope that allowed us to distinguish between the two genes. Using HB PDXs, we saw a higher expression of *RRM2*$^+$ cells than *RRM2B*$^+$ cells in both primary and metastatic tumors (**Figure 4-2B, b** vs**. c** and **f** vs**. g)**. Comparing HB PDXs derived from primary tumors to metastatic tumors, the latter appeared to have a relatively higher percentage of *RRM2*$^+$ cells (**Figure 4-2B, b** vs. **f)**. *RRM2* positivity in HB PDX tumors was well aligned with that of a cell proliferation marker Ki67 (**Figure 4-2B, d** and **h,**), supporting the role of RRM2 in cell proliferation. Lastly, analysis of a previously published gene expression profiles of 88 HB patient tumors[205] also showed a correlation of Ki67 with RRM2 expression, not with RRM2B expression, with both the pathologically- and molecularly-defined HB risk groups (**Figure 4-2C**).

To compare the role of RRM2 and RRM2B in HB cell proliferation, we overexpressed RRM2 and RRM2B as well as a TdTomato (TdT) empty vector in a human HB cell line HepG2[224, 225] (**Figure 4-3A**). To confirm that our exogenous proteins were enzymatically active we checked the levels of free NDPs, dNDPs, and dNTPs in the cells using targeted liquid chromatography/mass spectrometry (LC/MS). We were able to detect high levels of all nucleotides in our overexpressing cells compared to the control cells which were virtually undetectable for several of the nucleotides (**Figure 4-3B**). We also saw that nucleotide levels were higher in *RRM2*-overexpressing (*RRM2*^{OE}) compared to *RRM2B*-overexpressing (*RRM2B*^{OE}) cells correlating with the reported higher enzymatic activity of RRM2 (**Figure 4-3B**). We then tested the growth rate of these cell lines, and accordingly, saw that *RRM2*^{OE} cells showed a slight increase in growth rate compared to the TdT control cells, while no change was observed in the *RRM2B*^{OE} cells

Figure 4-1. RRM2 is upregulated in organoid transplantation model.
(A.) Schematic illustration showing the establishment of PNR genetic mouse, organoid, and orthotopic transplantation models. (B.) Flow chart for the comparative transcriptomic analysis of the tumors and organoids from the PNR and PPTR mouse models. (C.) Quantitative comparison of the three RNR subunits in PNR tumor tissues and organoids in the indicated groups. (D.) Quantitative comparison of the expression of three RNR subunits in PPTR tumor tissues and organoids in the indicated groups. *p* values were calculated by Student *t* test: * < 0.05; ** <0.01; *** <0.001; ****<0.0001.

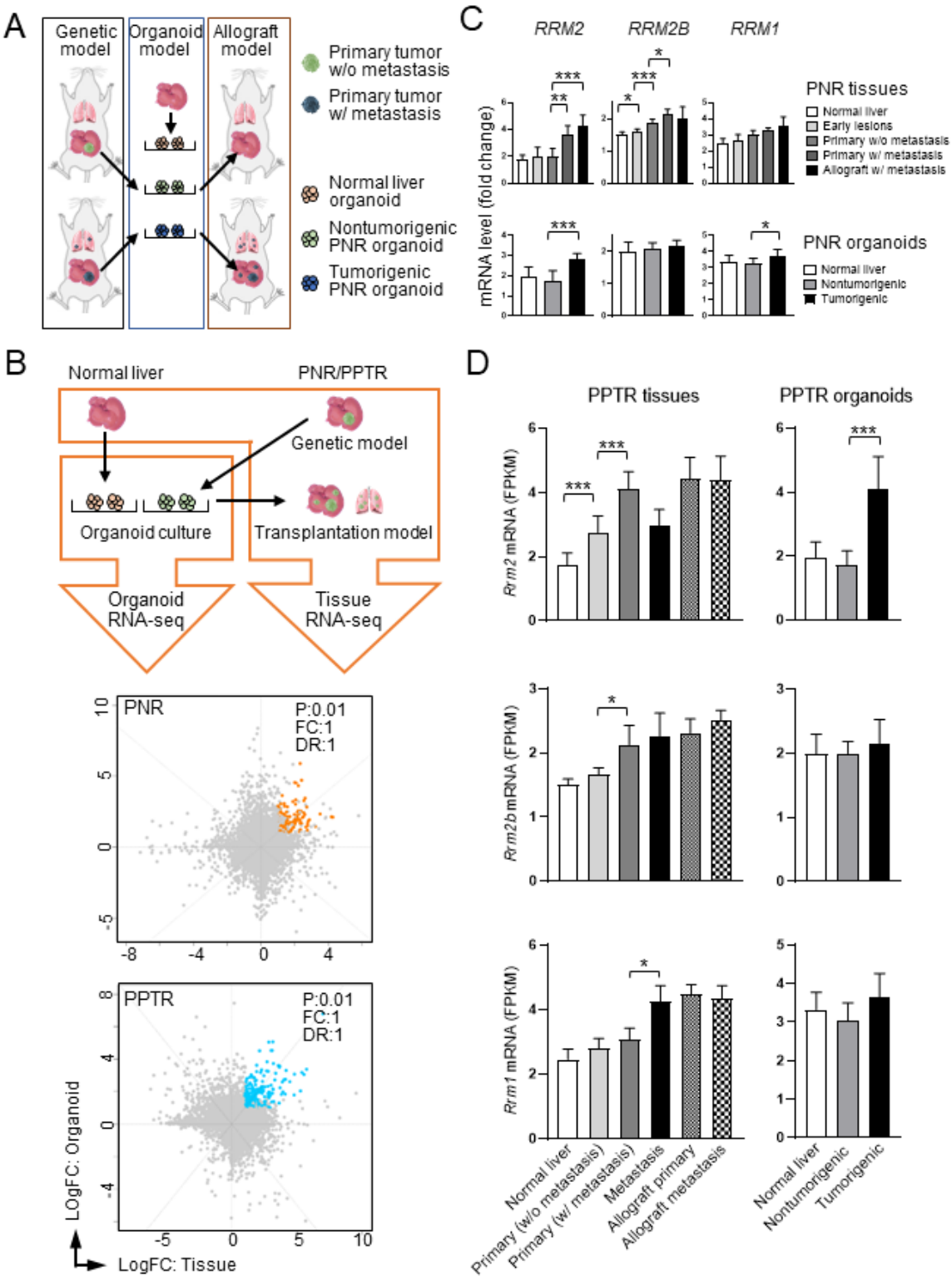
A
Genetic model
Organoid model
Allograft model
Primary tumor w/o metastasis
Primary tumor w/ metastasis
Normal liver organoid
Nontumorigenic PNR organoid
Tumorigenic PNR organoid
C
RRM2
RRM2B
RRM1
mRNA level (fold change)
PNR tissues
Normal liver
Early lesions
Primary w/o metastasis
Primary w/ metastasis
Allograft w/ metastasis
PNR organoids
Normal liver
Nontumorigenic
Tumorigenic
B
Normal liver
PNR/PPTR
Genetic model
Organoid culture
Transplantation model
Organoid RNA-seq
Tissue RNA-seq
PNR
P:0.01
FC:1
DR:1
PPTR
P:0.01
FC:1
DR:1
LOgFC: Organoid
LogFC: Tissue
D
PPTR tissues
PPTR organoids
Rrm2 mRNA (FPKM)
Rrm2b mRNA (FPKM)
Rrm1 mRNA (FPKM)
Normal liver
Primary (w/o metastasis)
Primary (w/ metastasis)
Metastasis
Allograft primary
Allograft metastasis
Normal liver
Nontumorigenic
Tumorigenic

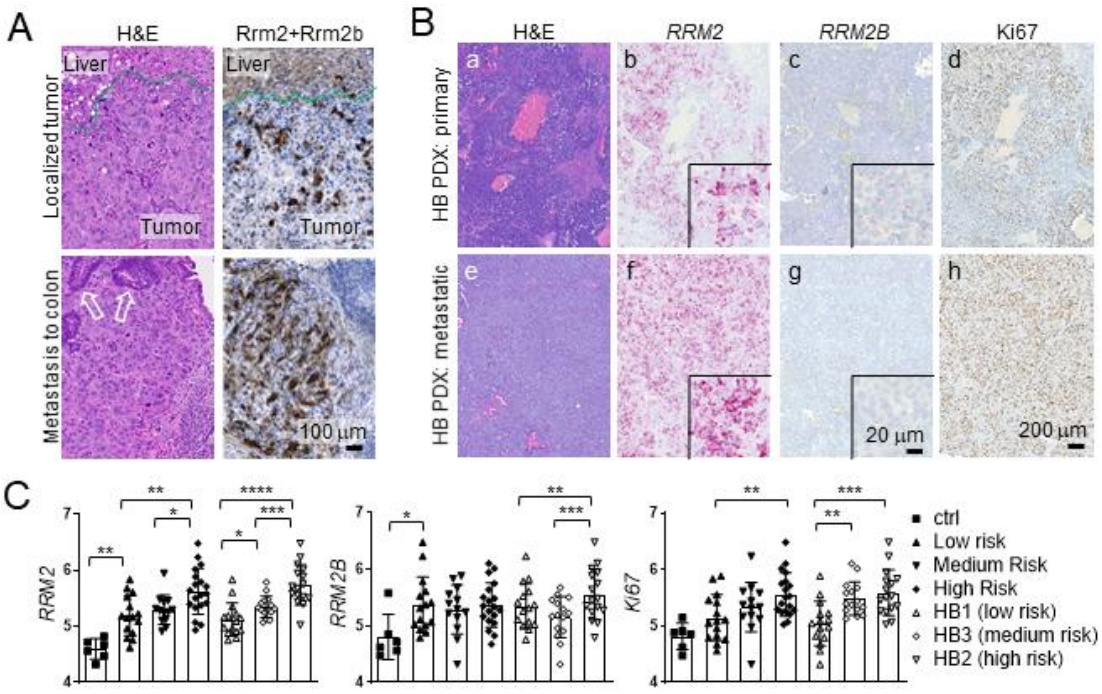

Figure 4-2. RRM2 is associated with HB disease progression.
A.) H&E (left) and RRM2/RRM2B IHC staining (right) on the serial sections of localized and metastatic PNR tumors. Dotted lines: tumor border; arrows: colonic polyps embedded in the tumor. All images share the same 100 µm scale bar. (B.) H&E staining (a, e), RNAscope staining for *RRM2* (b, f) and *RRM2B* (f, g), and Ki67 IHC staining (d, h) on serial sections of HB PDX tumors derived from primary and metastatic patient tumors. Al images share the same 200 µm scale bar. Insets in (b, c, f, g): higher magnification images; scale bars, 20 µm. (C.) Expression of the three RNR subunits in pathologically-defined (low, medium, and high) HB patient risk groups and molecularly-defined (HB1, HB3, and HB2) risk groups from a publicly available HB transcriptomics database.[205] *p* values were calculated by Student *t* test: * < 0.05; ** <0.01; *** <0.001; ****<0.0001.

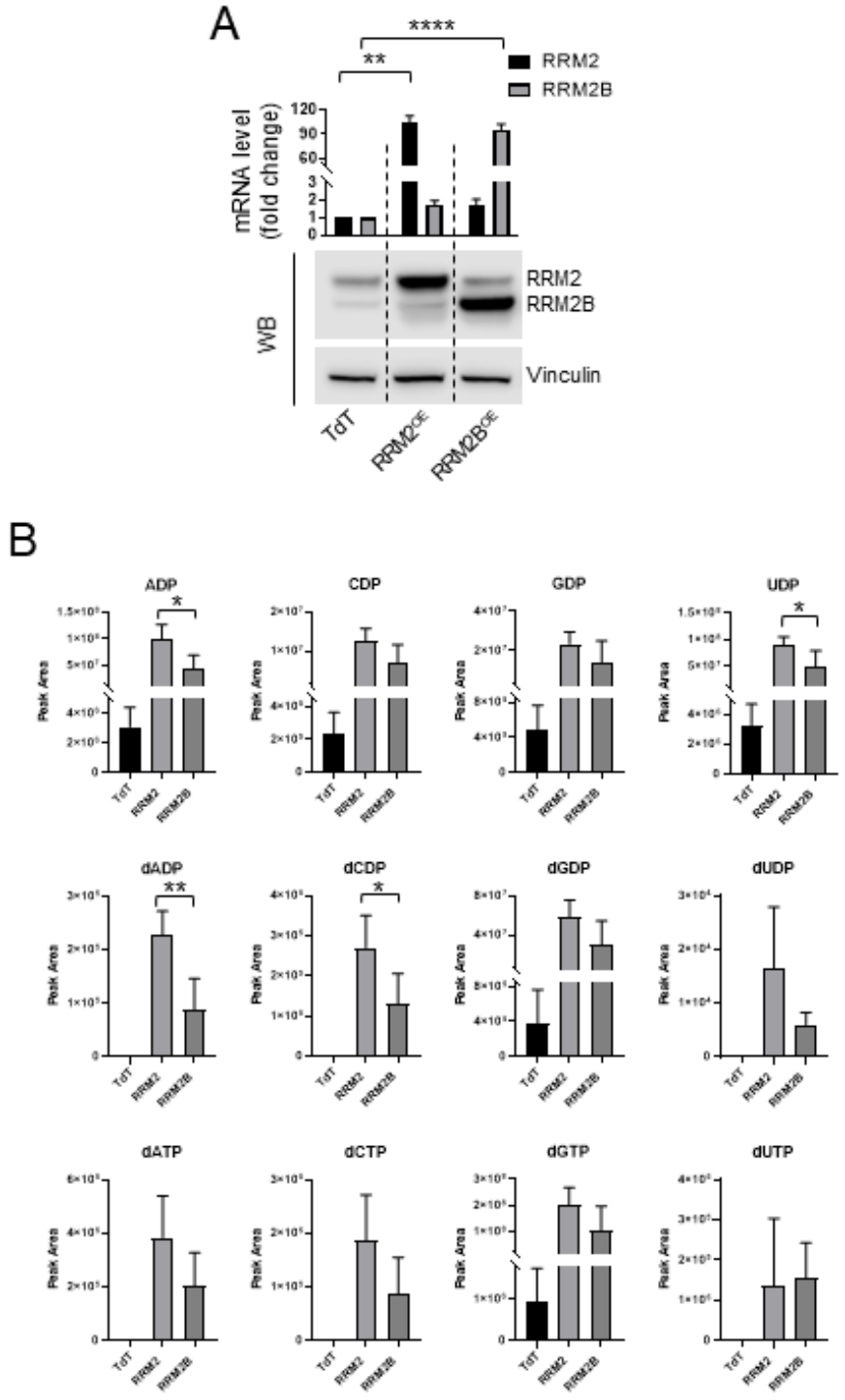

Figure 4-3. Overexpression of RRM2 and RRM2B in HepG2 cells.
(A.) Quantitative RT-PCR and immunoblotting of RRM2 and RRM2B in the indicated HepG2 cells. (B.) Quantitative analysis of nucleotide levels in TdT, *RRM2*^{OE}, and RRM2B^{OE} HepG2 cells using targeted LC/MS. *p* values were calculated by Student *t* test: * < 0.05; ** <0.01; *** <0.001; ****<0.0001.

(**Figure 4-4A**). Interestingly, when TdT, *RRM2*^{OE} and *RRM2B*^{OE} HepG2 cells were orthotopically transplanted into NOD scid gamma (NSG) mice, we saw a slight decrease in survival in the *RRM2B*^{OE} cells but not in the *RRM2*^{OE} cells (**Figure 4-4B**). This could partially be explained by the variability from orthotopic cell injections as the significance was not great. The minimal increase in growth observed in the *RRM2*^{OE} cells could be due to RRM2 already being highly expressed in HepG2 cells. To further see if RRM2 or RRM2B influenced cell growth we attempted to knockout (KO) the two genes. DepMap Portal shows *RRM2* is an essential gene and its KO leads to the death of all cancer cell lines tested. However, we tested a doxycycline-inducible shRNA targeting *RRM2*. We were able to see a clear dose-dependent knockdown of RRM2 which led to a significant decrease in cell growth with compared to the different controls (**Figure 4-4C, D**). With the help of Dr. Shondra Miller and Baranda Hansen, we were able to successfully KO *RRM2B* in two HepG2 cells clones that were grown from single cell selection using CRISPR/Cas9 (**Figure 4-4E**). KO of *RRM2B* showed no change in cell growth in HepG2 cells (**Figure 4-4F**). When these KO cells were orthotopically transplanted into NSG mice there was no change in survival in either of the two cell lines (**Figure 4-4G)**. Our nucleotide analysis results showed that *RRM2B*^{OE} cells were able to produce sufficient levels more so than the control TdT cells. We attempted to KO *RRM2* in the *RRM2B*^{OE} cells to see if the subunits were able to compensate for each other. However, this failed as we noticed an unusual bias towards in-frame indels that persisted in culture (**Figure 4-5A-C**). A wildtype copy of *RRM2* was also retained by all cells that survived long-term cultivation. Overall, these results indicate that RRM2 is the dominant RNR M2 subunit supporting HB cell growth. Although highly homologous in protein sequences, RRM2 and RRM2B likely play different roles in HB cells.

Drug Treatment Suppresses RRM2 but Induces RRM2B in HB Cells In Vitro and In Vivo

Upregulation of RRM2 has been reported in many adult solid tumors. Inhibitors have been developed which, however, only showed suboptimal benefits to adult patients with advanced solid tumors.[226-228] Since pediatric cancer is generally more sensitive to treatment than adult cancer, we decided to test two agents that have shown to inhibit RRM2 either directly or an upstream regulator, triapine[229] and MK1775[22] respectively. We tested two HB cell lines HepG2 and HB214, a previously reported HB PDX model,[230] that generated tumors with faithful HB histopathology when transplanted into NSG mouse liver.[195] Triapine and MK1775 showed comparable efficacies to other standard liver cancer chemotherapies including cisplatin, gemcitabine, vincristine, and SN38, an active form of irinotecan[231] (**Figure 4-6A**). When examining the response of the RNR subunits to drug treatment, we noticed that all the drugs tested led to a significant reduction in the RRM2 protein levels in both cell lines. However, interestingly, they also led to a significant increase in the RRM2B protein levels (**Figure 4-6B**). RNAseq profiling of cis-treated HepG2 cells showed that these drug-induced changes in RRM2 and RRM2B happened at the mRNA level as well (**Figure 4-6C**). We wanted to verify that the switching of the two subunits were

Figure 4-4. RRM2, not RRM2B, is associated with cell growth in vitro.
(A.) Growth curves of TdT, *RRM2*^{OE}, and *RRM2B*^{OE} HepG2 cells. (B.) Kaplan Meier curves of TdT, *RRM2*^{OE}, and *RRM2B*^{OE} cells orthotopically transplanted into NSG mice. (C.) RRM2 and RRM2B immunoblotting showing a dose-dependent knockdown of RRM2 in HepG2 cells. GAPDH shRNA was used as the control. (D.) Growth curves of the indicated HepG2 cells treated with 500 ng doxycycline (dox). (E.) Immunoblot showing knockout of RRM2B in two HepG2 cell lines. (F.) Growth curves of HepG2 (Ctrl), *RRM2B*^{KO1}, and *RRM2B*^{KO2} cells. (G.) Kaplan Meier curves of HepG2, *RRM2B*^{KO1}, and *RRM2B*^{KO2} cells orthotopically transplanted into NSG mice. *p* values were calculated by Student *t* test or Log Rank test for survival curves: * < 0.05; ** <0.01; *** <0.001; ****<0.0001.

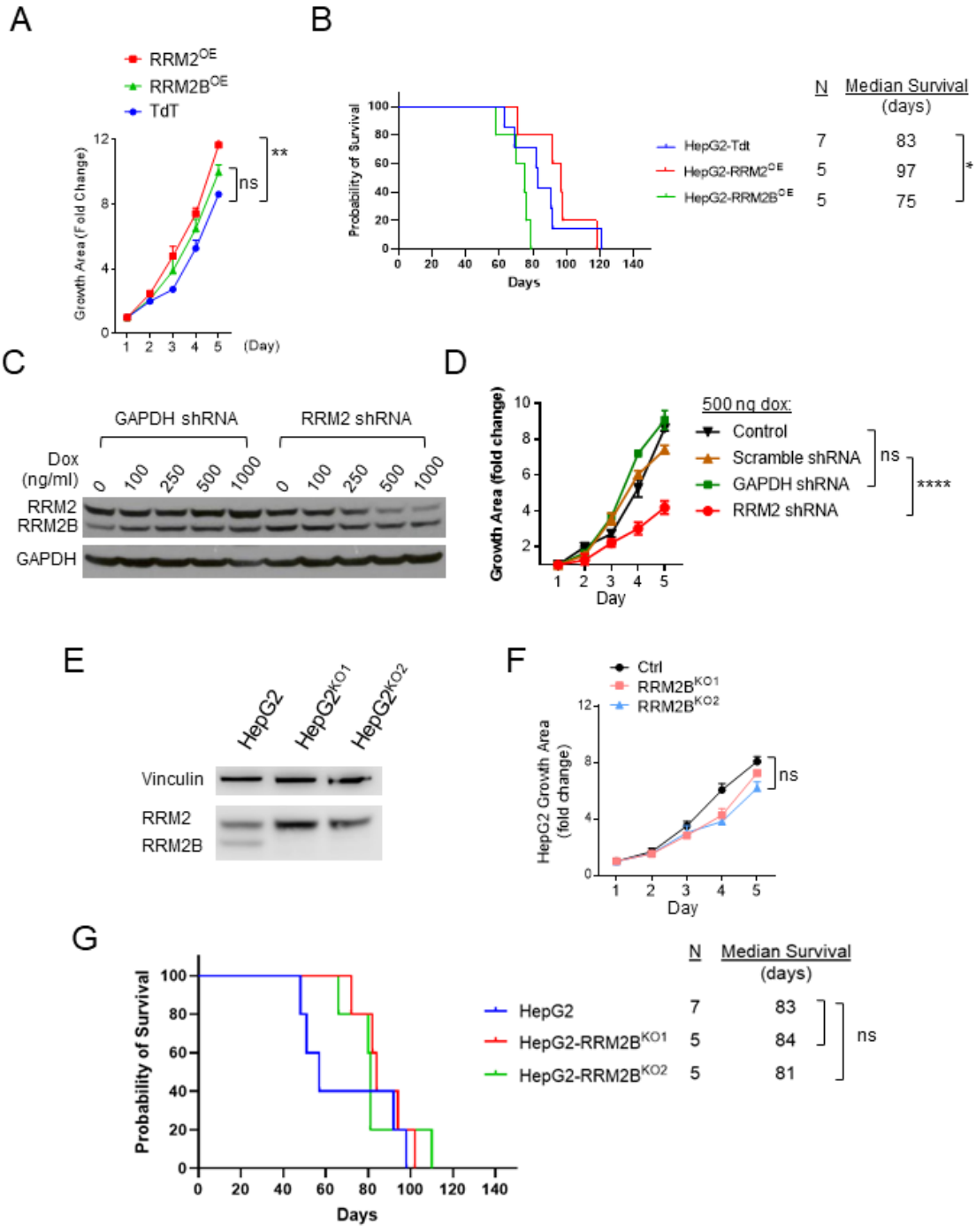
A
RRM2OE
RRM2BOE
TdT
Growth Area (Fold Change)
(Day)
ns
**
B
Probability of Survival
Days
N
Median Survival (days)
HepG2-Tdt 7 83
HepG2-RRM2OE 5 97
HepG2-RRM2BOE 5 75
*
C
GAPDH shRNA
RRM2 shRNA
Dox (ng/ml)
0 100 250 500 1000 0 100 250 500 1000
RRM2
RRM2B
GAPDH
D
Growth Area (fold change)
Day
500 ng dox:
Control
Scramble shRNA
GAPDH shRNA
RRM2 shRNA
ns
****
E
HepG2
HepG2KO1
HepG2KO2
Vinculin
RRM2
RRM2B
F
Ctrl
RRM2BKO1
RRM2BKO2
HepG2 Growth Area (fold change)
Day
ns
G
Probability of Survival
Days
N
Median Survival (days)
HepG2 7 83
HepG2-RRM2BKO1 5 84
HepG2-RRM2BKO2 5 81
ns

A

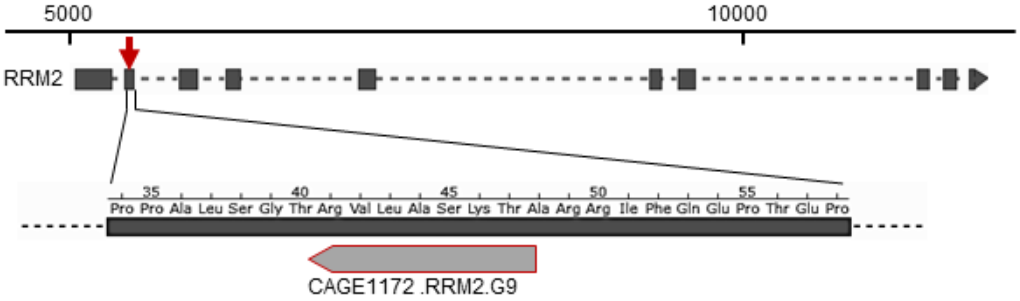

B

Indel Ranking	bp change	Clone%
#1	**0**	**13.9%**
#2	-1	9.2%
#3	**-18**	**7.2%**
#4	**-6**	**5.2%**
#5	**-12**	**4.5%**
#6	**-21**	**4.5%**
#7	**-24**	**4.2%**
#8	-13	3.7%
#9	**-3**	**3.7%**
#10	1	3.0%
	Total indel	86.10%
Total in-frame indel		**43.2%**

C

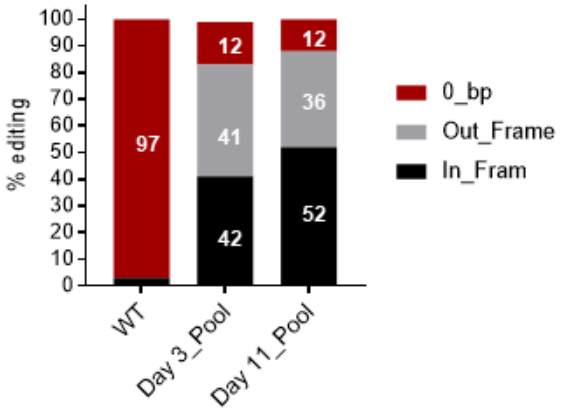

Figure 4-5. RRM2 is essential in HepG2 cells.
(A.) The position and sequence of *RRM2* guide RNA. (B.) Indels after attempted knockout of *RRM2* in HepG2 *RRM2B*^{OE} cells. (C.) Quantitative analysis of *RRM2* indels composition on Day 3 and Day 11 of in *RRM2B*^{OE} HepG2 cells.

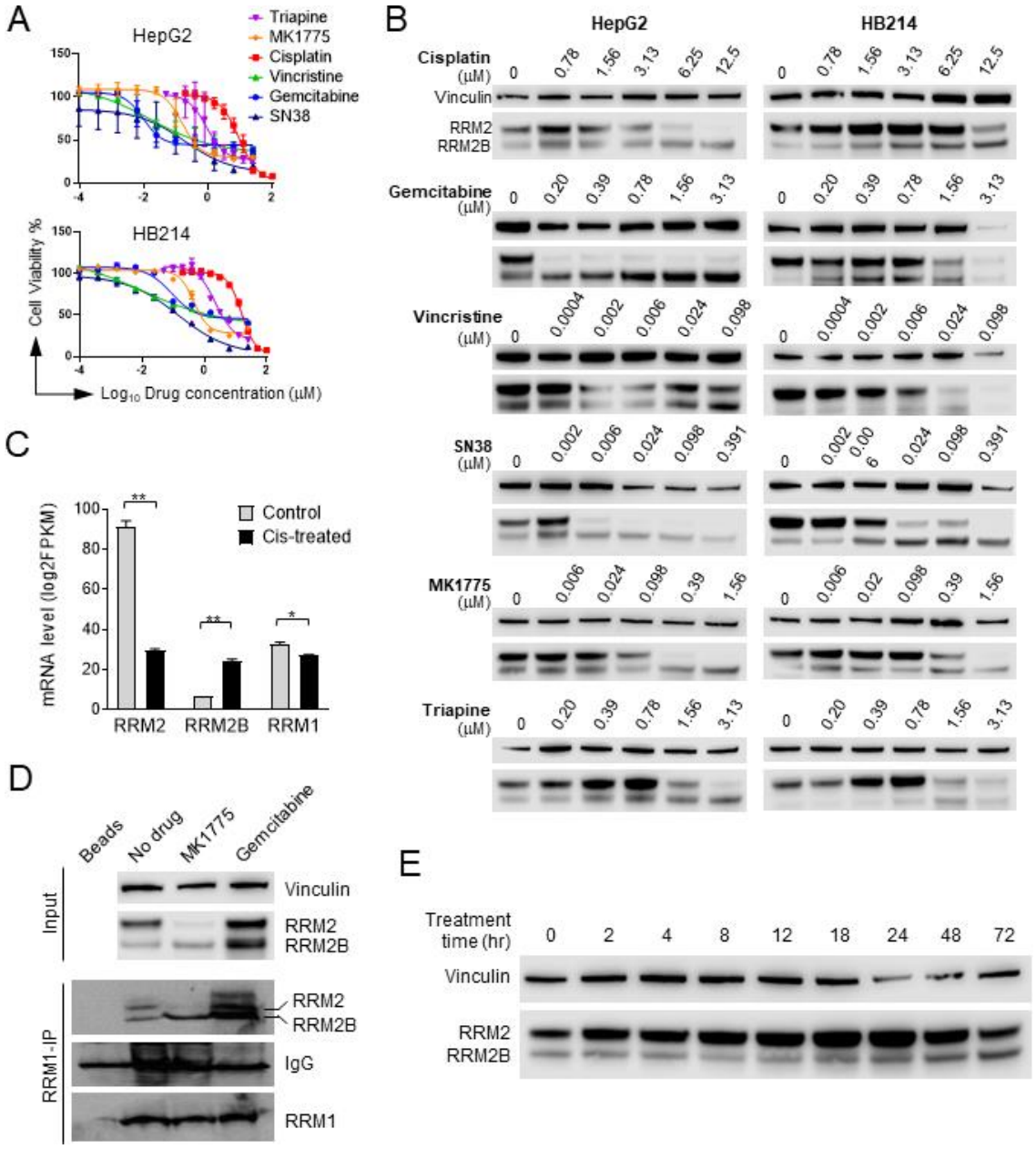

Figure 4-6. A drug-induced RRM2 to RRM2B subunit switch in HB cells.
(A.) Dose response curves of HepG2 and HB214 cells to the indicated chemotherapeutic agents and RRM2 inhibitors. (B.) RRM2 and RRM2B immunoblotting of HepG2 and HB214 cell lysates after treatment with the indicated drugs. (C.) RNR subunits mRNA levels detected by RNAseq in HepG2 cells treated with cisplatin. (D.) RRM1 co-IP assay using MK1775- and gemcitabine-treated HepG2 cells. (E.) A time-course study of RRM2 and RRM2B protein levels in cisplatin treated HepG2 cells by immunoblotting. *p* values were calculated by Student *t* test: * < 0.05; ** <0.01; *** <0.001; ****<0.0001.

binding to RRM1 to form the RNR complex. With the help of Dr. Nikolai Timchenko, we were able to immunoprecipitate RRM1 using MK1775- and gemcitabine-treated HepG2 cells which showed an evident RRM2B-RRM1 binding dominant over RRM2-RRM1 binding (**Figure 4-6D**). The elevated RRM2 in the Co-IP samples is possibly due to larger treatment batches needed for Co-IP versus western blotting. A more detailed time course study on cisplatin treated HepG2 cells revealed an induction of RRM2 within the first 24 hours before its level started decreasing, while increase in RRM2B levels occurred around 18-24 hours (**Figure 4-6E**). The other RNR subunit, RRM1, had consistent expression following treatment to chemotherapy except for the highest concentrations tested (**Figure 4-6C,** and **Figure 4-7**).

RRM2B has been shown to be regulated by the tumor suppressor TP53 and has even been shown to bind to RRM2B in HepG2 cells in untreated conditions.[232, 233] HepG2 cells have a wildtype *TP53* gene.[234] When examining HepG2 cells treated with cisplatin, triapine and gemcitabine, we found that there was a well correlated increase in TP53 and RRM2B protein levels with increasing drug concentrations (**Figure 4-8A**). We found in two HCC cell lines with *TP53* mutations, PLC/PRF/5 and Hep3B,[235] treatment with gemcitabine and a common HCC drug sorafenib failed to induce RRM2B as they did in HB cells (**Figure 4-8B**)

To determine if this RRM2 to RRM2B subunit switching induced by drug treatment also occurred in vivo, we treated HB214 subcutaneous models with saline or irinotecan for two weeks and examined *RRM2* and *RRM2B* levels via RNAscope. Compared to the untreated HB214 tumors, the treated tumors showed a marked loss of the typical punctate signals of *RRM2* mRNA in many areas as well as the loss of the tight association between *RRM2* and cell proliferation indicated by Ki67 IHC (**Figure 4-9a-f**). *RRM2* RNAscope staining on the treated HB214 tumors also showed an unusually high staining background that was never observed in untreated tumors, suggesting a potential *RRM2* mRNA degradation under drug treatment (**Figure 4-9 d** vs. **e** and **f**). On the other hand, irinotecan-treated HB214 tumors showed an evident increase in *RRM2B* mRNA signals compared to the control tumors, particularly in stressed areas with reduced *RRM2* mRNA signals (**Figure 4-9 g-i**). These in vitro and in vivo results, together, demonstrate an intriguing drug-induced RNR M2 subunit switching from RRM2 to RRM2B in HB cells.

Both RRM2 and RRM2B Contribute to HB Cell Drug Resistance, but Only RRM2B Supports Post-treatment Recovery

To determine the involvement of RRM2 and RRM2B in HB cell drug response, we treated TdT, $RRM2^{OE}$ and $RRM2B^{OE}$ HepG2 cells with six common liver cancer drugs and the two RRM2 inhibitors triapine and MK1775. We found overexpression of *RRM2* resulted in a slight increase in the IC50 of all the drugs tested except for SN38 (**Figure 4-10A, B**). $RRM2B^{OE}$ HepG2 cells also showed a limited increase in drug resistance in an extent less than $RRM2^{OE}$ cells. Compared to control TdT cells, $RRM2B^{OE}$ cells showed no differences in response to the two RRM2 inhibitors in addition to SN38

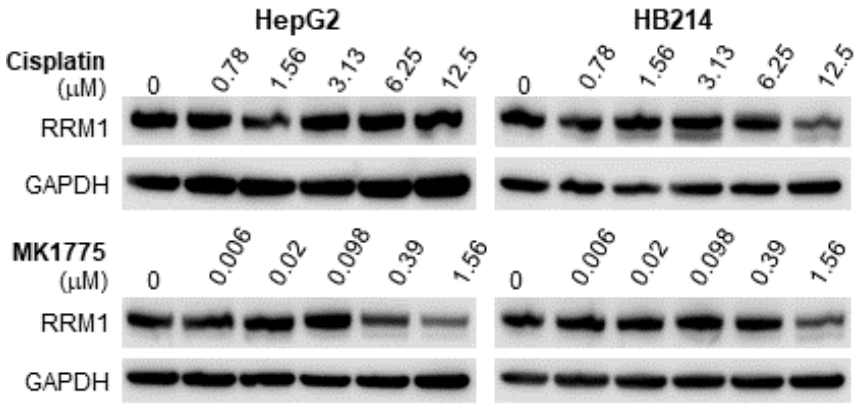

Figure 4-7. RRM1 is more stable than RRM2 and RRM2B following treatment. (A.) RRM1 immunoblotting in HepG2 and HB214 cells treated with cisplatin and MK1775, GAPDH used as loading control.

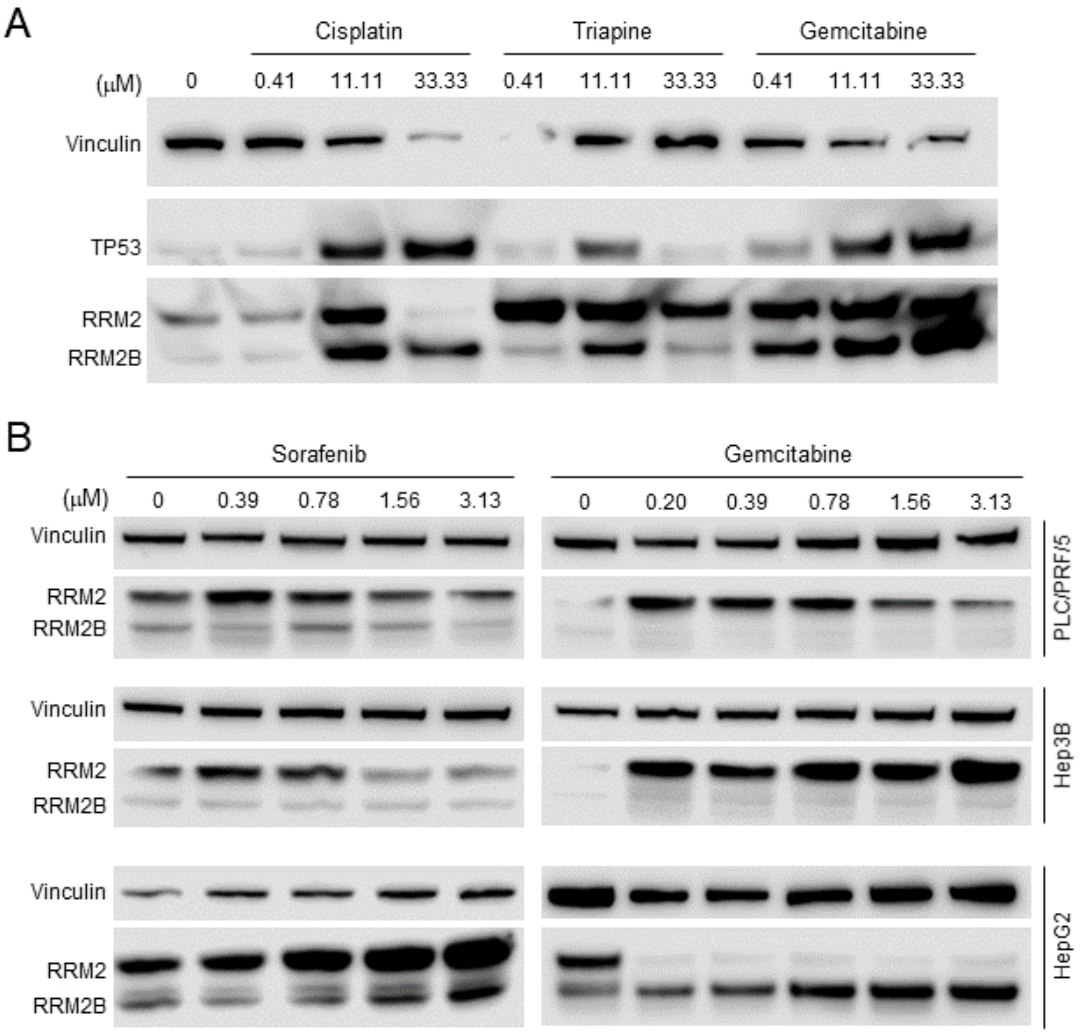

Figure 4-8. Drug-induced RRM2B upregulation in HB cells is associated with TP53.

(A.) TP53, RRM2 and RRM2B immunoblotting in HepG2 cells treated with cisplatin, triapine, and gemcitabine. (B.) RRM2 and RRM2B immunoblotting in two HCC cell lines PLC/PRF/5 and Hep3B, and HepG2 cells treated with sorafenib and gemcitabine.

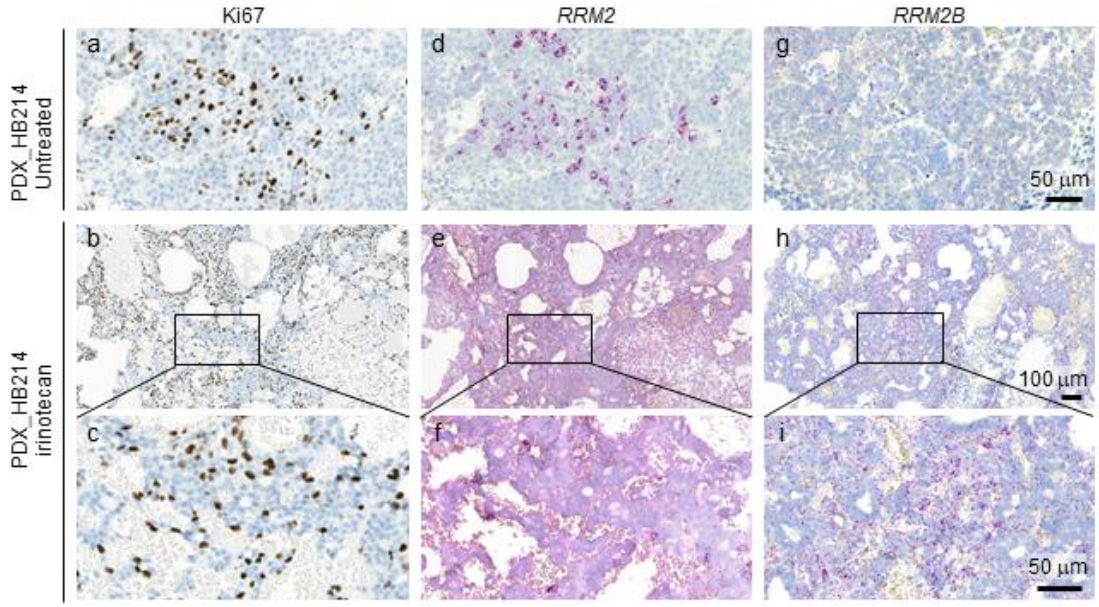

Figure 4-9. Drug-induced RRM2 to RRM2B subunit switch occurs in vivo.
Ki67 IHC (a-c), RNAscope for *RRM2* (d-f) and *RRM2B* (g-i) in untreated and irinotecan treated HB214 tumors. Images on the same row share the same scale bar.

A

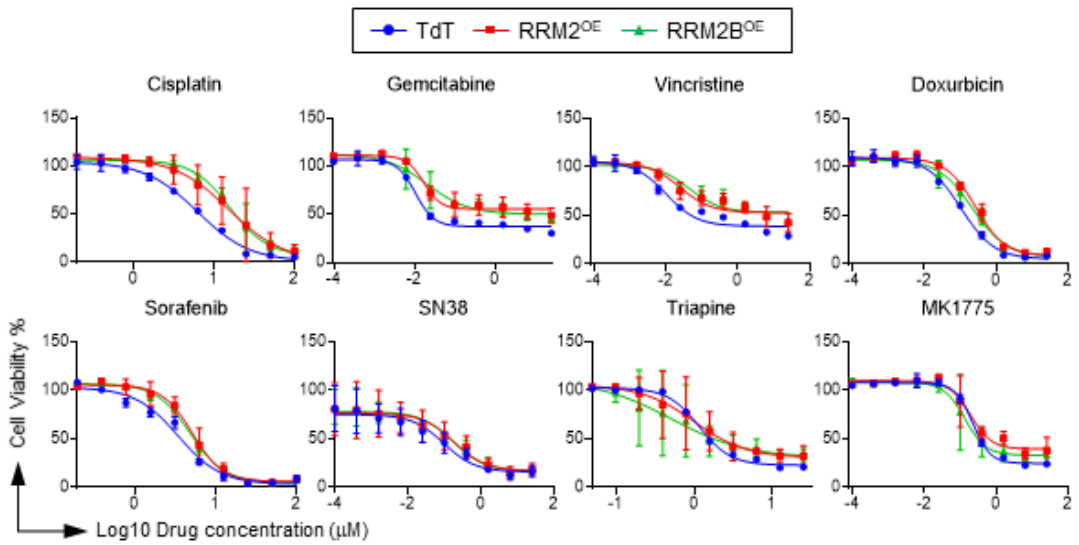

B

	Cisplatin	Gemcitabine	Vincristine	Doxorubicin	Sorafenib	SN38	Triapine	MK1775
IC_{50}: TdT	6.96	2.719	0.4259	0.16717	3.87	0.04027	2.289	0.6985
IC_{50}: $RRM2^{OE}$	18.6	11.74	4.771	0.4338	6.013	0.08771	4.108	2.465
IC_{50}: $RRM2B^{OE}$	19.56	9.865	5.916	0.3482	5.744	0.09294	3.27	1.042
P value: $RRM2^{OE}$ vs. TdT	**<0.0001**	**0.0031**	**0.0002**	**0.0002**	**0.0003**	0.2635	**0.0044**	**0.0266**
P value: $RRM2B^{OE}$ vs. TdT	**<0.0001**	**0.0044**	**<0.0001**	**0.022**	**0.0002**	0.1161	0.1508	0.49

C

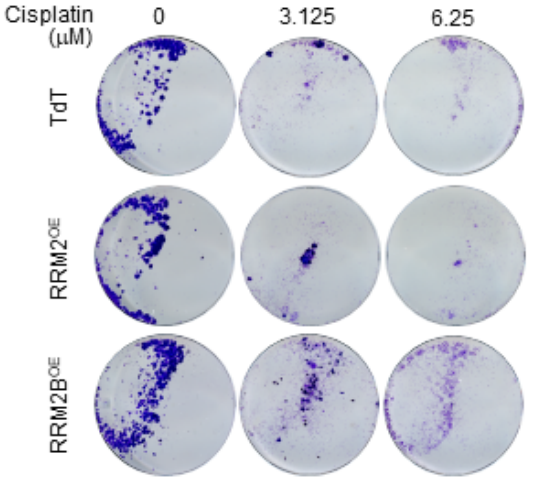

D

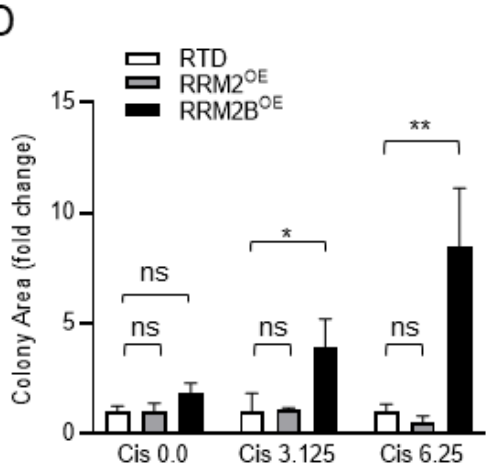

Figure 4-10. Both RRM2 and RRM2B contribute to HB cell drug resistance, but only RRM2B supports the post-treatment recovery of HB cells.
(A.) Dose response curves of TdT, *RRM2^{OE}* and *RRM2B^{OE}* HepG2 cells to the indicated drugs. (B.) List of the drug IC50 values and their comparisons between TdT, *RRM2^{OE}* and *RRM2B^{OE}* HepG2 cells. (C.) 12-day colony formation assay of the TdT, *RRM2^{OE}* and *RRM2B^{OE}* HepG2 cells following cisplatin treatment at the indicated concentrations. (D.) Quantitative comparison the of area occupied by cells in (C). *p* values were calculated by Extra Sum of Square F test or Student t test: * < 0.05; ** <0.01; *** <0.001; ****<0.0001.

(**Figure 4-10A, B**), consistent with the specificity of these two inhibitors to RRM2.

Since we have shown that elevation of RRM2B is maintained following treatment for 72 hours, we suspected that RRM2B might function mostly to improve the fitness of HB cells that had survived chemotherapy. To test this hypothesis, we treated TdT, *RRM2*^{OE} and *RRM2B*^{OE} HepG2 cells with cisplatin, the most commonly used drug for HB, for the same 72-hour time point at different concentrations. We then washed and removed the dead cells and seeded the remaining live cells at a low density and allowed them to recover for 12 days with fresh media. We found that, while no difference in the number of colonies grown from the untreated cells, *RRM2B*^{OE} cells exhibited a significantly higher ability to "relapse" from cisplatin treatment compared to the TdT and *RRM2*^{OE} cells (**Figure 4-10C, D**). TdT and *RRM2*^{OE} cells were similar in their ability to grow back after cisplatin treatment (**Figure 4-10C, D**).

To further confirm that RRM2B is important to the recovery of HB cells following treatment, we used the *RRM2B* knockout (*RRM2B*^{KO}) cells from (**Figure 4-4E**). We first wanted to verify that failing treatment, there was still no induction of RRM2B in these cells following cisplatin treatment (**Figure 4-11A**). We then tested the two KO cell lines against standard liver cancer chemotherapy agents as well as the two RRM2 inhibitors to check for changes in drug resistance. Interestingly, both *RRM2B*^{KO} cell lines showed no significant change in IC50 values to any of the drugs we tested (**Figure 4-11B**) showing that RRM2B is less important for initial drug response. However, when it came to post-treatment recovery both *RRM2B*^{KO} cell lines showed a significant decrease in their ability to form colonies at all concentrations tested following treatment with cisplatin when compared to the wild type HepG2 cells (**Figure 4-11C, D**). We then wanted to validate these results in the HB PDX cell lines HB214. Using the same CRISPR/Cas9 system, we were able to successfully KO *RRM2B* in HB214 (HB214^{KO}) (**Figure 4-12A**). HB214^{KO} cells showed a slight increase in IC50 values when compared to the parental cell line to some of the drugs tested including vincristine, doxorubicin, SN38, and MK1775 (**Figure 4-12B**). When HB214^{KO} cells were tested for post-treatment recovery, we saw a complete loss of colony formation ability when *RRM2B* was KO in HB214 compared to the control (**Figure 4-12C, D**). We then wanted to see if the *RRM2B* KO phenotype could be rescued by expression of exogenous RRM2B. Rescue cells (*RRM2B*$^{KO/Res}$) were generated by transfection of the HepG2 *RRM2B*^{KO} cells with the *RRM2B* overexpression vector (**Figure 4-13A**). We then compared these *RRM2B*$^{KO/Res}$ cells to their KO controls in their growth, drug response, and post-treatment recovery. Rescue of RRM2B did not have any change on cell growth similar to the other *RRM2B* manipulated cells (**Figure 4-13B** and **Figure 4-4B**). Both rescue cells lines showed an increase in IC50 values to several of the drugs tested comparable to the *RRM2B*^{OE} cell line (**Figure 4-13C** and **Figure 4-14**). Finally, RRM2B re-expression was able to partially rescue the colony formation ability of the KO cells at lower concentrations of cisplatin but not at the high concentration (**Figure 4-13D, E**). These results suggest RRM2 plays a more important role in cell growth and initial drug response, however, RRM2B plays a critical role in supporting the post-treatment recovery of HB cells.

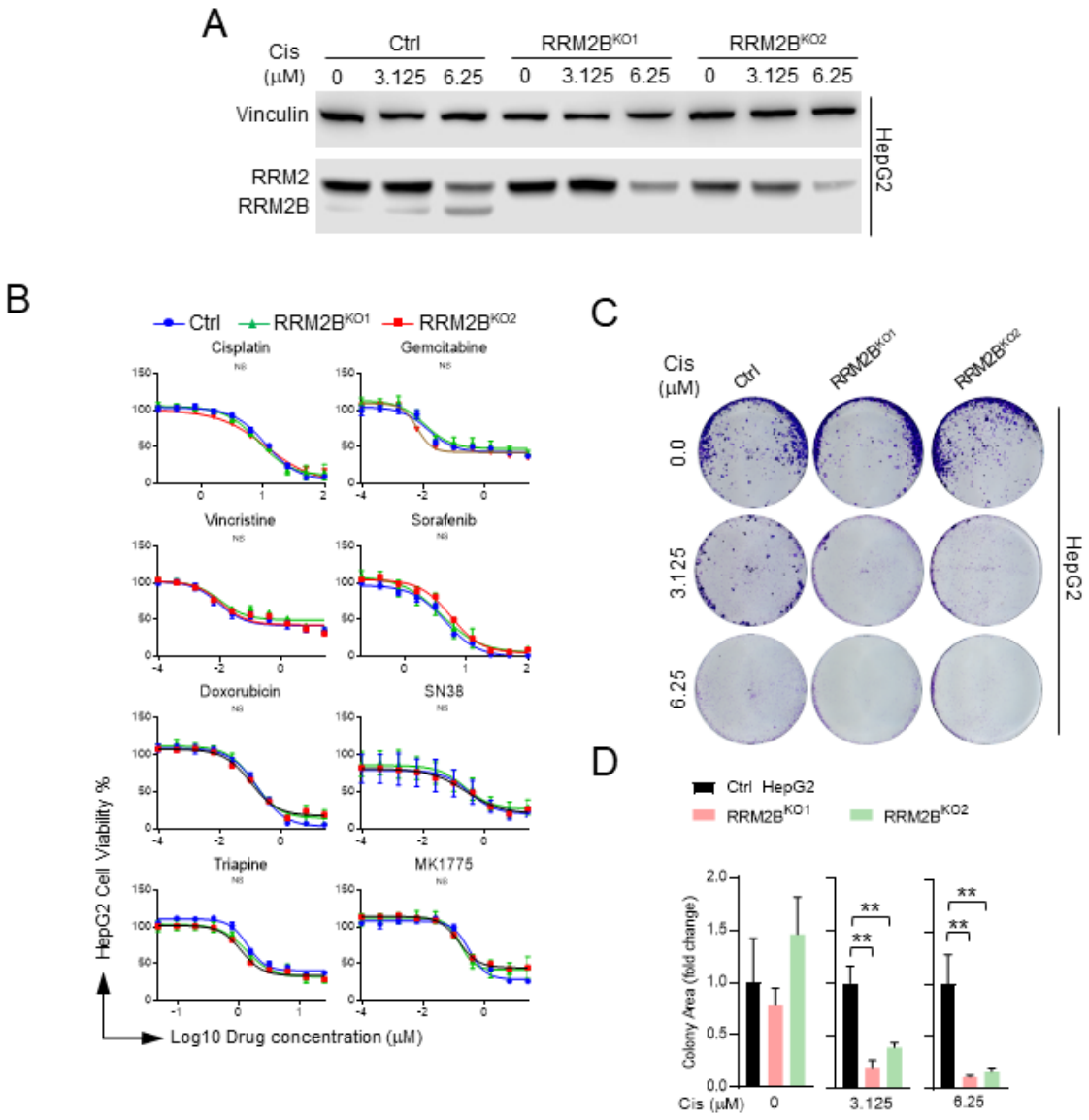

Figure 4-11. Knockout of RRM2B had no effect on drug resistance while decreasing post-treatment recovery in HepG2 cells.
(A.) RRM2 and RRM2B immunoblotting in untreated and cisplatin treated *RRM2B*^{KO} HepG2 cells. (B.) Dose response curves of HepG2 (Ctrl), *RRM2B*^{KO1}, and *RRM2B*^{KO1} HepG2 cells to the indicated drugs. (C.) 12-day colony formation assay of the HepG2 (Ctrl), *RRM2B*^{KO1}, and *RRM2B*^{KO1} HepG2 cells following cisplatin treatment at the indicated concentrations. (D.) Quantitative analysis of area occupied by cells in (C). *p* values were calculated by Extra Sum of Square F test or Student t test: * < 0.05; ** <0.01; *** <0.001; ****<0.0001.

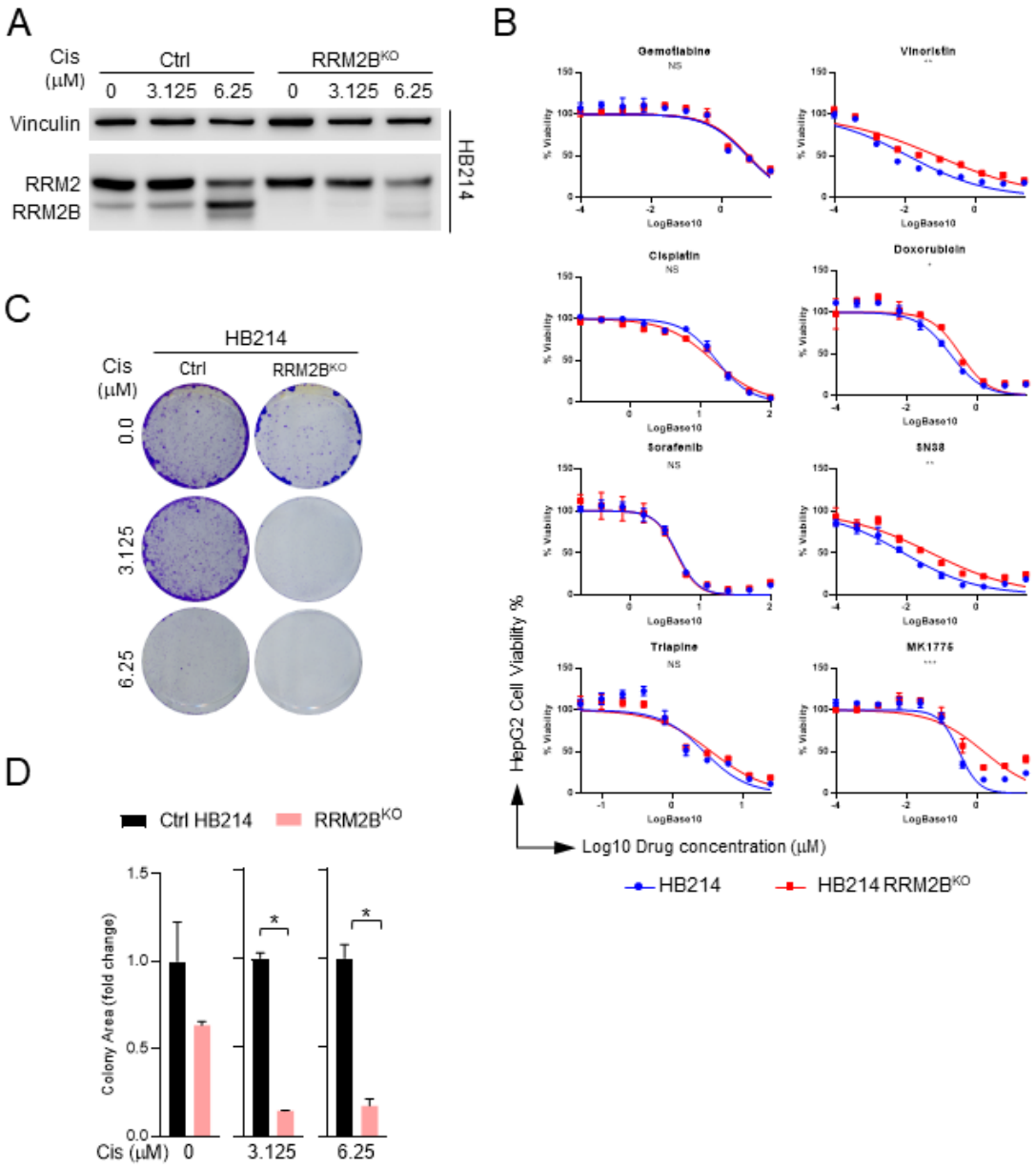

Figure 4-12. Knockout of RRM2B had minimal effect on drug resistance while decreasing post-treatment recovery in HB PDX cell line HB214.
(A.) RRM2 and RRM2B immunoblotting in untreated and cisplatin treated *RRM2B*^{KO} HB214 cells. (B.) Dose response curves of HB214 and *RRM2B*^{KO1} HB214 cells to the indicated drugs. (C.) 12-day colony formation assay of the HB214 and *RRM2B*^{KO1} HB214 cells following cisplatin treatment at the indicated concentrations. (D.) Quantitative analysis of area occupied by cells in (C). *p* values were calculated by Extra Sum of Square F test or Student t test: * < 0.05; ** <0.01; *** <0.001; ****<0.0001.

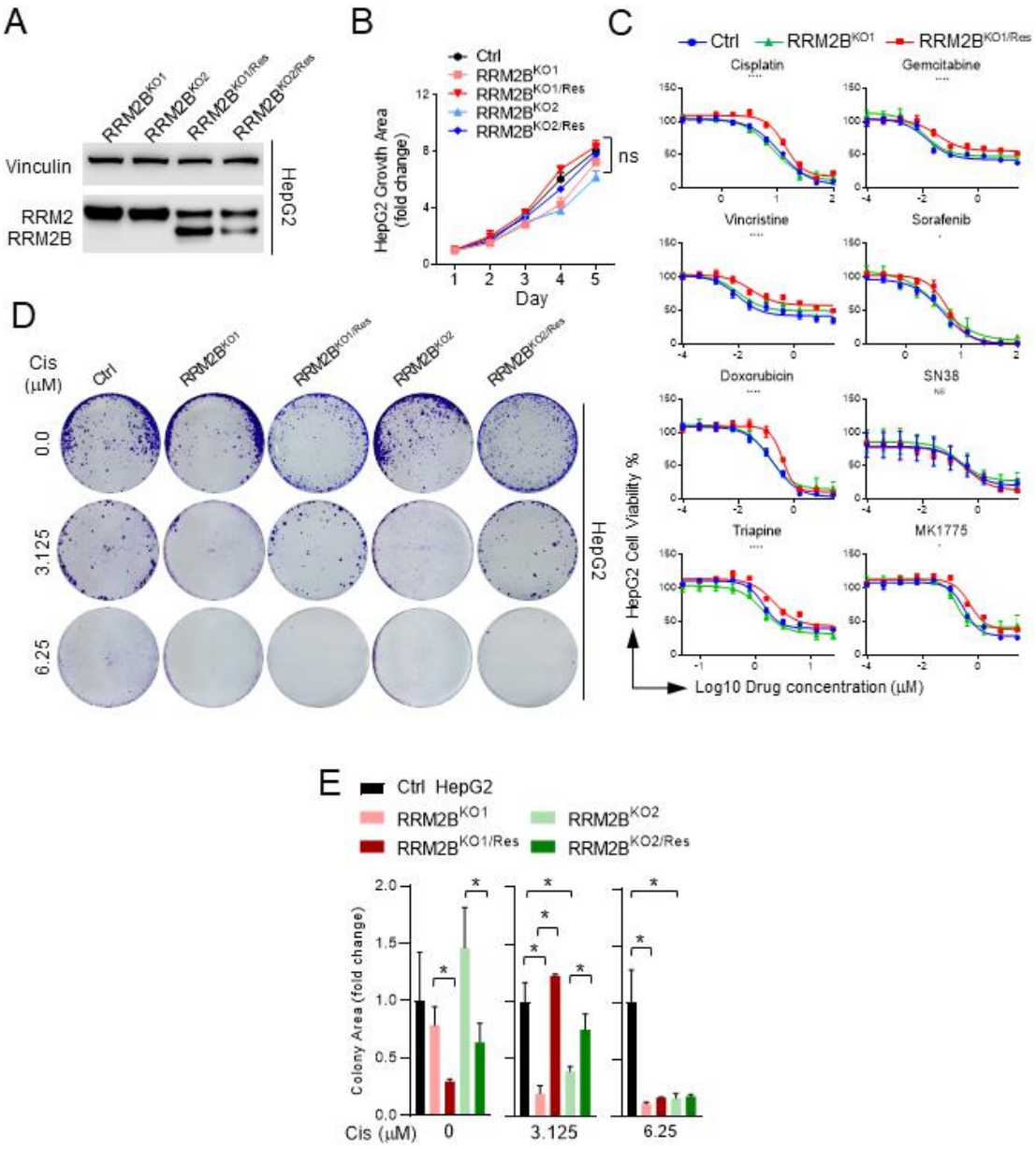

Figure 4-13. Re-expression of RRM2B can rescue partial cell recovery in HB cells. (A.) RRM2 and RRM2B immunoblotting in *RRM2B*^{KO} and *RRM2B*$^{KO/Res}$ HepG2 cells. (B.) Growth curves of HepG2 (Ctrl), *RRM2B*^{KO1}, *RRM2B*^{KO1}, *RRM2B*$^{KO1/Res}$, and *RRM2B*$^{KO2/Res}$ HepG2 cells. (C.) Dose response curves of *RRM2B*^{KO1} and *RRM2B*$^{KO1/Res}$ HepG2 cells to the indicated drugs. (D.) 12-day colony formation assay of the HepG2 (Ctrl), *RRM2B*^{KO1}, *RRM2B*^{KO1}, *RRM2B*$^{KO1/Res}$, and *RRM2B*$^{KO2/Res}$ HepG2 cells following cisplatin treatment at the indicated concentrations. (E.) Quantitative analysis of area occupied by cells in (D). *p* values were calculated by Extra Sum of Square F test or Student t test: * < 0.05; ** <0.01; *** <0.001; ****<0.0001.

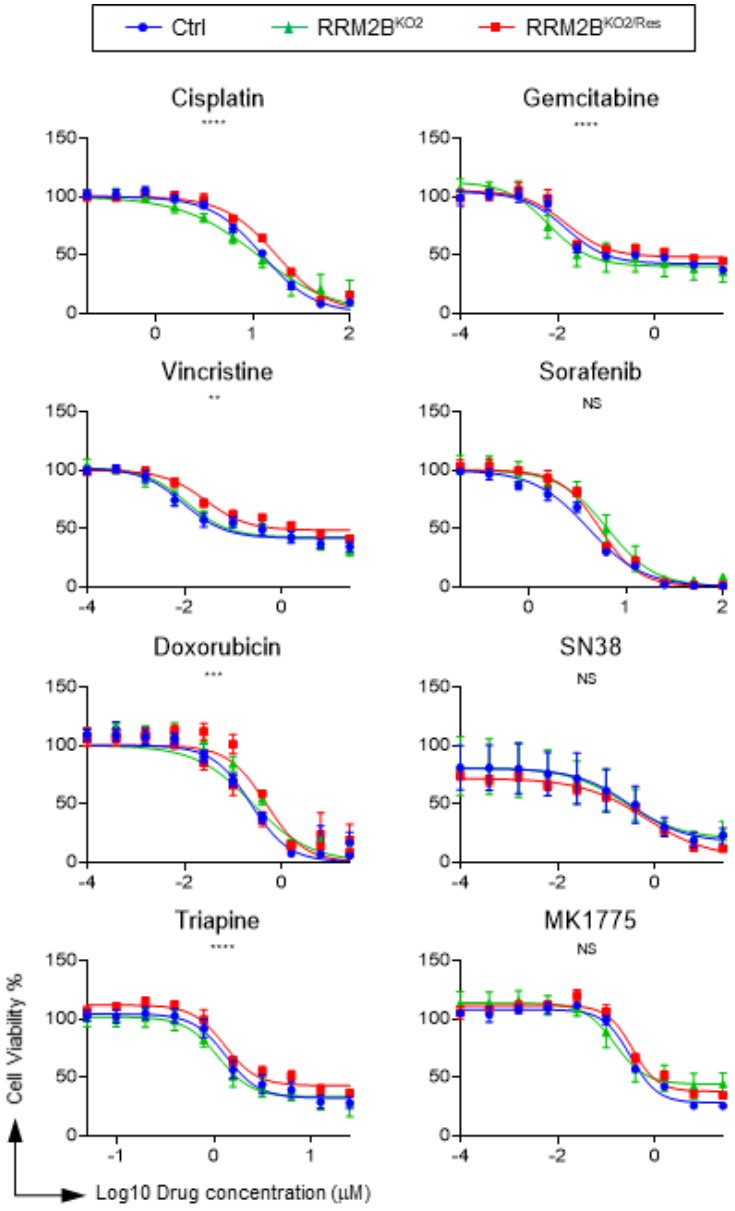

Figure 4-14. Drug response curves of control, *RRM2B^{KO2}*, and *RRM2B$^{KO2/Res}$* HepG2 cells.

Dose response curves of *RRM2B^{KO2}* and *RRM2B$^{KO2/Res}$* HepG2 cells to the indicated drugs.). *p* values were calculated by Extra Sum of Square F test: * < 0.05; ** <0.01; *** <0.001; ****<0.0001.

RRM2 and RRM2B Are Involved in Distinct Cellular Processes in HB Cells and Patient Tumors

With the help of Dr. Qingfei Pan we performed a series of transcriptomic analyses of the HB cell and patient tumors in an effort to understand the systemic involvement of RRM2 and RRM2B in HB tumorigenesis. Using these patient transcriptomic profiles, which were divided into $RRM2^{High}$ and $RRM2B^{High}$ samples, we were able to identify a set of RRM2 and RRM2B hub genes whose expression was highly correlated with RRM2 and RRM2B expression respectively, including both the upstream regulators and downstream targets (**Figure 4-15A, B**). RNA-seq data of 374 HCC patient tumors in The Cancer Genome Atlas (TCGA) database were also downloaded and analyzed simultaneously since we have shown that RRM2 was also tightly associated with HCC progression. We found that the hub genes were similar for each gene between HB and HCC patient tumors (**Figure 4-15A, B**), while there was no overlap between *RRM2* and *RRM2B* hub genes in either tumor types (**Figure 4-16A**). A hypergeometric distribution method found that *RRM2* hub genes are mostly enriched in the pathways involved in cell proliferation and DNA repair (RRM2-associated pathways, or $PTWAY^{RRM2}$) while RRM2B hub genes participated strongly in stress and inflammatory response pathways (RRM2B-associated pathways, or $PTWAY^{RRM2B}$) (**Figure 4-16B**). These enriched pathways correlate with the observed phenotypes we have seen in our *RRM2* and *RRM2B* manipulated cells and suggest that RRM2 and RRM2B could be playing similar roles in HB patient tumors.

A Reversed RRM2B to RRM2 Subunit Switching in HB Cells Recovering from Drug Treatment

Our data suggested that inhibiting RRM2B would work as an effective combinatorial treatment to standard chemotherapies. However, no RRM2B-specific inhibitors have been developed, likely due to the low expression of this RNR M2 subunit in growing tumor cells. We tested two drugs that could potentially inhibit RRM2B, deferoxamine[236] and KU60019[237], however, neither of which showed RRM2B-specific inhibition at the protein level, nor in our $RRM2B^{OE}$ cells (**Figure 4-17A, B**). Since our data indicated that RRM2 was important to HB cell growth, we hypothesized that HB cells would regain RRM2 expression in order for them to resume growth after treatment. In turn, RRM2 inhibition might be an effective approach to prevent HB relapse. When cisplatin treated HepG2 cells were allowed to regrow, we found that the level of RRM2 did come back up and became the dominant M2 subunit again while RRM2B levels decreased (**Figure 4-18A**). This reversed RRM2B to RRM2 switching occurred quickly and at a high level in cells that were initially treated with a relatively low concentration of cisplatin (3.1 mM), and much more slowly and at a markedly lower level in cells treated with a high dose of cisplatin (12.5 mM) (**Figure 4-18A**). We then moved onto the in vivo tumors and found an expected reduction in *RRM2B* mRNA level over time in HB214 tumors post irinotecan treatment, and the reestablishment of strong *RRM2* expression in proliferating cells (**Figure 4-18B, a-f**). In an HB PDX derived from a recurrent patient

Figure 4-15. Identification of hub genes associated with RRM2 and RRM2B in HB and HCC patient tumors.

(A.) Microarray data from 46 HB patient tumors and sequencing data from 374 HCC patients tumors were divided into thirds to separate $RRM2^{High}$ samples and $RRM2B^{High}$ samples. (B.) Hub genes associated with *RRM2* and *RRM2B* in HB and HCC patient cohorts inferred by SJARACNe. Edge width is corresponding to the correlation strength measured by mutual information. Red and blue edges indicate positive and negative correlations of each hub gene, respectively.

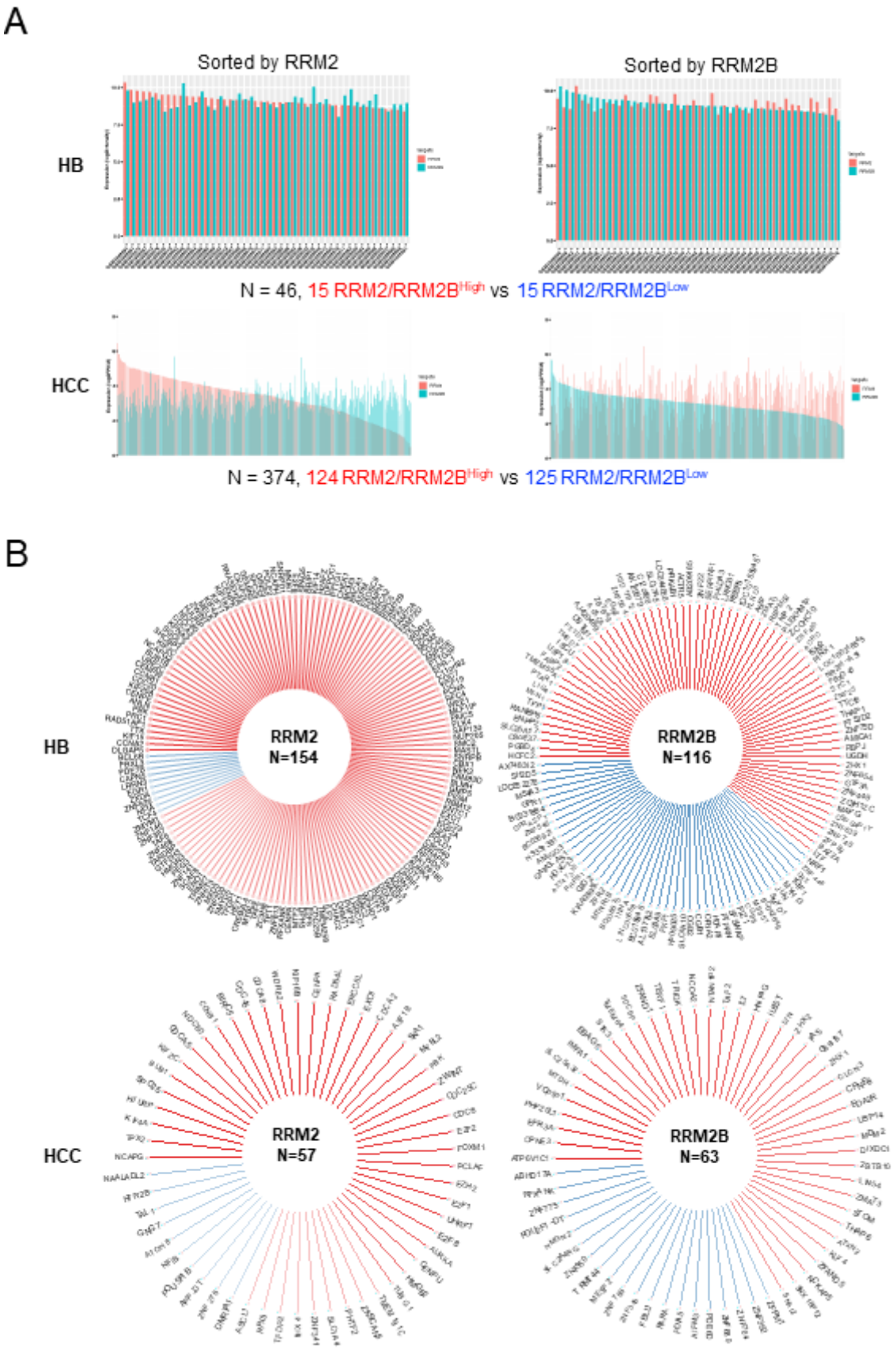
A
Sorted by RRM2
Sorted by RRM2B
HB
N = 46, 15 RRM2/RRM2B^High vs 15 RRM2/RRM2B^Low
HCC
N = 374, 124 RRM2/RRM2B^High vs 125 RRM2/RRM2B^Low
B
HB
RRM2
N=154
RRM2B
N=116
HCC
RRM2
N=57
RRM2B
N=63

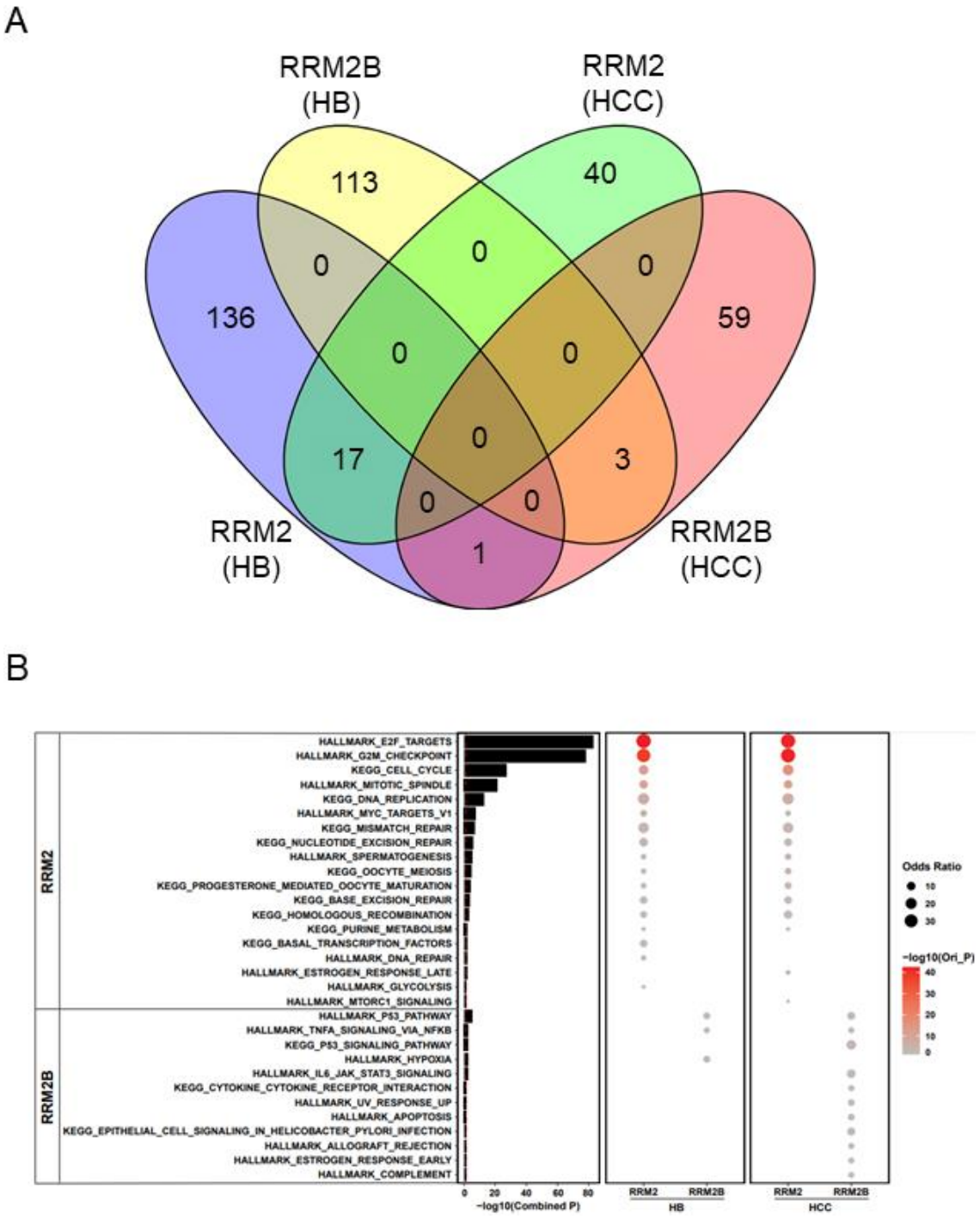

Figure 4-16. RRM2 and RRM2B are involved in distinct cellular processes in HB and HCC patient tumors.

(A.) Venn plot showing the overlap statistics of the four hub gene list. (B.) Gene set enrichment analysis of HALLMARK and KEGG gene sets of the 4 hub gene lists using Fisher's Exact Test. The size and color intensity indicate the odds ratio and statistical significance, respectively. The *p* values of the bar plot were combined from HB and HCC primary patient cohorts using the Stouffer method.

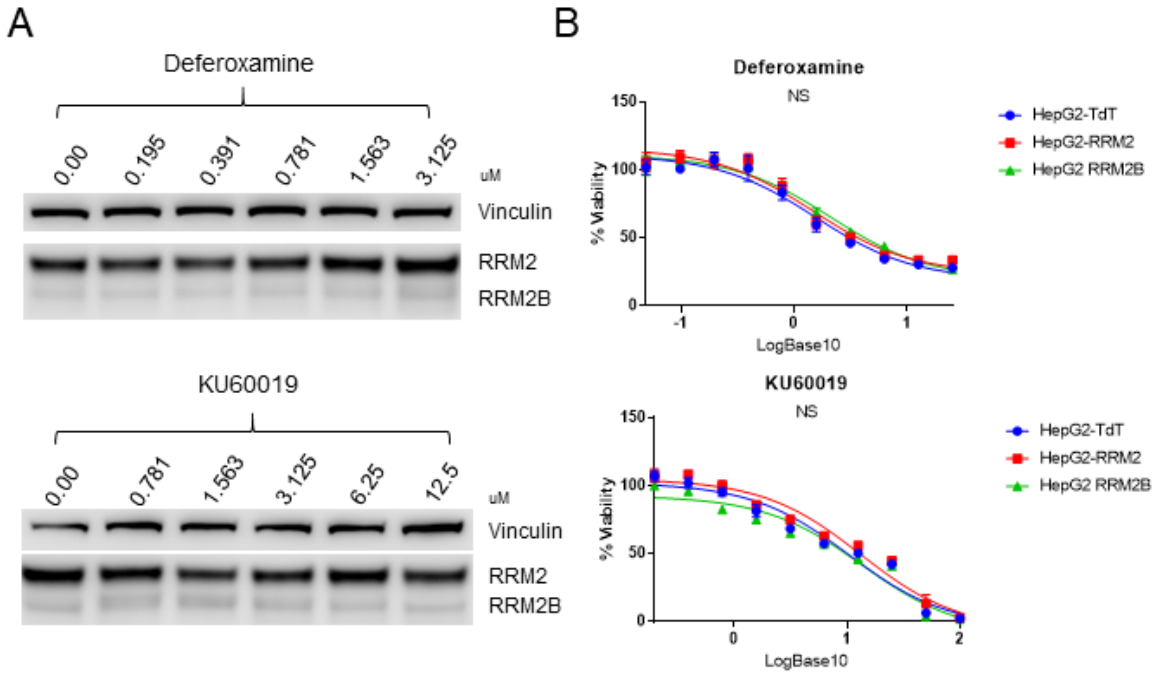

Figure 4-17. No effective RRM2B inhibitors.
(A.) Immunoblot for RRM2 and RRM2B in HepG2 cells treated with deferoxamine and KU60019. (B.) Dose response curves of TdT, *RRM2*^{OE}, and *RRM2B*^{OE} HepG2 cells to deferoxamine and KU60019. *p* values were calculated by Extra Sum of Square F test: * < 0.05; ** <0.01; *** <0.001; ****<0.0001.

Figure 4-18. A reversed RRM2B to RRM2 subunit switching in relapsed HB cells and tumors.

(A.) RRM2 and RRM2B immunoblotting of HepG2 cells recovered from the indicated cisplatin treatment. (B.) Ki67 IHC and *RRM2* and *RRM2B* RNAscope HB214 tumors post irinotecan treatment and a HB PDX model derived from a recurrent patient tumor. All images on the same row share the same scale bar. (C.) ZIP synergy analysis of the two RRM2 inhibitors in combination with SN38 in HB214 cells. (D.) Tumor volume measurements in mice treated with the indicated drug or drug combination. Arrow: drug withdraw on Day 21. (E.) Tumor volume measurements in mice treated with the indicated drug or drug combination. Arrow: drug withdraw on Day 14. MK1775 was maintained in the last group (red line). (F.) RRM2 and RRM2B immunoblotting of the HB214 tumors collected post the indicated treatment. ZIP scores calculated using SynergyFinder2.0.[196]

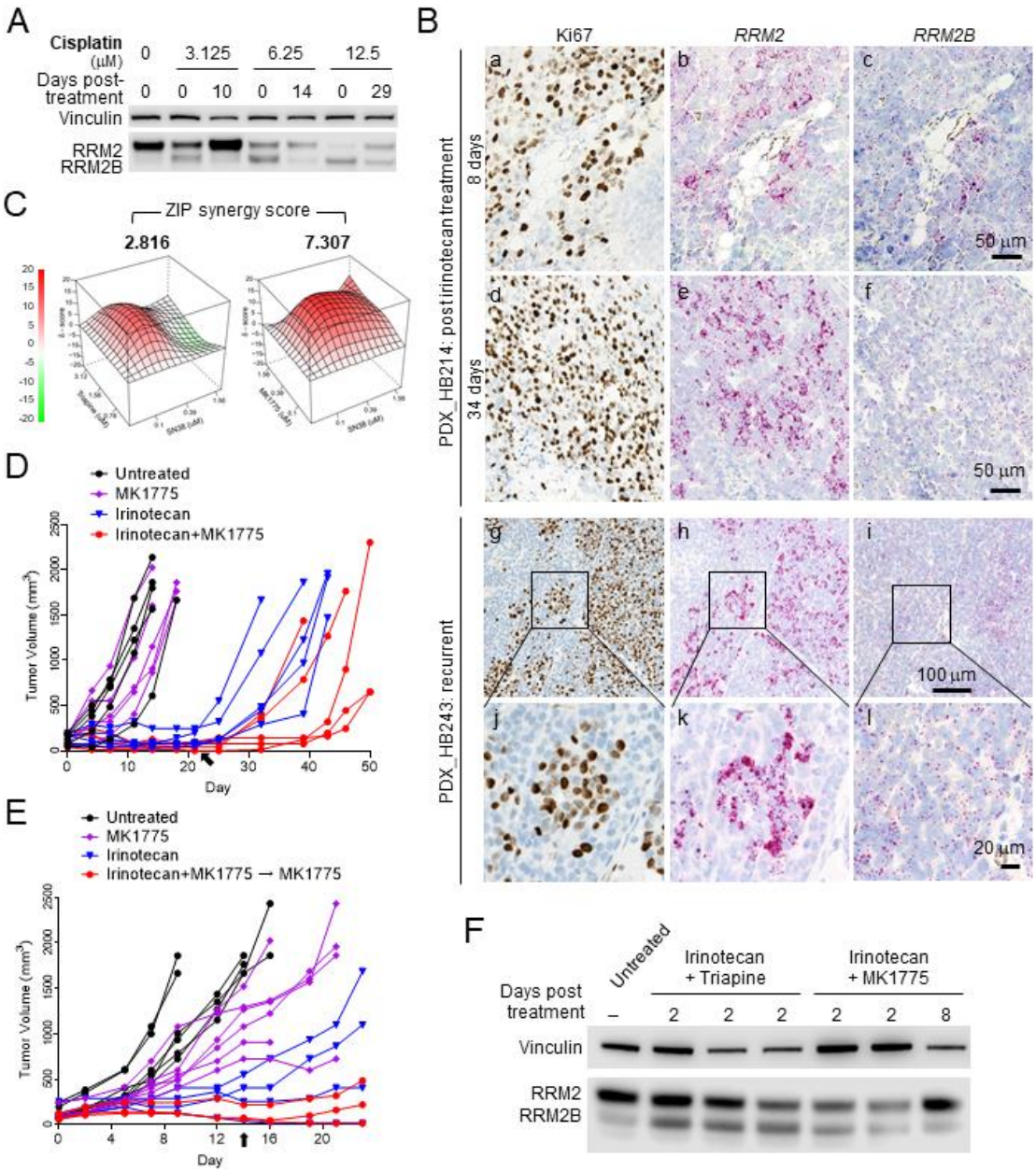
A
Cisplatin (μM)
0
3.125
6.25
12.5
Days post-treatment
0
0
10
0
14
0
29
Vinculin
RRM2
RRM2B
B
Ki67
RRM2
RRM2B
PDX_HB214: post irinotecan treatment
8 days
34 days
PDX_HB243: recurrent
50 μm
100 μm
20 μm
C
ZIP synergy score
2.816
7.307
D
Untreated
MK1775
Irinotecan
Irinotecan+MK1775
Tumor Volume (mm³)
Day
E
Untreated
MK1775
Irinotecan
Irinotecan+MK1775 → MK1775
Tumor Volume (mm³)
Day
F
Untreated
Irinotecan + Triapine
Irinotecan + MK1775
Days post treatment
–
2
2
2
2
2
8
Vinculin
RRM2
RRM2B

tumor (HB243)[230], we similarly found high levels of *RRM2* and low levels of *RRM2B* in $Ki67^+$ cells (**Figure 4-18B, d-l,**).

Based on these results, we tested the efficacy of combining RRM2 inhibitors with chemotherapy in preventing HB relapse. To identify the synergistic combinations, we first tested HepG2 and HB214 cells for combinatorial treatments of the two RRM2 inhibitors, triapine and MK1775, with other chemotherapeutic agents in vitro. We found that SN38, the active form of irinotecan, showed good synergy with both triapine and MK1775 in HB214 (**Figure 4-18C**). With the help of Dr. Stefano Cairo and Dr. Emilie Endersie we then tested triapine/irinotecan and MK1775/irinotecan combinatorial treatment in the HB214 subcutaneous PDX model. Triapine treatment caused rapid body weight loss and all animals had to be removed from the study early (data not shown). Treatment with irinotecan and a low dose of MK1775, which had minimal toxicity or anti-tumor efficacy by itself, showed no additional benefit in tumor suppression compared to irinotecan alone during the three weeks of treatment. However, a modest but statistically significant delay in tumor relapse was observed in mice which previously received the MK1775/irinotecan combinatorial treatment (**Figure 4-18D**). Based on this result, we tested the possibility of continuing this low dose MK1775 as a "maintenance therapy" in a second in vivo test. We shortened MK1775/irinotecan combinatorial treatment to two weeks and then MK1775 alone afterwards. We found that, compared to irinotecan monotherapy, this MK1775/irinotecan-MK1775 treatment regimen was able to delay tumor relapse for approximately 10 days (**Figure 4-18E**). We collected tumor samples from different post-treatment time points and confirmed there was an evident subunit switching from RRM2 to RRM2B in tumors right after treatment and a reversed switching in relapsed tumors (**Figure 4-18F**). These results show a promise in combining RRM2 inhibition with chemotherapy to prevent HB relapse. Future optimization on the drug dose will be necessary as this low-dose of MK1775 we used was only able to delay but not prevent the eventual tumor relapse in both tests.

Overall, out study demonstrates a subunit switching between RRM2 and RRM2B in HB cells in the context of cell proliferation and survival (**Figure 4-19**). RRM2 switches to RRM2B when drug treatment inhibits cell proliferation and induces stress; once helping cells survive the stress, RRM2B switches back to RRM2 to support cell regrowth.

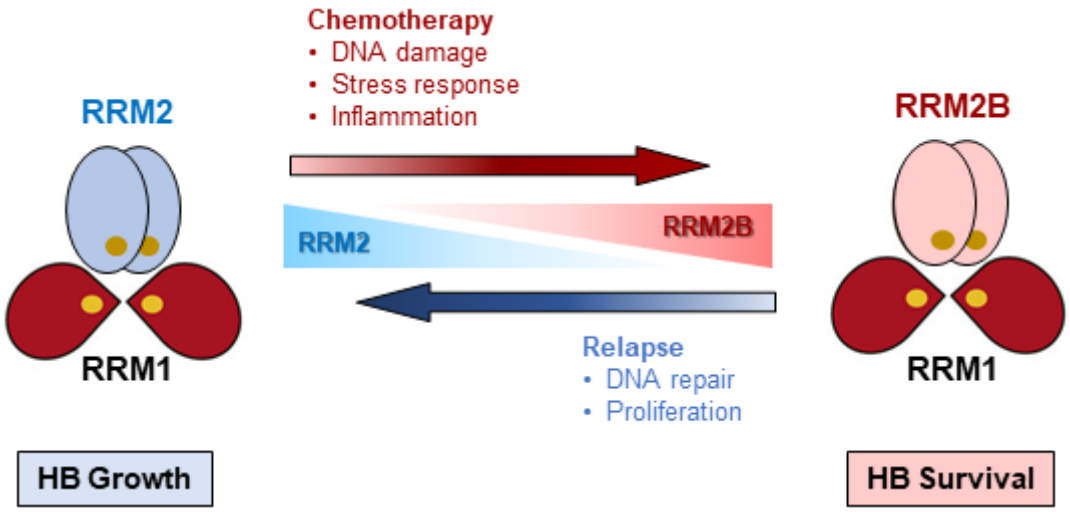

Figure 4-19. A working model of RRM2 and RRM2B subunit switching in HB growth, drug response, and relapse.
Schematic representation of the dynamic relationship between RRM2 and RRM2B.

CHAPTER 5. DISCUSSION

Rare pediatric cancers present one of the greatest challenges to the oncology community because of the limited number of patients available for therapeutic and biological investigations. HB is a very rare cancer but the most common liver cancer in children. HB is also one of the most genetically simple cancer types with low numbers of genomic abnormalities.[126] Little is known how some HB tumors, with minimal alterations in their genomic profiles, manage to progress into highly advanced stages and develop drug resistance. Studies have shown that the drug resistance of many adult solid tumors can be mediated by an adaptive and often reversible cellular state tumor cells turn on under stressful conditions.[211, 212, 238, 239] Past HB studies have mainly focused on the "natural" biology driving advanced tumor progression in an effort to find better treatment for the high-risk forms of this disease that are resistant to standard treatment.[43, 195, 240] With the increasing appreciation of cancer cell plasticity in drug resistance through studies in adults, understanding mechanisms that enable HB cells to survive drug treatment and support subsequent relapse has become a potential path leading to a better treatment of this pediatric cancer.

RRM2 is well known for its upregulation in adult solid tumors and its essential role in supporting cell proliferation.[217-221] RRM2B has also been reported to contribute to stress response and drug resistance of cancer cells.[111, 115, 241] RRM2B subunit switching had been reported before under hypoxic conditions.[116] However, we believe this work is one of first studies that has revealed a dynamic, reversible switching between the two RNR M2 subunits under chemotherapy and depicted a biological picture on how HB cells transit between a growing state and a surviving state from a point of RNR dynamics.

In **Figure 4-7** I show this dynamic switching of the two RNR2 subunits following different chemotherapy treatments. However, this is from a pool of cells, and it is possible that this response is not occurring in every cell and that some cells have high RRM2B while others do not. Validating this subunit switching at the single cell level would further prove the importance of RRM2B in response to chemotherapy. This could be done by attaching a fluorescent tag to endogenous RRM2 (GFP) and RRM2B (RFP). Upon treatment you would be able to perform live cell imaging of a single cell and monitor the change in fluorescence from green to red and actively monitor the dynamic relationship between these two proteins.

The mechanism of RRM2B induction following chemotherapy needs to be investigated further. We show in **Figure 4-9** that there is an association between TP53 expression and RRM2B expression in HepG2 cells. There is also chromatin immunoprecipitation sequencing (ChIP-seq) data available that shows binding of TP53 to RRM2B in HepG2 cells[233]. However, this ChIP-seq was performed in untreated HepG2 cells. This same experiment should be done in treated HepG2 cells with increasing concentrations of therapeutic agents to further validate TP53 dependent induction of RRM2B following treatment. Furthermore, obe could introduce loss of

function mutations of TP53 in to HepG2 cells such as R249S[242] and test whether is similarly induces RRM2B expression both at the RNA level and protein level following treatment. One could then re-introduce wild type TP53 to see if induction can be rescued.

As mentioned previously, RRM2 is cell cycle regulated, and therefore has been a target for chemotherapy as a way of targeting proliferative cells, several of which I mentioned earlier (**Chapter 2)**. There are two current downsides to RRM2 inhibitors. First is the lack of specificity of these inhibitors. Several compounds that inhibit RRM2, specifically target the non-heme iron group in RRM2. These compounds will also target other metalloproteins which can lead to severe side effects or decrease the effectiveness of these compounds due to the saturation of multiple targets. The second downside is that a number of drugs need the RRM1/RRM2 holocomplex in order for them to engage the binding pocket. This leads other compounds to compete for the binding pocket such as nucleosides and allosteric regulators and thereby decrease the drug's efficacy. Both reasons highlight the need for RRM2 specific inhibitors.

siRNAs have been developed to target RRM2 and have shown effectiveness when working in combination with other drugs in several cancer types including pancreatic adenocarcinoma,[87] clear cell renal carcinoma,[80] and CML.[83] However, difficulties in siRNA delivery makes siRNA-based therapy clinically challenging. In fact, a few different applications have been developed using liposomes or nanoparticles which increase the efficacy of the siRNA by increasing the solubility and half-life.[220] Although these delivery systems have seen increased efficacy in vivo in pancreatic carcinoma[221] and even HCC [222], more clinical validation is warranted.

Our study suggests that RRM2B-specific inhibitors, when developed, can be very promising anti-cancer agents when combined with standard treatment for its non-essential role in normal cells but its critical role in drug resistance and cancer relapse. The idea of targeting the cellular response to stress is not novel. Programed death receptor and ligand 1 (PD-1/PD-L1) plays an important role in the ability of cytotoxic T cells to kill cancer cells with an increased expression of PD-L1 inducing T cell anergy thus allowing cancer cells to evade killing. It has been reported that stress response from chemotherapy causes an increase in translation of PD-L1 thus decreasing the efficacy of cytotoxic T cells.[243] Targeting of PD-L1 with a PERK inhibitor that increased the activity of cytotoxic T cells showed synergistic effects in vivo.

In that regard, I believe determining the therapeutic value of RRM2B warrants further investigation. In **Chapter 4** I was able to successfully knockout RRM2B in two HB cell lines. While we did see a decrease in colony formation in the KO cells, a common issue with single cell selection following a gene KO, are cells losing dependency of the selected target. However, using a degradation tag (dTAG) system would be able to work around this problem. dTAGs are a method of targeted degradation that by attaching a chemical probe to the target of interest, once can initiate its selective degradation with a heterobifunctional degrader that will bridge the probe (and target of interest) to an E3 ubiquitin ligase.[244] With this system, RRM2B could be specifically

degraded without influencing the dependencies in cells and in mice and would be able to more accurately determine the therapeutic value of RRM2B.

There have not been any reported specific inhibitors of RRM2B until the discovery of compound DFO, mentioned in **Chapter 2**, which was able to bind to RRM2B with higher affinity than to RRM2. When this compound was tested in our hands, we saw no clear inhibition of RRM2B or RRM2 **Figure 4-18**. The lack of RRM2B inhibitors could be because of two main reasons. First is the lack of RRM2B expression in many tumors. Even though there have been some tumors reported to have elevated expression mentioned before, most tumors have low levels unless the tumor is actively stressed recently via hypoxia or chemotherapy. Second is the homology between RRM2 and RRM2B subunits. It would be difficult to design small molecule inhibitors to specifically bind to RRM2B without binding to RRM2 as well.

siRNA have been used to target RRM2B in a similar fashion as RRM2. siRNA inhibition of RRM2B was able to increase sensitivity to radiation in esophageal squamous cell carcinoma[245] and increase the efficacy of 5-FU in oral cancer.[246] These findings are similar to our own suggesting that inhibition of RRM2B could prevent cells from responding to stress from chemotherapy treatment.

One potential method that we would like to try in the future is targeting RRM2B with the use of Proteolysis Targeting Chimeras (PROTACs). PROTACs are a unique targeting technology that makes use of the host's own machinery to degrade the target. PROTACs can bind to their protein of interest (POI) and bring it to the proximity of an E3 ubiquitin ligase, resulting in a stable PROTAC-POI-E3 ternary complex and subsequently proteasomal degradation.[247, 248] One of the advantages of using PROTACs is that the inhibition process is not impeded by traditional targeting stumbling blocks such as competition of substrates or occupancy driven events. This allows PROTACs to achieve greater efficacy at lower concentrations.[249]

Finally, even though RRM2 and RRM2B perform similar enzymatic functions when bound to RRM1, it is clear from the hub gene analysis (**Figure 4-16)** that these two proteins serve different functions in pediatric liver cancer. Elucidating this dynamic relationship needs further studies. One possible relationship between RRM2B and cell survival is with the mitochondria and reactive oxygen species (ROS). As mentioned in **Chapter 2** RRM2B is also responsible for the synthesis of mtDNA. In HB, cisplatin is the most commonly used drug for treatment. Cisplatin not only damages nuclear DNA, it targets mtDNA as well.[250] Excessive mtDNA damage can lead to increase in oxidative stress and the increased production of ROS and eventual cell death.[251] RRM2B has been shown to suppress the oxidative stress pathway[23], contain catalase activity to scavenge ROS[252], and repair mtDNA under stress.[253] The decrease in colony formation observed in **Chapter 4** could be due to the cells inability to handle the oxidative stress and increase in ROS caused by cisplatin treatment leading to eventual cell senescence and death. This hypothesis could be tested by monitoring mitochondrial activity before and after treatment in control cells as well as the RRM2B KO and OE cells we generated. A common gene for monitoring mitochondrial activity is

mitochondrial transcription factor A (TFAM).[254] One could also monitor active ROS production in live cells using fluorescent imaging or flow cytometry. This would be able to determine whether inhibition of RRM2B increases ROS in the cells.

Taken together, in this study, we showed that upregulation of RRM2 is strongly associated with high-risk HB. In an attempt to suppress this molecule with standard chemotherapy as well as its inhibitors, we found that, when RRM2 was effectively suppressed by these drugs, there was a surprising induction of RRM2B, another RNR M2 subunit that shares a high protein homology with RRM2. We confirmed that RRM2B had a lower RNR enzymatic activity than RRM2 as reported and had limited participation in the proliferation or the initial drug response of HB cells. However, we found that RRM2B was critical to the fitness of the HB cells that survived initial drug treatment, allowing them to relapse much more efficiently post drug treatment. When HB cells resumed proliferation during relapse, RRM2 became the dominant RNR M2 subunit again and RRM2B gradually dropped to its low, pre-treatment level. Adding a low-dose of RRM2 inhibitor MK1775 to irinotecan was able to delay the tumor relapse in an HB PDX model compared to irinotecan treatment alone. Computational analysis of publicly available HB and HCC patient transcriptomic profiles and our RNR-manipulated HB cells revealed distinct cellular network associated with these two RNR M2 subunits. Consistent with the cell and tumor phenotypes we observed, $PTWAY^{RRM2}$ is primarily inolved in cell proliferation and DNA repair while $PTWAY^{RRM2B}$ participates heavily in stress and inflammatory responses.

LIST OF REFERENCES

1. Spector LG, Birch J. The epidemiology of hepatoblastoma. Pediatr Blood Cancer 2012;59:776-9http://dx.doi.org/10.1002/pbc.24215.

2. Feusner J, Buckley J, Robison L, et al. Prematurity and hepatoblastoma: more than just an association? J Pediatr 1998;133:585-6http://dx.doi.org/10.1016/s0022-3476(98)70084-8.

3. Feng J, He Y, Wei L, et al. Assessment of Survival of Pediatric Patients With Hepatoblastoma Who Received Chemotherapy Following Liver Transplant or Liver Resection. JAMA Netw Open 2019;2:e1912676http://dx.doi.org/10.1001/jamanetworkopen.2019.12676.

4. Shi Y, Geller JI, Ma IT, et al. Relapsed hepatoblastoma confined to the lung is effectively treated with pulmonary metastasectomy. J Pediatr Surg 2016;51:525-9http://dx.doi.org/10.1016/j.jpedsurg.2015.10.053.

5. Hishiki T, Matsunaga T, Sasaki F, et al. Outcome of hepatoblastomas treated using the Japanese Study Group for Pediatric Liver Tumor (JPLT) protocol-2: report from the JPLT. Pediatr Surg Int 2011;27:1-8http://dx.doi.org/10.1007/s00383-010-2708-0.

6. Hu HM, Zhang WL, Wang YZ, et al. Treatment outcomes for hepatoblastoma children with pulmonary metastasis and extrapulmonary involvement: experience of 36 cases at a single institution. Transl Cancer Res 2020;9:6402-6411http://dx.doi.org/10.21037/tcr-20-1876.

7. Aronson DC, Czauderna P, Maibach R, et al. The treatment of hepatoblastoma: Its evolution and the current status as per the SIOPEL trials. J Indian Assoc Pediatr Surg 2014;19:201-7http://dx.doi.org/10.4103/0971-9261.142001.

8. Colon NC, Chung DH. Neuroblastoma. Adv Pediatr 2011;58:297-311http://dx.doi.org/10.1016/j.yapd.2011.03.011.

9. Balyasny S, Lee SM, Desai AV, et al. Association Between Participation in Clinical Trials and Overall Survival Among Children With Intermediate- or High-risk Neuroblastoma. JAMA Netw Open 2021;4:e2116248http://dx.doi.org/10.1001/jamanetworkopen.2021.16248.

10. Rikhi RR, Spady KK, Hoffman RI, et al. Hepatoblastoma: A Need for Cell Lines and Tissue Banks to Develop Targeted Drug Therapies. Front Pediatr 2016;4:22http://dx.doi.org/10.3389/fped.2016.00022.

11. Zhu L, Finkelstein D, Gao C, et al. Multi-organ Mapping of Cancer Risk. Cell 2016;166:1132-1146 e7http://dx.doi.org/10.1016/j.cell.2016.07.045.

12. Adams JM, Jafar-Nejad H. The Roles of Notch Signaling in Liver Development and Disease. Biomolecules 2019;9http://dx.doi.org/10.3390/biom9100608.

13. Li L, Qian M, Chen IH, et al. Acquisition of Cholangiocarcinoma Traits during Advanced Hepatocellular Carcinoma Development in Mice. Am J Pathol 2018;188:656-671http://dx.doi.org/10.1016/j.ajpath.2017.11.013.

14. Chang JC. Cancer stem cells: Role in tumor growth, recurrence, metastasis, and treatment resistance. Medicine (Baltimore) 2016;95:S20-S25http://dx.doi.org/10.1097/MD.0000000000004766.

15. Gunti S, Hoke ATK, Vu KP, et al. Organoid and Spheroid Tumor Models: Techniques and Applications. Cancers (Basel) 2021;13http://dx.doi.org/10.3390/cancers13040874.

16. Aye Y, Li M, Long MJ, et al. Ribonucleotide reductase and cancer: biological mechanisms and targeted therapies. Oncogene 2015;34:2011-21http://dx.doi.org/10.1038/onc.2014.155.

17. Zhuang S, Li L, Zang Y, et al. RRM2 elicits the metastatic potential of breast cancer cells by regulating cell invasion, migration and VEGF expression via the PI3K/AKT signaling. Oncol Lett 2020;19:3349-3355http://dx.doi.org/10.3892/ol.2020.11428.

18. Wang J, Yi Y, Chen Y, et al. Potential mechanism of RRM2 for promoting Cervical Cancer based on weighted gene co-expression network analysis. Int J Med Sci 2020;17:2362-2372http://dx.doi.org/10.7150/ijms.47356.

19. Jiang X, Li Y, Zhang N, et al. RRM2 silencing suppresses malignant phenotype and enhances radiosensitivity via activating cGAS/STING signaling pathway in lung adenocarcinoma. Cell Biosci 2021;11:74http://dx.doi.org/10.1186/s13578-021-00586-5.

20. Yang Y, Lin J, Guo S, et al. RRM2 protects against ferroptosis and is a tumor biomarker for liver cancer. Cancer Cell Int 2020;20:587http://dx.doi.org/10.1186/s12935-020-01689-8.

21. Zhan Y, Jiang L, Jin X, et al. Inhibiting RRM2 to enhance the anticancer activity of chemotherapy. Biomed Pharmacother 2021;133:110996http://dx.doi.org/10.1016/j.biopha.2020.110996.

22. Pfister SX, Markkanen E, Jiang Y, et al. Inhibiting WEE1 Selectively Kills Histone H3K36me3-Deficient Cancers by dNTP Starvation. Cancer Cell 2015;28:557-568http://dx.doi.org/10.1016/j.ccell.2015.09.015.

23. Kuo ML, Sy AJ, Xue L, et al. RRM2B suppresses activation of the oxidative stress pathway and is up-regulated by p53 during senescence. Sci Rep 2012;2:822http://dx.doi.org/10.1038/srep00822.

24. Venkatramani R, Spector LG, Georgieff M, et al. Congenital abnormalities and hepatoblastoma: a report from the Children's Oncology Group (COG) and the Utah Population Database (UPDB). Am J Med Genet A 2014;164A:2250-5http://dx.doi.org/10.1002/ajmg.a.36638.

25. Clericuzio CL, Chen E, McNeil DE, et al. Serum alpha-fetoprotein screening for hepatoblastoma in children with Beckwith-Wiedemann syndrome or isolated hemihyperplasia. J Pediatr 2003;143:270-2http://dx.doi.org/10.1067/S0022-3476(03)00306-8.

26. Darbari A, Sabin KM, Shapiro CN, et al. Epidemiology of primary hepatic malignancies in U.S. children. Hepatology 2003;38:560-6http://dx.doi.org/10.1053/jhep.2003.50375.

27. Ranganathan S, Lopez-Terrada D, Alaggio R. Hepatoblastoma and Pediatric Hepatocellular Carcinoma: An Update. Pediatr Dev Pathol 2020;23:79-95http://dx.doi.org/10.1177/1093526619875228.

28. Ng K, Mogul DB. Pediatric Liver Tumors. Clin Liver Dis 2018;22:753-772http://dx.doi.org/10.1016/j.cld.2018.06.008.

29. Wu JT, Book L, Sudar K. Serum alpha fetoprotein (AFP) levels in normal infants. Pediatr Res 1981;15:50-2http://dx.doi.org/10.1203/00006450-198101000-00012.

30. Abenoza P, Manivel JC, Wick MR, et al. Hepatoblastoma: an immunohistochemical and ultrastructural study. Hum Pathol 1987;18:1025-35http://dx.doi.org/10.1016/s0046-8177(87)80219-8.

31. Ruck P, Xiao JC, Pietsch T, et al. Hepatic stem cells in the human liver. Histopathology 1996;29:590-2http://dx.doi.org/10.1046/j.1365-2559.1996.d01-547.x.

32. Wang LL, Filippi RZ, Zurakowski D, et al. Effects of neoadjuvant chemotherapy on hepatoblastoma: a morphologic and immunohistochemical study. Am J Surg Pathol 2010;34:287-99http://dx.doi.org/10.1097/PAS.0b013e3181ce5f1e.

33. Towbin AJ, Meyers RL, Woodley H, et al. 2017 PRETEXT: radiologic staging system for primary hepatic malignancies of childhood revised for the Paediatric

Hepatic International Tumour Trial (PHITT). Pediatr Radiol 2018;48:536-554http://dx.doi.org/10.1007/s00247-018-4078-z.

34. Lopez-Terrada D, Alaggio R, de Davila MT, et al. Towards an international pediatric liver tumor consensus classification: proceedings of the Los Angeles COG liver tumors symposium. Mod Pathol 2014;27:472-91http://dx.doi.org/10.1038/modpathol.2013.80.

35. Meyers RL, Maibach R, Hiyama E, et al. Risk-stratified staging in paediatric hepatoblastoma: a unified analysis from the Children's Hepatic tumors International Collaboration. Lancet Oncol 2017;18:122-131http://dx.doi.org/10.1016/S1470-2045(16)30598-8.

36. Haas JE, Feusner JH, Finegold MJ. Small cell undifferentiated histology in hepatoblastoma may be unfavorable. Cancer 2001;92:3130-4http://dx.doi.org/10.1002/1097-0142(20011215)92:12<3130::aid-cncr10115>3.0.co;2-#.

37. Kiruthiga KG, Ramakrishna B, Saha S, et al. Histological and immunohistochemical study of hepatoblastoma: correlation with tumour behaviour and survival. J Gastrointest Oncol 2018;9:326-337http://dx.doi.org/10.21037/jgo.2018.01.08.

38. Totoki Y, Tatsuno K, Covington KR, et al. Trans-ancestry mutational landscape of hepatocellular carcinoma genomes. Nat Genet 2014;46:1267-73http://dx.doi.org/10.1038/ng.3126.

39. Takigawa Y, Brown AM. Wnt signaling in liver cancer. Curr Drug Targets 2008;9:1013-24http://dx.doi.org/10.2174/138945008786786127.

40. Anna CH, Sills RC, Foley JF, et al. Beta-catenin mutations and protein accumulation in all hepatoblastomas examined from B6C3F1 mice treated with anthraquinone or oxazepam. Cancer Res 2000;60:2864-8.

41. Hayashi SM, Ton TV, Hong HH, et al. Genetic alterations in the Catnb gene but not the H-ras gene in hepatocellular neoplasms and hepatoblastomas of B6C3F(1) mice following exposure to diethanolamine for 2 years. Chem Biol Interact 2003;146:251-61http://dx.doi.org/10.1016/j.cbi.2003.07.001.

42. Buendia MA. Genetic alterations in hepatoblastoma and hepatocellular carcinoma: common and distinctive aspects. Med Pediatr Oncol 2002;39:530-5http://dx.doi.org/10.1002/mpo.10180.

43. Tao J, Calvisi DF, Ranganathan S, et al. Activation of beta-catenin and Yap1 in human hepatoblastoma and induction of hepatocarcinogenesis in mice.

Gastroenterology 2014;147:690-701http://dx.doi.org/10.1053/j.gastro.2014.05.004.

44. Prokurat A, Kluge P, Kosciesza A, et al. Transitional liver cell tumors (TLCT) in older children and adolescents: a novel group of aggressive hepatic tumors expressing beta-catenin. Med Pediatr Oncol 2002;39:510-8http://dx.doi.org/10.1002/mpo.10177.

45. Eichenmuller M, Trippel F, Kreuder M, et al. The genomic landscape of hepatoblastoma and their progenies with HCC-like features. J Hepatol 2014;61:1312-20http://dx.doi.org/10.1016/j.jhep.2014.08.009.

46. Nagae G, Yamamoto S, Fujita M, et al. Genetic and epigenetic basis of hepatoblastoma diversity. Nat Commun 2021;12:5423http://dx.doi.org/10.1038/s41467-021-25430-9.

47. Kikuchi A, Yamamoto H, Sato A. Selective activation mechanisms of Wnt signaling pathways. Trends Cell Biol 2009;19:119-29http://dx.doi.org/10.1016/j.tcb.2009.01.003.

48. Pai SG, Carneiro BA, Mota JM, et al. Wnt/beta-catenin pathway: modulating anticancer immune response. J Hematol Oncol 2017;10:101http://dx.doi.org/10.1186/s13045-017-0471-6.

49. Clevers H. Wnt/beta-catenin signaling in development and disease. Cell 2006;127:469-80http://dx.doi.org/10.1016/j.cell.2006.10.018.

50. Litten JB, Chen TT, Schultz R, et al. Activated NOTCH2 is overexpressed in hepatoblastomas: an immunohistochemical study. Pediatr Dev Pathol 2011;14:378-83http://dx.doi.org/10.2350/10-09-0900-OA.1.

51. Lopez-Terrada D, Gunaratne PH, Adesina AM, et al. Histologic subtypes of hepatoblastoma are characterized by differential canonical Wnt and Notch pathway activation in DLK+ precursors. Hum Pathol 2009;40:783-94http://dx.doi.org/10.1016/j.humpath.2008.07.022.

52. Kremer N, Walther AE, Tiao GM. Management of hepatoblastoma: an update. Curr Opin Pediatr 2014;26:362-9http://dx.doi.org/10.1097/MOP.0000000000000081.

53. Semeraro M, Branchereau S, Maibach R, et al. Relapses in hepatoblastoma patients: clinical characteristics and outcome--experience of the International Childhood Liver Tumour Strategy Group (SIOPEL). Eur J Cancer 2013;49:915-22http://dx.doi.org/10.1016/j.ejca.2012.10.003.

54. Wanaguru D, Shun A, Price N, et al. Outcomes of pulmonary metastases in hepatoblastoma--is the prognosis always poor? J Pediatr Surg 2013;48:2474-8http://dx.doi.org/10.1016/j.jpedsurg.2013.08.023.

55. Feng TC, Zai HY, Jiang W, et al. Survival and analysis of prognostic factors for hepatoblastoma: based on SEER database. Ann Transl Med 2019;7:555http://dx.doi.org/10.21037/atm.2019.09.76.

56. Kelly D, Sharif K, Brown RM, et al. Hepatocellular carcinoma in children. Clin Liver Dis 2015;19:433-47http://dx.doi.org/10.1016/j.cld.2015.01.010.

57. Allan BJ, Wang B, Davis JS, et al. A review of 218 pediatric cases of hepatocellular carcinoma. J Pediatr Surg 2014;49:166-71; discussion 171http://dx.doi.org/10.1016/j.jpedsurg.2013.09.050.

58. Lee CL, Ko YC. Survival and distribution pattern of childhood liver cancer in Taiwan. Eur J Cancer 1998;34:2064-7http://dx.doi.org/10.1016/s0959-8049(98)00281-0.

59. Chang MH, You SL, Chen CJ, et al. Decreased incidence of hepatocellular carcinoma in hepatitis B vaccinees: a 20-year follow-up study. J Natl Cancer Inst 2009;101:1348-55http://dx.doi.org/10.1093/jnci/djp288.

60. Khanna R, Verma SK. Pediatric hepatocellular carcinoma. World J Gastroenterol 2018;24:3980-3999http://dx.doi.org/10.3748/wjg.v24.i35.3980.

61. Tummala KS, Brandt M, Teijeiro A, et al. Hepatocellular Carcinomas Originate Predominantly from Hepatocytes and Benign Lesions from Hepatic Progenitor Cells. Cell Rep 2017;19:584-600http://dx.doi.org/10.1016/j.celrep.2017.03.059.

62. Moore SW, Millar AJ, Hadley GP, et al. Hepatocellular carcinoma and liver tumors in South African children: a case for increased prevalence. Cancer 2004;101:642-9http://dx.doi.org/10.1002/cncr.20398.

63. Di Tommaso L, Destro A, Seok JY, et al. The application of markers (HSP70 GPC3 and GS) in liver biopsies is useful for detection of hepatocellular carcinoma. J Hepatol 2009;50:746-54http://dx.doi.org/10.1016/j.jhep.2008.11.014.

64. Capurro M, Wanless IR, Sherman M, et al. Glypican-3: a novel serum and histochemical marker for hepatocellular carcinoma. Gastroenterology 2003;125:89-97http://dx.doi.org/10.1016/s0016-5085(03)00689-9.

65. Bioulac-Sage P, Sempoux C, Balabaud C. Hepatocellular adenoma: Classification, variants and clinical relevance. Semin Diagn Pathol 2017;34:112-125http://dx.doi.org/10.1053/j.semdp.2016.12.007.

66. Sergi CM. Hepatocellular Carcinoma, Fibrolamellar Variant: Diagnostic Pathologic Criteria and Molecular Pathology Update. A Primer. Diagnostics (Basel) 2015;6http://dx.doi.org/10.3390/diagnostics6010003.

67. Honeyman JN, Simon EP, Robine N, et al. Detection of a recurrent DNAJB1-PRKACA chimeric transcript in fibrolamellar hepatocellular carcinoma. Science 2014;343:1010-4http://dx.doi.org/10.1126/science.1249484.

68. Luo JH, Ren B, Keryanov S, et al. Transcriptomic and genomic analysis of human hepatocellular carcinomas and hepatoblastomas. Hepatology 2006;44:1012-24http://dx.doi.org/10.1002/hep.21328.

69. Aronson DC, Meyers RL. Malignant tumors of the liver in children. Semin Pediatr Surg 2016;25:265-275http://dx.doi.org/10.1053/j.sempedsurg.2016.09.002.

70. Czauderna P, Mackinlay G, Perilongo G, et al. Hepatocellular carcinoma in children: results of the first prospective study of the International Society of Pediatric Oncology group. J Clin Oncol 2002;20:2798-804http://dx.doi.org/10.1200/JCO.2002.06.102.

71. Kim A, Widemann BC, Krailo M, et al. Phase 2 trial of sorafenib in children and young adults with refractory solid tumors: A report from the Children's Oncology Group. Pediatr Blood Cancer 2015;62:1562-6http://dx.doi.org/10.1002/pbc.25548.

72. Murawski M, Weeda VB, Maibach R, et al. Hepatocellular Carcinoma in Children: Does Modified Platinum- and Doxorubicin-Based Chemotherapy Increase Tumor Resectability and Change Outcome? Lessons Learned From the SIOPEL 2 and 3 Studies. J Clin Oncol 2016;34:1050-6http://dx.doi.org/10.1200/JCO.2014.60.2250.

73. Nordlund P, Reichard P. Ribonucleotide reductases. Annu Rev Biochem 2006;75:681-706http://dx.doi.org/10.1146/annurev.biochem.75.103004.142443.

74. Jordan A, Reichard P. Ribonucleotide reductases. Annu Rev Biochem 1998;67:71-98http://dx.doi.org/10.1146/annurev.biochem.67.1.71.

75. Bester AC, Roniger M, Oren YS, et al. Nucleotide deficiency promotes genomic instability in early stages of cancer development. Cell 2011;145:435-46http://dx.doi.org/10.1016/j.cell.2011.03.044.

76. Chabes A, Georgieva B, Domkin V, et al. Survival of DNA damage in yeast directly depends on increased dNTP levels allowed by relaxed feedback inhibition

of ribonucleotide reductase. Cell 2003;112:391-401http://dx.doi.org/10.1016/s0092-8674(03)00075-8.

77. Reichard P. Interactions between deoxyribonucleotide and DNA synthesis. Annu Rev Biochem 1988;57:349-74http://dx.doi.org/10.1146/annurev.bi.57.070188.002025.

78. Fersht AR. Fidelity of replication of phage phi X174 DNA by DNA polymerase III holoenzyme: spontaneous mutation by misincorporation. Proc Natl Acad Sci U S A 1979;76:4946-50http://dx.doi.org/10.1073/pnas.76.10.4946.

79. Jordheim LP, Seve P, Tredan O, et al. The ribonucleotide reductase large subunit (RRM1) as a predictive factor in patients with cancer. Lancet Oncol 2011;12:693-702http://dx.doi.org/10.1016/S1470-2045(10)70244-8.

80. Engstrom Y, Eriksson S, Jildevik I, et al. Cell cycle-dependent expression of mammalian ribonucleotide reductase. Differential regulation of the two subunits. J Biol Chem 1985;260:9114-6.

81. Mann GJ, Musgrove EA, Fox RM, et al. Ribonucleotide reductase M1 subunit in cellular proliferation, quiescence, and differentiation. Cancer Res 1988;48:5151-6.

82. Bjorklund S, Skog S, Tribukait B, et al. S-phase-specific expression of mammalian ribonucleotide reductase R1 and R2 subunit mRNAs. Biochemistry 1990;29:5452-8http://dx.doi.org/10.1021/bi00475a007.

83. Fan H, Huang A, Villegas C, et al. The R1 component of mammalian ribonucleotide reductase has malignancy-suppressing activity as demonstrated by gene transfer experiments. Proc Natl Acad Sci U S A 1997;94:13181-6http://dx.doi.org/10.1073/pnas.94.24.13181.

84. Gautam A, Bepler G. Suppression of lung tumor formation by the regulatory subunit of ribonucleotide reductase. Cancer Res 2006;66:6497-502http://dx.doi.org/10.1158/0008-5472.CAN-05-4462.

85. Zhang X, Taoka R, Liu D, et al. Knockdown of RRM1 with Adenoviral shRNA Vectors to Inhibit Tumor Cell Viability and Increase Chemotherapeutic Sensitivity to Gemcitabine in Bladder Cancer Cells. Int J Mol Sci 2021;22http://dx.doi.org/10.3390/ijms22084102.

86. Davidson JD, Ma L, Flagella M, et al. An increase in the expression of ribonucleotide reductase large subunit 1 is associated with gemcitabine resistance in non-small cell lung cancer cell lines. Cancer Res 2004;64:3761-6http://dx.doi.org/10.1158/0008-5472.CAN-03-3363.

87. Bepler G, Kusmartseva I, Sharma S, et al. RRM1 modulated in vitro and in vivo efficacy of gemcitabine and platinum in non-small-cell lung cancer. J Clin Oncol 2006;24:4731-7http://dx.doi.org/10.1200/JCO.2006.06.1101.

88. Nakahira S, Nakamori S, Tsujie M, et al. Involvement of ribonucleotide reductase M1 subunit overexpression in gemcitabine resistance of human pancreatic cancer. Int J Cancer 2007;120:1355-63http://dx.doi.org/10.1002/ijc.22390.

89. Reid G, Wallant NC, Patel R, et al. Potent subunit-specific effects on cell growth and drug sensitivity from optimised siRNA-mediated silencing of ribonucleotide reductase. J RNAi Gene Silencing 2009;5:321-30.

90. Ohtaka K, Kohya N, Sato K, et al. Ribonucleotide reductase subunit M1 is a possible chemoresistance marker to gemcitabine in biliary tract carcinoma. Oncol Rep 2008;20:279-86.

91. Toffalorio F, Giovannetti E, De Pas T, et al. Expression of gemcitabine- and cisplatin-related genes in non-small-cell lung cancer. Pharmacogenomics J 2010;10:180-90http://dx.doi.org/10.1038/tpj.2009.53.

92. Rosell R, Danenberg KD, Alberola V, et al. Ribonucleotide reductase messenger RNA expression and survival in gemcitabine/cisplatin-treated advanced non-small cell lung cancer patients. Clin Cancer Res 2004;10:1318-25http://dx.doi.org/10.1158/1078-0432.ccr-03-0156.

93. Kato T, Ono H, Fujii M, et al. Cytoplasmic RRM1 activation as an acute response to gemcitabine treatment is involved in drug resistance of pancreatic cancer cells. PLoS One 2021;16:e0252917http://dx.doi.org/10.1371/journal.pone.0252917.

94. DeGregori J, Kowalik T, Nevins JR. Cellular targets for activation by the E2F1 transcription factor include DNA synthesis- and G1/S-regulatory genes. Mol Cell Biol 1995;15:4215-24http://dx.doi.org/10.1128/MCB.15.8.4215.

95. Trimarchi JM, Lees JA. Sibling rivalry in the E2F family. Nat Rev Mol Cell Biol 2002;3:11-20http://dx.doi.org/10.1038/nrm714.

96. Chabes A, Thelander L. Controlled protein degradation regulates ribonucleotide reductase activity in proliferating mammalian cells during the normal cell cycle and in response to DNA damage and replication blocks. J Biol Chem 2000;275:17747-53http://dx.doi.org/10.1074/jbc.M000799200.

97. Guittet O, Hakansson P, Voevodskaya N, et al. Mammalian p53R2 protein forms an active ribonucleotide reductase in vitro with the R1 protein, which is expressed both in resting cells in response to DNA damage and in proliferating cells. J Biol Chem 2001;276:40647-51http://dx.doi.org/10.1074/jbc.M106088200.

98. Wettergren Y, Kullberg A, Levan G. Drug-specific rearrangements of chromosome 12 in hydroxyurea-resistant mouse SEWA cells: support for chromosomal breakage model of gene amplification. Somat Cell Mol Genet 1994;20:267-85http://dx.doi.org/10.1007/BF02254717.

99. Zhou B, Mo X, Liu X, et al. Human ribonucleotide reductase M2 subunit gene amplification and transcriptional regulation in a homogeneous staining chromosome region responsible for the mechanism of drug resistance. Cytogenet Cell Genet 2001;95:34-42http://dx.doi.org/10.1159/000057014.

100. Zhang YW, Jones TL, Martin SE, et al. Implication of checkpoint kinase-dependent up-regulation of ribonucleotide reductase R2 in DNA damage response. J Biol Chem 2009;284:18085-95http://dx.doi.org/10.1074/jbc.M109.003020.

101. Liu X, Zhou B, Xue L, et al. Nuclear factor Y regulation and promoter transactivation of human ribonucleotide reductase subunit M2 gene in a Gemcitabine resistant KB clone. Biochem Pharmacol 2004;67:1499-511http://dx.doi.org/10.1016/j.bcp.2003.12.026.

102. Yan T, Li HY, Wu JS, et al. Astaxanthin inhibits gemcitabine-resistant human pancreatic cancer progression through EMT inhibition and gemcitabine resensitization. Oncol Lett 2017;14:5400-5408http://dx.doi.org/10.3892/ol.2017.6836.

103. Huang N, Guo W, Ren K, et al. LncRNA AFAP1-AS1 Supresses miR-139-5p and Promotes Cell Proliferation and Chemotherapy Resistance of Non-small Cell Lung Cancer by Competitively Upregulating RRM2. Front Oncol 2019;9:1103http://dx.doi.org/10.3389/fonc.2019.01103.

104. Zhao H, Zheng GH, Li GC, et al. Long noncoding RNA LINC00958 regulates cell sensitivity to radiotherapy through RRM2 by binding to microRNA-5095 in cervical cancer. J Cell Physiol 2019;234:23349-23359http://dx.doi.org/10.1002/jcp.28902.

105. Osako Y, Yoshino H, Sakaguchi T, et al. Potential tumorsuppressive role of microRNA99a3p in sunitinibresistant renal cell carcinoma cells through the regulation of RRM2. Int J Oncol 2019;54:1759-1770http://dx.doi.org/10.3892/ijo.2019.4736.

106. Wang C, Zhang W, Fu M, et al. Establishment of human pancreatic cancer gemcitabineresistant cell line with ribonucleotide reductase overexpression. Oncol Rep 2015;33:383-90http://dx.doi.org/10.3892/or.2014.3599.

107. Zhou S, Li J, Xu H, et al. Liposomal curcumin alters chemosensitivity of breast cancer cells to Adriamycin via regulating microRNA expression. Gene 2017;622:1-12http://dx.doi.org/10.1016/j.gene.2017.04.026.

108. Liu C, Li Y, Hu R, et al. Knockdown of ribonucleotide reductase regulatory subunit M2 increases the drug sensitivity of chronic myeloid leukemia to imatinibbased therapy. Oncol Rep 2019;42:571-580http://dx.doi.org/10.3892/or.2019.7194.

109. Putluri N, Maity S, Kommagani R, et al. Pathway-centric integrative analysis identifies RRM2 as a prognostic marker in breast cancer associated with poor survival and tamoxifen resistance. Neoplasia 2014;16:390-402http://dx.doi.org/10.1016/j.neo.2014.05.007.

110. Elford HL, Freese M, Passamani E, et al. Ribonucleotide reductase and cell proliferation. I. Variations of ribonucleotide reductase activity with tumor growth rate in a series of rat hepatomas. J Biol Chem 1970;245:5228-33.

111. Tanaka H, Arakawa H, Yamaguchi T, et al. A ribonucleotide reductase gene involved in a p53-dependent cell-cycle checkpoint for DNA damage. Nature 2000;404:42-9http://dx.doi.org/10.1038/35003506.

112. Lin ZP, Belcourt MF, Cory JG, et al. Stable suppression of the R2 subunit of ribonucleotide reductase by R2-targeted short interference RNA sensitizes p53(-/-) HCT-116 colon cancer cells to DNA-damaging agents and ribonucleotide reductase inhibitors. J Biol Chem 2004;279:27030-8http://dx.doi.org/10.1074/jbc.M402056200.

113. Lin ZP, Belcourt MF, Carbone R, et al. Excess ribonucleotide reductase R2 subunits coordinate the S phase checkpoint to facilitate DNA damage repair and recovery from replication stress. Biochem Pharmacol 2007;73:760-72http://dx.doi.org/10.1016/j.bcp.2006.11.014.

114. Shao J, Zhou B, Zhu L, et al. In vitro characterization of enzymatic properties and inhibition of the p53R2 subunit of human ribonucleotide reductase. Cancer Res 2004;64:1-6http://dx.doi.org/10.1158/0008-5472.can-03-3048.

115. Wang X, Zhenchuk A, Wiman KG, et al. Regulation of p53R2 and its role as potential target for cancer therapy. Cancer Lett 2009;276:1-7http://dx.doi.org/10.1016/j.canlet.2008.07.019.

116. Foskolou IP, Jorgensen C, Leszczynska KB, et al. Ribonucleotide Reductase Requires Subunit Switching in Hypoxia to Maintain DNA Replication. Mol Cell 2017;66:206-220 e9http://dx.doi.org/10.1016/j.molcel.2017.03.005.

117. Baugh EH, Ke H, Levine AJ, et al. Why are there hotspot mutations in the TP53 gene in human cancers? Cell Death Differ 2018;25:154-160http://dx.doi.org/10.1038/cdd.2017.180.

118. Cho EC, Kuo ML, Cheng JH, et al. RRM2B-Mediated Regulation of Mitochondrial Activity and Inflammation under Oxidative Stress. Mediators Inflamm 2015;2015:287345http://dx.doi.org/10.1155/2015/287345.

119. Nakano K, Balint E, Ashcroft M, et al. A ribonucleotide reductase gene is a transcriptional target of p53 and p73. Oncogene 2000;19:4283-9http://dx.doi.org/10.1038/sj.onc.1203774.

120. Cho EC, Kuo ML, Liu X, et al. Tumor suppressor FOXO3 regulates ribonucleotide reductase subunit RRM2B and impacts on survival of cancer patients. Oncotarget 2014;5:4834-44http://dx.doi.org/10.18632/oncotarget.2044.

121. Byun DS, Chae KS, Ryu BK, et al. Expression and mutation analyses of P53R2, a newly identified p53 target for DNA repair in human gastric carcinoma. Int J Cancer 2002;98:718-23http://dx.doi.org/10.1002/ijc.10253.

122. Devlin HL, Mack PC, Burich RA, et al. Impairment of the DNA repair and growth arrest pathways by p53R2 silencing enhances DNA damage-induced apoptosis in a p53-dependent manner in prostate cancer cells. Mol Cancer Res 2008;6:808-18http://dx.doi.org/10.1158/1541-7786.MCR-07-2027.

123. Liu X, Zhou B, Xue L, et al. Ribonucleotide reductase subunits M2 and p53R2 are potential biomarkers for metastasis of colon cancer. Clin Colorectal Cancer 2007;6:374-81http://dx.doi.org/10.3816/CCC.2007.n.007.

124. Li Y, Dowbenko D, Lasky LA. AKT/PKB phosphorylation of p21Cip/WAF1 enhances protein stability of p21Cip/WAF1 and promotes cell survival. J Biol Chem 2002;277:11352-61http://dx.doi.org/10.1074/jbc.M109062200.

125. Smith ML, Seo YR. p53 regulation of DNA excision repair pathways. Mutagenesis 2002;17:149-56http://dx.doi.org/10.1093/mutage/17.2.149.

126. Grobner SN, Worst BC, Weischenfeldt J, et al. The landscape of genomic alterations across childhood cancers. Nature 2018;555:321-327http://dx.doi.org/10.1038/nature25480.

127. Ekhart C, Doodeman VD, Rodenhuis S, et al. Influence of polymorphisms of drug metabolizing enzymes (CYP2B6, CYP2C9, CYP2C19, CYP3A4, CYP3A5, GSTA1, GSTP1, ALDH1A1 and ALDH3A1) on the pharmacokinetics of cyclophosphamide and 4-hydroxycyclophosphamide. Pharmacogenet Genomics 2008;18:515-23http://dx.doi.org/10.1097/FPC.0b013e3282fc9766.

128. Algeciras-Schimnich A, O'Kane DJ, Snozek CL. Pharmacogenomics of tamoxifen and irinotecan therapies. Clin Lab Med 2008;28:553-67http://dx.doi.org/10.1016/j.cll.2008.05.004.

129. Queckenberg C, Erlinghagen V, Baken BC, et al. Pharmacokinetics and pharmacogenetics of capecitabine and its metabolites following replicate administration of two 500 mg tablet formulations. Cancer Chemother Pharmacol 2015;76:1081-91http://dx.doi.org/10.1007/s00280-015-2840-6.

130. Trujillo-Paolillo A, Tesser-Gamba F, Petrilli AS, et al. CYP genes in osteosarcoma: Their role in tumorigenesis, pulmonary metastatic microenvironment and treatment response. Oncotarget 2017;8:38530-38540http://dx.doi.org/10.18632/oncotarget.15869.

131. Hagleitner MM, Coenen MJ, Gelderblom H, et al. A First Step toward Personalized Medicine in Osteosarcoma: Pharmacogenetics as Predictive Marker of Outcome after Chemotherapy-Based Treatment. Clin Cancer Res 2015;21:3436-41http://dx.doi.org/10.1158/1078-0432.CCR-14-2638.

132. Valencia-Cervantes J, Huerta-Yepez S, Aquino-Jarquin G, et al. Hypoxia increases chemoresistance in human medulloblastoma DAOY cells via hypoxiainducible factor 1alphamediated downregulation of the CYP2B6, CYP3A4 and CYP3A5 enzymes and inhibition of cell proliferation. Oncol Rep 2019;41:178-190http://dx.doi.org/10.3892/or.2018.6790.

133. Darwish MH, Farah RA, Farhat GN, et al. Association of CYP3A4/5 genotypes and expression with the survival of patients with neuroblastoma. Mol Med Rep 2015;11:1462-8http://dx.doi.org/10.3892/mmr.2014.2835.

134. Egbelakin A, Ferguson MJ, MacGill EA, et al. Increased risk of vincristine neurotoxicity associated with low CYP3A5 expression genotype in children with acute lymphoblastic leukemia. Pediatr Blood Cancer 2011;56:361-7http://dx.doi.org/10.1002/pbc.22845.

135. Bader P, Fuchs J, Wenderoth M, et al. Altered expression of resistance associated genes in hepatoblastoma xenografts incorporated into mice following treatment with adriamycin or cisplatin. Anticancer Res 1998;18:3127-32.

136. Molina-Ortiz D, Torres-Zarate C, Cardenas-Cardos R, et al. MDR1 not CYP3A4 gene expression is the predominant mechanism of innate drug resistance in pediatric soft tissue sarcoma patients. Cancer Biomark 2018;22:317-324http://dx.doi.org/10.3233/CBM-171027.

137. Gsur A, Zochbauer S, Gotzl M, et al. MDR1 RNA expression as a prognostic factor in acute myeloid leukemia: an update. Leuk Lymphoma 1993;12:91-4http://dx.doi.org/10.3109/10428199309059575.

138. Fazlina N, Maha A, Zarina AL, et al. Assessment of P-gp and MRP1 activities using MultiDrugQuant Assay Kit: a preliminary study of correlation between protein expressions and its functional activities in newly diagnosed acute leukaemia patients. Malays J Pathol 2008;30:87-93.

139. Li Y, Zhao L, Li N, et al. miR-9 regulates the multidrug resistance of chronic myelogenous leukemia by targeting ABCB1. Oncol Rep 2017;37:2193-2200http://dx.doi.org/10.3892/or.2017.5464.

140. Korita PV, Wakai T, Shirai Y, et al. Multidrug resistance-associated protein 2 determines the efficacy of cisplatin in patients with hepatocellular carcinoma. Oncol Rep 2010;23:965-72http://dx.doi.org/10.3892/or_00000721.

141. Ferrandis E, Da Silva J, Riou G, et al. Coactivation of the MDR1 and MYCN genes in human neuroblastoma cells during the metastatic process in the nude mouse. Cancer Res 1994;54:2256-61.

142. Hu R, Yan Y, Li Q, et al. Increased drug efflux along with midkine gene high expression in childhood B-lineage acute lymphoblastic leukemia cells. Int J Hematol 2010;92:105-10http://dx.doi.org/10.1007/s12185-010-0613-x.

143. Pongstaporn W, Pakakasama S, Chaksangchaichote P, et al. MDR1 C3435T and C1236T polymorphisms: association with high-risk childhood acute lymphoblastic leukemia. Asian Pac J Cancer Prev 2015;16:2839-43http://dx.doi.org/10.7314/apjcp.2015.16.7.2839.

144. Schaich M, Kestel L, Pfirrmann M, et al. A MDR1 (ABCB1) gene single nucleotide polymorphism predicts outcome of temozolomide treatment in glioblastoma patients. Ann Oncol 2009;20:175-81http://dx.doi.org/10.1093/annonc/mdn548.

145. Chen CJ, Chin JE, Ueda K, et al. Internal duplication and homology with bacterial transport proteins in the mdr1 (P-glycoprotein) gene from multidrug-resistant human cells. Cell 1986;47:381-9http://dx.doi.org/10.1016/0092-8674(86)90595-7.

146. Mansoori B, Mohammadi A, Davudian S, et al. The Different Mechanisms of Cancer Drug Resistance: A Brief Review. Adv Pharm Bull 2017;7:339-348http://dx.doi.org/10.15171/apb.2017.041.

147. Izycka-Swieszewska E, Bien E, Stefanowicz J, et al. Malignant Gliomas as Second Neoplasms in Pediatric Cancer Survivors: Neuropathological Study. Biomed Res Int 2018;2018:4596812http://dx.doi.org/10.1155/2018/4596812.

148. Pollack IF, Finkelstein SD, Woods J, et al. Expression of p53 and prognosis in children with malignant gliomas. N Engl J Med 2002;346:420-7http://dx.doi.org/10.1056/NEJMoa012224.

149. Iqbal W, Demidova EV, Serrao S, et al. RRM2B Is Frequently Amplified Across Multiple Tumor Types: Implications for DNA Repair, Cellular Survival, and Cancer Therapy. Front Genet 2021;12:628758http://dx.doi.org/10.3389/fgene.2021.628758.

150. Takagi M, Yoshida M, Nemoto Y, et al. Loss of DNA Damage Response in Neuroblastoma and Utility of a PARP Inhibitor. J Natl Cancer Inst 2017;109http://dx.doi.org/10.1093/jnci/djx062.

151. Ballinger ML, Goode DL, Ray-Coquard I, et al. Monogenic and polygenic determinants of sarcoma risk: an international genetic study. Lancet Oncol 2016;17:1261-71http://dx.doi.org/10.1016/S1470-2045(16)30147-4.

152. Chen C, Bartenhagen C, Gombert M, et al. Next-generation-sequencing of recurrent childhood high hyperdiploid acute lymphoblastic leukemia reveals mutations typically associated with high risk patients. Leuk Res 2015;39:990-1001http://dx.doi.org/10.1016/j.leukres.2015.06.005.

153. Klein S, Abraham M, Bulvik B, et al. CXCR4 Promotes Neuroblastoma Growth and Therapeutic Resistance through miR-15a/16-1-Mediated ERK and BCL2/Cyclin D1 Pathways. Cancer Res 2018;78:1471-1483http://dx.doi.org/10.1158/0008-5472.CAN-17-0454.

154. Laetsch TW, Liu X, Vu A, et al. Multiple components of the spliceosome regulate Mcl1 activity in neuroblastoma. Cell Death Dis 2014;5:e1072http://dx.doi.org/10.1038/cddis.2014.40.

155. Aries IM, Bodaar K, Karim SA, et al. PRC2 loss induces chemoresistance by repressing apoptosis in T cell acute lymphoblastic leukemia. J Exp Med 2018;215:3094-3114http://dx.doi.org/10.1084/jem.20180570.

156. Tarek N, Hayes-Jordan A, Salvador L, et al. Recurrent desmoplastic small round cell tumor responding to an mTOR inhibitor containing regimen. Pediatr Blood Cancer 2018;65http://dx.doi.org/10.1002/pbc.26768.

157. Becher OJ, Gilheeney SW, Khakoo Y, et al. A phase I study of perifosine with temsirolimus for recurrent pediatric solid tumors. Pediatr Blood Cancer 2017;64http://dx.doi.org/10.1002/pbc.26409.

158. Vo KT, Karski EE, Nasholm NM, et al. Phase 1 study of sirolimus in combination with oral cyclophosphamide and topotecan in children and young adults with

relapsed and refractory solid tumors. Oncotarget 2017;8:23851-23861http://dx.doi.org/10.18632/oncotarget.12904.

159. Krueger DA, Care MM, Holland K, et al. Everolimus for subependymal giant-cell astrocytomas in tuberous sclerosis. N Engl J Med 2010;363:1801-11http://dx.doi.org/10.1056/NEJMoa1001671.

160. Rodrik-Outmezguine VS, Okaniwa M, Yao Z, et al. Overcoming mTOR resistance mutations with a new-generation mTOR inhibitor. Nature 2016;534:272-6http://dx.doi.org/10.1038/nature17963.

161. Hosoi H, Dilling MB, Liu LN, et al. Studies on the mechanism of resistance to rapamycin in human cancer cells. Mol Pharmacol 1998;54:815-24http://dx.doi.org/10.1124/mol.54.5.815.

162. Folgiero V, Miele E, Carai A, et al. IDO1 involvement in mTOR pathway: a molecular mechanism of resistance to mTOR targeting in medulloblastoma. Oncotarget 2016;7:52900-52911http://dx.doi.org/10.18632/oncotarget.9284.

163. Schultz KR, Carroll A, Heerema NA, et al. Long-term follow-up of imatinib in pediatric Philadelphia chromosome-positive acute lymphoblastic leukemia: Children's Oncology Group study AALL0031. Leukemia 2014;28:1467-71http://dx.doi.org/10.1038/leu.2014.30.

164. Aoe M, Shimada A, Muraoka M, et al. ABL kinase mutation and relapse in 4 pediatric Philadelphia chromosome-positive acute lymphoblastic leukemia cases. Int J Hematol 2014;99:609-15http://dx.doi.org/10.1007/s12185-014-1565-3.

165. Yang K, Fu LW. Mechanisms of resistance to BCR-ABL TKIs and the therapeutic strategies: A review. Crit Rev Oncol Hematol 2015;93:277-92http://dx.doi.org/10.1016/j.critrevonc.2014.11.001.

166. Mody R, Naranjo A, Van Ryn C, et al. Irinotecan-temozolomide with temsirolimus or dinutuximab in children with refractory or relapsed neuroblastoma (COG ANBL1221): an open-label, randomised, phase 2 trial. Lancet Oncol 2017;18:946-957http://dx.doi.org/10.1016/S1470-2045(17)30355-8.

167. Goldman S, Smith L, Galardy P, et al. Rituximab with chemotherapy in children and adolescents with central nervous system and/or bone marrow-positive Burkitt lymphoma/leukaemia: a Children's Oncology Group Report. Br J Haematol 2014;167:394-401http://dx.doi.org/10.1111/bjh.13040.

168. Hiraga J, Tomita A, Sugimoto T, et al. Down-regulation of CD20 expression in B-cell lymphoma cells after treatment with rituximab-containing combination chemotherapies: its prevalence and clinical significance. Blood 2009;113:4885-93http://dx.doi.org/10.1182/blood-2008-08-175208.

169. Al-Rohil RN, Torres-Cabala CA, Patel A, et al. Loss of CD30 expression after treatment with brentuximab vedotin in a patient with anaplastic large cell lymphoma: a novel finding. J Cutan Pathol 2016;43:1161-1166http://dx.doi.org/10.1111/cup.12797.

170. Janiszewska H, Styczynski J, Kolodziej B, et al. Changes in the MDR1 gene expression after short-term ex vivo therapy with prednisolone have prognostic impact in childhood acute lymphoblastic leukemia. Ann Hematol 2009;88:1193-8http://dx.doi.org/10.1007/s00277-009-0739-1.

171. Boot A, Huang MN, Ng AWT, et al. In-depth characterization of the cisplatin mutational signature in human cell lines and in esophageal and liver tumors. Genome Res 2018;28:654-665http://dx.doi.org/10.1101/gr.230219.117.

172. Hirsch TZ, Pilet J, Morcrette G, et al. Integrated Genomic Analysis Identifies Driver Genes and Cisplatin-Resistant Progenitor Phenotype in Pediatric Liver Cancer. Cancer Discov 2021;11:2524-2543http://dx.doi.org/10.1158/2159-8290.CD-20-1809.

173. Farmer P, Bonnefoi H, Anderle P, et al. A stroma-related gene signature predicts resistance to neoadjuvant chemotherapy in breast cancer. Nat Med 2009;15:68-74http://dx.doi.org/10.1038/nm.1908.

174. Byers LA, Diao L, Wang J, et al. An epithelial-mesenchymal transition gene signature predicts resistance to EGFR and PI3K inhibitors and identifies Axl as a therapeutic target for overcoming EGFR inhibitor resistance. Clin Cancer Res 2013;19:279-90http://dx.doi.org/10.1158/1078-0432.CCR-12-1558.

175. Li R, Wu C, Liang H, et al. Knockdown of TWIST enhances the cytotoxicity of chemotherapeutic drugs in doxorubicin-resistant HepG2 cells by suppressing MDR1 and EMT. Int J Oncol 2018;53:1763-1773http://dx.doi.org/10.3892/ijo.2018.4495.

176. Manegold C, Zatloukal P, Krejcy K, et al. Gemcitabine in non-small cell lung cancer (NSCLC). Invest New Drugs 2000;18:29-42http://dx.doi.org/10.1023/a:1006327729228.

177. Wang J, Lohman GJ, Stubbe J. Enhanced subunit interactions with gemcitabine-5'-diphosphate inhibit ribonucleotide reductases. Proc Natl Acad Sci U S A 2007;104:14324-9http://dx.doi.org/10.1073/pnas.0706803104.

178. Bonate PL, Arthaud L, Cantrell WR, Jr., et al. Discovery and development of clofarabine: a nucleoside analogue for treating cancer. Nat Rev Drug Discov 2006;5:855-63http://dx.doi.org/10.1038/nrd2055.

179. Aye Y, Stubbe J. Clofarabine 5'-di and -triphosphates inhibit human ribonucleotide reductase by altering the quaternary structure of its large subunit. Proc Natl Acad Sci U S A 2011;108:9815-20http://dx.doi.org/10.1073/pnas.1013274108.

180. Gonzalez H, Leblond V, Azar N, et al. Severe autoimmune hemolytic anemia in eight patients treated with fludarabine. Hematol Cell Ther 1998;40:113-8.

181. Shao J, Zhou B, Chu B, et al. Ribonucleotide reductase inhibitors and future drug design. Curr Cancer Drug Targets 2006;6:409-31http://dx.doi.org/10.2174/156800906777723949.

182. Sterkers Y, Preudhomme C, Lai JL, et al. Acute myeloid leukemia and myelodysplastic syndromes following essential thrombocythemia treated with hydroxyurea: high proportion of cases with 17p deletion. Blood 1998;91:616-22.

183. Hehlmann R, Heimpel H, Hasford J, et al. Randomized comparison of busulfan and hydroxyurea in chronic myelogenous leukemia: prolongation of survival by hydroxyurea. The German CML Study Group. Blood 1993;82:398-407.

184. Temperini C, Innocenti A, Scozzafava A, et al. N-hydroxyurea--a versatile zinc binding function in the design of metalloenzyme inhibitors. Bioorg Med Chem Lett 2006;16:4316-20http://dx.doi.org/10.1016/j.bmcl.2006.05.068.

185. Shah KN, Wilson EA, Malla R, et al. Targeting Ribonucleotide Reductase M2 and NF-kappaB Activation with Didox to Circumvent Tamoxifen Resistance in Breast Cancer. Mol Cancer Ther 2015;14:2411-21http://dx.doi.org/10.1158/1535-7163.MCT-14-0689.

186. Nutting CM, van Herpen CM, Miah AB, et al. Phase II study of 3-AP Triapine in patients with recurrent or metastatic head and neck squamous cell carcinoma. Ann Oncol 2009;20:1275-9http://dx.doi.org/10.1093/annonc/mdn775.

187. Finch RA, Liu M, Grill SP, et al. Triapine (3-aminopyridine-2-carboxaldehyde-thiosemicarbazone): A potent inhibitor of ribonucleotide reductase activity with broad spectrum antitumor activity. Biochem Pharmacol 2000;59:983-91http://dx.doi.org/10.1016/s0006-2952(99)00419-0.

188. Cory JG, Cory AH, Rappa G, et al. Inhibitors of ribonucleotide reductase. Comparative effects of amino- and hydroxy-substituted pyridine-2-carboxaldehyde thiosemicarbazones. Biochem Pharmacol 1994;48:335-44http://dx.doi.org/10.1016/0006-2952(94)90105-8.

189. Zhu L, Zhou B, Chen X, et al. Inhibitory mechanisms of heterocyclic carboxaldehyde thiosemicabazones for two forms of human ribonucleotide

reductase. Biochem Pharmacol 2009;78:1178-85http://dx.doi.org/10.1016/j.bcp.2009.06.103.

190. Aye Y, Long MJC, Stubbe J. Mechanistic studies of semicarbazone triapine targeting human ribonucleotide reductase in vitro and in mammalian cells: tyrosyl radical quenching not involving reactive oxygen species. J Biol Chem 2012;287:35768-35778http://dx.doi.org/10.1074/jbc.M112.396911.

191. Zhou B, Su L, Hu S, et al. A small-molecule blocking ribonucleotide reductase holoenzyme formation inhibits cancer cell growth and overcomes drug resistance. Cancer Res 2013;73:6484-93http://dx.doi.org/10.1158/0008-5472.CAN-13-1094.

192. Koppenhafer SL, Goss KL, Terry WW, et al. Inhibition of the ATR-CHK1 Pathway in Ewing Sarcoma Cells Causes DNA Damage and Apoptosis via the CDK2-Mediated Degradation of RRM2. Mol Cancer Res 2020;18:91-104http://dx.doi.org/10.1158/1541-7786.MCR-19-0585.

193. Nicolle D, Fabre M, Simon-Coma M, et al. Patient-derived mouse xenografts from pediatric liver cancer predict tumor recurrence and advise clinical management. Hepatology 2016;64:1121-35http://dx.doi.org/10.1002/hep.28621.

194. Kats D, Ricker CA, Berlow NE, et al. Volasertib preclinical activity in high-risk hepatoblastoma. Oncotarget 2019;10:6403-6417http://dx.doi.org/10.18632/oncotarget.27237.

195. Fan L, Pan Q, Yang W, et al. A developmentally prometastatic niche to hepatoblastoma in neonatal liver mediated by the Cxcl1/Cxcr2 axis. Hepatology 2022http://dx.doi.org/10.1002/hep.32412.

196. Ianevski A, Giri AK, Aittokallio T. SynergyFinder 2.0: visual analytics of multi-drug combination synergies. Nucleic Acids Res 2020;48:W488-W493http://dx.doi.org/10.1093/nar/gkaa216.

197. Sentmanat MF, Peters ST, Florian CP, et al. A Survey of Validation Strategies for CRISPR-Cas9 Editing. Sci Rep 2018;8:888http://dx.doi.org/10.1038/s41598-018-19441-8.

198. Connelly JP, Pruett-Miller SM. CRIS.py: A Versatile and High-throughput Analysis Program for CRISPR-based Genome Editing. Sci Rep 2019;9:4194http://dx.doi.org/10.1038/s41598-019-40896-w.

199. Valanejad L, Cast A, Wright M, et al. PARP1 activation increases expression of modified tumor suppressors and pathways underlying development of aggressive hepatoblastoma. Commun Biol 2018;1:67http://dx.doi.org/10.1038/s42003-018-0077-8.

200. Li B, Dewey CN. RSEM: accurate transcript quantification from RNA-Seq data with or without a reference genome. BMC Bioinformatics 2011;12:323http://dx.doi.org/10.1186/1471-2105-12-323.

201. Langmead B, Salzberg SL. Fast gapped-read alignment with Bowtie 2. Nat Methods 2012;9:357-9http://dx.doi.org/10.1038/nmeth.1923.

202. Ritchie ME, Phipson B, Wu D, et al. limma powers differential expression analyses for RNA-sequencing and microarray studies. Nucleic Acids Res 2015;43:e47http://dx.doi.org/10.1093/nar/gkv007.

203. Subramanian A, Tamayo P, Mootha VK, et al. Gene set enrichment analysis: a knowledge-based approach for interpreting genome-wide expression profiles. Proc Natl Acad Sci U S A 2005;102:15545-50http://dx.doi.org/10.1073/pnas.0506580102.

204. Khatamian A, Paull EO, Califano A, et al. SJARACNe: a scalable software tool for gene network reverse engineering from big data. Bioinformatics 2019;35:2165-2166http://dx.doi.org/10.1093/bioinformatics/bty907.

205. Sumazin P, Chen Y, Trevino LR, et al. Genomic analysis of hepatoblastoma identifies distinct molecular and prognostic subgroups. Hepatology 2017;65:104-121http://dx.doi.org/10.1002/hep.28888.

206. Cancer Genome Atlas Research Network. Electronic address wbe, Cancer Genome Atlas Research N. Comprehensive and Integrative Genomic Characterization of Hepatocellular Carcinoma. Cell 2017;169:1327-1341 e23http://dx.doi.org/10.1016/j.cell.2017.05.046.

207. Du X, Yu A, Tao W. The non-canonical Hippo/Mst pathway in lymphocyte development and functions. Acta Biochim Biophys Sin (Shanghai) 2015;47:60-4http://dx.doi.org/10.1093/abbs/gmu112.

208. Allan BJ, Parikh PP, Diaz S, et al. Predictors of survival and incidence of hepatoblastoma in the paediatric population. Hpb 2013;15:741-746http://dx.doi.org/10.1111/hpb.12112.

209. Litten JB, Tomlinson GE. Liver tumors in children. Oncologist 2008;13:812-20http://dx.doi.org/10.1634/theoncologist.2008-0011.

210. Hubbard AK, Spector LG, Fortuna G, et al. Trends in International Incidence of Pediatric Cancers in Children Under 5 Years of Age: 1988-2012. JNCI Cancer Spectr 2019;3:pkz007http://dx.doi.org/10.1093/jncics/pkz007.

211. Bell CC, Gilan O. Principles and mechanisms of non-genetic resistance in cancer. Br J Cancer 2019http://dx.doi.org/10.1038/s41416-019-0648-6.

212. Craig AJ, von Felden J, Garcia-Lezana T, et al. Tumour evolution in hepatocellular carcinoma. Nat Rev Gastroenterol Hepatol 2019http://dx.doi.org/10.1038/s41575-019-0229-4.

213. Greene BL, Kang G, Cui C, et al. Ribonucleotide Reductases: Structure, Chemistry, and Metabolism Suggest New Therapeutic Targets. Annu Rev Biochem 2020;89:45-75http://dx.doi.org/10.1146/annurev-biochem-013118-111843.

214. Elledge SJ, Zhou Z, Allen JB. Ribonucleotide reductase: regulation, regulation, regulation. Trends Biochem Sci 1992;17:119-23http://dx.doi.org/10.1016/0968-0004(92)90249-9.

215. Herrick J, Sclavi B. Ribonucleotide reductase and the regulation of DNA replication: an old story and an ancient heritage. Mol Microbiol 2007;63:22-34http://dx.doi.org/10.1111/j.1365-2958.2006.05493.x.

216. Qiu W, Zhou B, Darwish D, et al. Characterization of enzymatic properties of human ribonucleotide reductase holoenzyme reconstituted in vitro from hRRM1, hRRM2, and p53R2 subunits. Biochem Biophys Res Commun 2006;340:428-34http://dx.doi.org/10.1016/j.bbrc.2005.12.019.

217. Lee B, Ha SY, Song DH, et al. High expression of ribonucleotide reductase subunit M2 correlates with poor prognosis of hepatocellular carcinoma. Gut Liver 2014;8:662-8http://dx.doi.org/10.5009/gnl13392.

218. Yang Y, Li S, Cao J, et al. RRM2 Regulated By LINC00667/miR-143-3p Signal Is Responsible For Non-Small Cell Lung Cancer Cell Progression. Onco Targets Ther 2019;12:9927-9939http://dx.doi.org/10.2147/OTT.S221339.

219. Han P, Lin ZR, Xu LH, et al. Ribonucleotide reductase M2 subunit expression and prognostic value in nasopharyngeal carcinoma. Mol Med Rep 2015;12:401-9http://dx.doi.org/10.3892/mmr.2015.3360.

220. Yoshida Y, Tsunoda T, Doi K, et al. KRAS-mediated up-regulation of RRM2 expression is essential for the proliferation of colorectal cancer cell lines. Anticancer Res 2011;31:2535-9.

221. Sun H, Yang B, Zhang H, et al. RRM2 is a potential prognostic biomarker with functional significance in glioma. Int J Biol Sci 2019;15:533-543http://dx.doi.org/10.7150/ijbs.30114.

222. Cho EC, Yen Y. Novel regulators and molecular mechanisms of p53R2 and its disease relevance. Biochimie 2016;123:81-4http://dx.doi.org/10.1016/j.biochi.2016.01.008.

223. Zhang K, Wu J, Wu X, et al. p53R2 inhibits the proliferation of human cancer cells in association with cell-cycle arrest. Mol Cancer Ther 2011;10:269-78http://dx.doi.org/10.1158/1535-7163.MCT-10-0728.

224. Lopez-Terrada D, Cheung SW, Finegold MJ, et al. Hep G2 is a hepatoblastoma-derived cell line. Hum Pathol 2009;40:1512-5http://dx.doi.org/10.1016/j.humpath.2009.07.003.

225. Woodfield SE, Shi Y, Patel RH, et al. A Novel Cell Line Based Orthotopic Xenograft Mouse Model That Recapitulates Human Hepatoblastoma. Sci Rep 2017;7:17751http://dx.doi.org/10.1038/s41598-017-17665-8.

226. Souglakos J, Boukovinas I, Taron M, et al. Ribonucleotide reductase subunits M1 and M2 mRNA expression levels and clinical outcome of lung adenocarcinoma patients treated with docetaxel/gemcitabine. Br J Cancer 2008;98:1710-5http://dx.doi.org/10.1038/sj.bjc.6604344.

227. Mortazavi A, Ling Y, Martin LK, et al. A phase I study of prolonged infusion of triapine in combination with fixed dose rate gemcitabine in patients with advanced solid tumors. Invest New Drugs 2013;31:685-95http://dx.doi.org/10.1007/s10637-012-9863-1.

228. Farrell JJ, Moughan J, Wong JL, et al. Precision Medicine and Pancreatic Cancer: A Gemcitabine Pathway Approach. Pancreas 2016;45:1485-1493http://dx.doi.org/10.1097/MPA.0000000000000710.

229. Finch RA, Liu MC, Cory AH, et al. Triapine (3-aminopyridine-2-carboxaldehyde thiosemicarbazone; 3-AP): an inhibitor of ribonucleotide reductase with antineoplastic activity. Adv Enzyme Regul 1999;39:3-12http://dx.doi.org/10.1016/s0065-2571(98)00017-x.

230. Nicolle D, Fabre M, Simon-Coma M, et al. Patient-derived xenografts from pediatric liver cancer predict tumor recurrence and advise clinical management. Hepatology 2016http://dx.doi.org/10.1002/hep.28621.

231. Bailly C. Irinotecan: 25 years of cancer treatment. Pharmacol Res 2019;148:104398http://dx.doi.org/10.1016/j.phrs.2019.104398.

232. Yousefi B, Rahmati M, Ahmadi Y. The roles of p53R2 in cancer progression based on the new function of mutant p53 and cytoplasmic p21. Life Sci 2014;99:14-7http://dx.doi.org/10.1016/j.lfs.2014.01.063.

233. Partridge EC, Chhetri SB, Prokop JW, et al. Occupancy maps of 208 chromatin-associated proteins in one human cell type. Nature 2020;583:720-728http://dx.doi.org/10.1038/s41586-020-2023-4.

234. Lee YR, Park SY. P53 expression in hepatocellular carcinoma: influence on the radiotherapeutic response of the hepatocellular carcinoma. Clin Mol Hepatol 2015;21:230-1http://dx.doi.org/10.3350/cmh.2015.21.3.230.

235. Hsu IC, Tokiwa T, Bennett W, et al. p53 gene mutation and integrated hepatitis B viral DNA sequences in human liver cancer cell lines. Carcinogenesis 1993;14:987-92http://dx.doi.org/10.1093/carcin/14.5.987.

236. Buss JL, Torti FM, Torti SV. The role of iron chelation in cancer therapy. Curr Med Chem 2003;10:1021-34http://dx.doi.org/10.2174/0929867033457638.

237. Jin MH, Oh DY. ATM in DNA repair in cancer. Pharmacol Ther 2019;203:107391http://dx.doi.org/10.1016/j.pharmthera.2019.07.002.

238. Meacham CE, Morrison SJ. Tumour heterogeneity and cancer cell plasticity. Nature 2013;501:328-37http://dx.doi.org/10.1038/nature12624.

239. Marine JC, Dawson SJ, Dawson MA. Non-genetic mechanisms of therapeutic resistance in cancer. Nat Rev Cancer 2020;20:743-756http://dx.doi.org/10.1038/s41568-020-00302-4.

240. Bell D, Ranganathan S, Tao J, et al. Novel Advances in Understanding of Molecular Pathogenesis of Hepatoblastoma: A Wnt/beta-Catenin Perspective. Gene Expr 2017;17:141-154http://dx.doi.org/10.3727/105221616X693639.

241. Azimi A, Majidinia M, Shafiei-Irannejad V, et al. Suppression of p53R2 gene expression with specific siRNA sensitizes HepG2 cells to doxorubicin. Gene 2018;642:249-255http://dx.doi.org/10.1016/j.gene.2017.11.008.

242. Friedler A, DeDecker BS, Freund SM, et al. Structural distortion of p53 by the mutation R249S and its rescue by a designed peptide: implications for "mutant conformation". J Mol Biol 2004;336:187-96http://dx.doi.org/10.1016/j.jmb.2003.12.005.

243. Suresh S, Chen B, Zhu J, et al. eIF5B drives integrated stress response-dependent translation of PD-L1 in lung cancer. Nat Cancer 2020;1:533-545http://dx.doi.org/10.1038/s43018-020-0056-0.

244. Nabet B, Roberts JM, Buckley DL, et al. The dTAG system for immediate and target-specific protein degradation. Nat Chem Biol 2018;14:431-441http://dx.doi.org/10.1038/s41589-018-0021-8.

245. Yokomakura N, Natsugoe S, Okumura H, et al. Improvement in radiosensitivity using small interfering RNA targeting p53R2 in esophageal squamous cell carcinoma. Oncol Rep 2007;18:561-7.

246. Yanamoto S, Iwamoto T, Kawasaki G, et al. Silencing of the p53R2 gene by RNA interference inhibits growth and enhances 5-fluorouracil sensitivity of oral cancer cells. Cancer Lett 2005;223:67-76http://dx.doi.org/10.1016/j.canlet.2004.10.019.

247. An S, Fu L. Small-molecule PROTACs: An emerging and promising approach for the development of targeted therapy drugs. EBioMedicine 2018;36:553-562http://dx.doi.org/10.1016/j.ebiom.2018.09.005.

248. Gadd MS, Testa A, Lucas X, et al. Structural basis of PROTAC cooperative recognition for selective protein degradation. Nat Chem Biol 2017;13:514-521http://dx.doi.org/10.1038/nchembio.2329.

249. Sun X, Gao H, Yang Y, et al. PROTACs: great opportunities for academia and industry. Signal Transduct Target Ther 2019;4:64http://dx.doi.org/10.1038/s41392-019-0101-6.

250. Kleih M, Bopple K, Dong M, et al. Direct impact of cisplatin on mitochondria induces ROS production that dictates cell fate of ovarian cancer cells. Cell Death Dis 2019;10:851http://dx.doi.org/10.1038/s41419-019-2081-4.

251. Guo C, Sun L, Chen X, et al. Oxidative stress, mitochondrial damage and neurodegenerative diseases. Neural Regen Res 2013;8:2003-14http://dx.doi.org/10.3969/j.issn.1673-5374.2013.21.009.

252. Liu X, Xue L, Yen Y. Redox property of ribonucleotide reductase small subunit M2 and p53R2. Methods Mol Biol 2008;477:195-206http://dx.doi.org/10.1007/978-1-60327-517-0_15.

253. Chen YF, Lin IH, Guo YR, et al. Rrm2b deletion causes mitochondrial metabolic defects in renal tubules. Sci Rep 2019;9:13238http://dx.doi.org/10.1038/s41598-019-49663-3.

254. Araujo LF, Siena ADD, Placa JR, et al. Mitochondrial transcription factor A (TFAM) shapes metabolic and invasion gene signatures in melanoma. Sci Rep 2018;8:14190http://dx.doi.org/10.1038/s41598-018-31170-6.

VITA

Anthony Brown (Tony) was born in 1994 in Fairbanks, AK to Katrina and Dennis Brown. He graduated from McGavock High School in 2012. He received his Bachelor of Science in Biochemistry and Biology Health Science from Tennessee Technological University in 2016. He began the Integrated Program of Biomedical Sciences doctoral program in the Cancer and Developmental Biology track in 2017. In February 2018 Tony joined the lab of Dr. Liqin Zhu in the Pharmacy and Pharmaceutical Sciences department at St. Jude Children's Research Hospital. There he studied the role of RRM2 and RRM2B subunit switching in hepatoblastoma drug resistance and relapse. Tony anticipates graduation with a Doctor of Philosophy degree in July 2022.